Preclinical models and molecular biomarkers

Tools to improve treatment in endometrial carcinoma

Tina Fonnes

Thesis for the Degree of Philosophiae Doctor (PhD)
University of Bergen, Norway
2018

UNIVERSITY OF BERGEN

Preclinical models and molecular biomarkers

Tools to improve treatment in endometrial carcinoma

Tina Fonnes

Thesis for the Degree of Philosophiae Doctor (PhD)
at the University of Bergen

2018

Date of defence: 30.11.2018

Year: 2018

Title: Preclinical models and molecular biomarkers

Name: Tina Fonnes

Print: Skipnes Kommunikasjon / University of Bergen

Scientific environment

This PhD-project was conducted within the Bergen Gynaecologic Cancer Research Group at the Department of Clinical Science, University of Bergen, with professor Camilla Krakstad as the main supervisor. The group was founded by the late professor Helga Salvesen, which co-supervised this PhD-project until she died unexpectedly in January 2016. More than 20 members with wide professional backgrounds are currently employed, including PhD-students, post-docs, senior researchers, and technical staff. The research group is located at Kvinneklinikken, and is cooperating closely with the Department of Obstetrics and Gynecology, Haukeland University Hospital. A major resource for the Bergen Gynaecologic Cancer Research Group is the local biobank of gynecologic malignancies which was initiated in 2001. Patients are continuously included, and the biobank now contains biological samples as well as clinical-, pathological-, imaging- and follow-up data from more than 4000 women.

Professor Emmet McCormack is head of the research group Translational Molecular Imaging in Cancer at the Department of Clinical Science, University of Bergen, and has co-supervised this PhD-project. By using state-of-the-art preclinical models and advanced imaging modalities his group aims to develop novel treatments and imaging strategies for various human cancers. Also co-supervising this PhD is Professor Bjørn Tore Gjertsen, PI of the Signalling-Targeted Therapy Group at the Department of Clinical Science, University of Bergen.

The Bergen Gynaecologic Cancer Research Group and all supervisors are affiliated with the Centre for Cancer Biomarkers (CCBIO), a "Norwegian Centre of Excellency" since 2013. The purpose of CCBIO is to discover, validate and translate cancer biomarkers through preclinical and clinical studies in order to improve diagnosis and treatment of cancer. CCBIO also offers student courses, seminars, and

hosts an annual international cancer symposium, providing a professional environment that is capable of delivering high-quality results within the field of cancer research.

This PhD-project was financially supported by the University of Bergen, Helse Vest, the Norwegian Cancer Society (628837), the Research Council of Norway (239840), and the Bergen Research Foundation. This work was also partly supported by CCBIO, a Centre of Excellence funded by the Research Council of Norway funding scheme, project number 223250.

Acknowledgements

During my years as a PhD-student I have met a lot of wonderful people which have willingly and patiently shared their knowledge and skills with me; without you I would not have been able to do this, and I owe you all my gratitude.

Camilla - as my main supervisor you have guided me safely through this PhD period. I appreciate all the efforts you have made to help me improve my skills and my sense of critical thinking. You are hardworking and result-oriented, and I am convinced that you will continue to deliver excellent research for many years to come. Emmet – I am always impressed by your innovative ideas and wide scientific insight. Bjørn Tore - your passion for research and medicine is remarkable, and it was your enthusiasm for science that first inspired me to apply for this PhD position. Helga also co-supervised this project until her unexpected death. Her achievements were remarkable, and she was truly an inspiration – both professionally and personally.

Special thanks to all my colleagues in the Bergen Gynaecological Cancer Research Group throughout these years: Ann-Helen, Anna, Britt, Camilla, David, Elin, Ellen, Elisabeth, Erica, Erling, Frederik, Grete, Havjin, Hege, Hilde, Hildegunn, Ingfrid, Ingvild, Jone, Julie, Kadri, Kanthida, Karen, Katharina, Konstantina, Kristina, Kristine, Liv Cecilie, Mari, Madeleine, Njål, Reidun, Sigmund, Siv, Therese and Vikram. The years I have spent with you will be remembered.

Ingvild - your thorough feedback has been indispensable, providing much needed SPSS-support and patiently reading through manuscripts. I greatly appreciate it. Reidun - thanks for teaching me all the skills I needed, and for helping me solve both big and small problems in the lab. Elin – thanks for all our fruitful discussions, planning sessions and cooperation at the animal facilities, you have been a highly appreciated member of “team mouse”. Therese - the office was never the same without you. Thanks for all the good talks, laughs and shared frustrations. Hilde – I

have really enjoyed our friendship, and I appreciate all the talks, laughs and social events.

The biobank of gynecological malignancies is an invaluable asset for our research group, and it has been kept up to date by a highly dedicated and skilled staff. Britt Edvardsen, Elisabeth Enge, Hege F. Berg, Reidun Kopperud, Kadri Madisoo, Ellen Valen and Ann-Helen Pridesis; you have all done an excellent job in keeping track of biological samples and updated clinical data.

Thanks to Heidi Espedal, Emmet McCormack, Tina Pavlin, Mihaela Popa, Cecilie Brekke Rygh and Mireia Mayoral Safont who have provided me with expert advice and technical support regarding small animal imaging.

I would like to thank all the co-authors of the included papers, here listed in alphabetical order; Lars A. Akslen, Frederic Amant, Anna Berg, Hege F. Berg, Njål Brekke, Line Bjørge, Per-Henrik D. Edqvist, Heidi Espedal, Kristine E. Fasmer, Ingfrid S. Haldorsen, Reidun Kopperud, Camilla Krakstad, Janusz Marcickiewicz, Emmet McCormack, Therese B. Onyango, Tina Pavlin, Mihaela Popa, Cecilie B. Rygh, Helga B. Salvesen, Kristina Sortland, Anne C. Staff, Elin Strand, Ingvild L. Tangen, Solveig Tingulstad, Jone Trovik, Nicole C. Visser and Henrica M.J. Werner.

Thank you to the Centre for Cancer Biomarkers and the Department of Clinical Science at the University of Bergen and to Kvinneklinikken, Haukeland University Hospital (HUS) for allowing me to carry out this PhD-project in such an inspiring and professional environment. A warm thanks to all the women that have participated in this study; your contributions are vital for acquiring new knowledge about endometrial carcinoma. Also, as a veterinarian I would like to acknowledge all the mice that were sacrificed in our projects in order to gain new insight in human cancer.

To all my friends outside the research environment – life would not have been the same without you, and each and every one of you mean a lot to me. Thanks to my

parents, Sonni and Gunnar, for teaching me the value of hard work and for encouraging me to perform my best. My brother Emil; our friendly debates are greatly appreciated. And last, but not least, thank you to my two beautiful sons Marcus and Theodor for constantly reminding me of what is really important in life. Your warm hugs, cheerful smiles and endless love have meant the world to me during these years, and will continue to do so for many years to come.

Abbreviations

ADC:	Apparent diffusion coefficient
AKT:	Protein kinase B
ALCAM:	Activated leukocyte cell adhesion molecule
AF680:	Alexa 680 fluorophore
ALL:	Acute lymphoblastic leukemia
AML:	Acute myeloid leukemia
ASRGL1:	Asparaginase-like protein 1
BLI:	Bioluminescent imaging
BSA:	Bovine serum albumin
CAH:	Complex atypical hyperplasia
CI:	Confidence interval
CT:	Computed tomography
DCE:	Dynamic contrast enhanced
DNA:	Deoxyribonucleic acid
DWI:	Diffusion weighted images
EBRT:	External beam radiotherapy
EGFR:	Epidermal growth factor receptor
EMEM:	Eagle's minimum essential medium
EpCAM:	Epithelial cell adhesion molecule
ERα:	Estrogen receptor alpha
FBS:	Fetal bovine serum
^{18}F-FDG:	Fluorine-18-fluorodeoxyglucose
^{18}F-FLT:	Fluorine-18-fluorothymidine
FFPE:	Formalin fixed paraffin embedded
FIGO:	International Federation of Gynecology and Obstetrics
FOV:	Field of view
GEM:	Genetically engineered models
HER2:	Human epidermal growth factor 2
HR:	Hazard ratio

HUS:	Haukeland University Hospital
ICC:	Intraclass correlation coefficient
IGFR1α:	Insulin-like growth factor 1 receptor alpha
IHC:	Immunohistochemistry
KRAS:	KRAS proto-oncogene
L1CAM:	L1 cell adhesion molecule
Luc+:	Luciferase expressing
MLH1:	MutL homolog 1
MMR:	Mismatch repair
MoMaTEC:	Molecular Markers in Treatment of Endometrial Cancer
MRI:	Magnetic resonance imaging
MSI:	Microsatellite-instable
mTOR:	Mammalian target of rapamycin
MTV:	Metabolic tumor volume
NIRF:	Near-infrared fluorescent imaging
NSG:	Non-obese diabetic severe combined immune deficiency gamma
OMI:	Optical molecular imaging
OR:	Odds ratio
PBS:	Phosphate buffered saline
PDX:	Patient derived xenograft
PE:	Phycoerythrin
PET:	Positron emission tomography
PFS:	Progression free survival
PIK3CA:	Phosphatidylinositol-4,5 bisphosphate 3-kinase catalytic subunit alpha
PI3K:	Phosphatidylinositol-4,5 bisphosphate 3-kinase
POLE:	Polymerase ε
PR:	Progesterone receptor
PTEN:	Phosphatase and Tensin homolog
RARE:	Rapid acquisition with relaxation enhancement
RNA:	Ribonucleic acid

ROI:	Region of interest
SI:	Staining index
SCNA:	Somatic copy number alteration
SUV:	Standard uptake value
SUV_{max}:	Maximum standard uptake value
SUV_{mean}:	Mean standard uptake value
TCGA:	The Cancer Genome Atlas
TE:	Echo time
TLG:	Total lesion glycolysis
TMA:	Tissue microarray
TP53:	Tumor protein p53
TR:	Repetition time
VOI:	Volume of interest

Abstract

Background: Endometrial carcinoma is the fourth most common cancer in European women, and incidence is increasing. No major improvements in treatment or survival have been achieved over the last decades, and an individualized treatment approach may improve the likelihood of a beneficial outcome for endometrial carcinoma patients. Identifying robust biomarkers that can improve risk-stratification and help select patients likely to benefit from specific treatments is vital. There is also a need for representative preclinical models in order to discover and validate new targeted therapies.

Aim: To investigate potential new biomarkers in endometrial carcinoma, and to develop robust and reliable preclinical models to improve translational research.

Material and methods: Endometrial carcinoma cell lines or patient derived primary tumor cells were implanted in the uterus of female mice to generate orthotopic endometrial carcinoma mouse models. We then applied several advanced imaging techniques to monitor development of disease in these models, including optical molecular imaging (OMI), magnetic resonance imaging (MRI) and positron emission tomography/computed tomography (PET/CT).

Patients treated for endometrial carcinoma have been prospectively entered in a biobank of gynaecological malignancies and clinicopathological data, imaging data and biological samples have been collected. Tissue samples were evaluated by immunohistochemistry and microarray in order to explore expression of asparaginase-like protein 1 (ASRGL1) in endometrial carcinoma, relating the level of ASRGL1 to survival as well as imaging- and clinicopathological parameters.

Results: Bioluminescent imaging (BLI), MRI, and PET/CT using fluorine-18-fluorodeoxyglucose (^{18}F-FDG) or fluorine-18-fluorothymidine (^{18}F-FLT) as tracer were all found to be feasible methods for monitoring of disease in orthotopic mouse models of endometrial carcinoma. With the exception of BLI, these imaging modalities were also demonstrated to visualize uterine tumors in patient derived xenografts (PDX) (**Paper I**).

Epithelial adherence molecule (EpCAM) was found to be highly expressed in both endometrial carcinoma cell lines and in hysterectomy specimens from patients diagnosed with endometrial carcinoma. Near infrared fluorescence (NIRF) imaging using an Alexa 680 fluorophore (AF680)-conjugated anti-EpCAM antibody and BLI generated comparable images of uterine tumors in cell line based orthotopic endometrial carcinoma mouse models. EpCAM-AF680 NIRF was however superior to BLI in early delineation of metastatic disease. EpCAM-AF680 NIRF imaging was found to visualize uterine tumors in multiple orthotopic PDX models, with better contrast and earlier detection of tumors compared to ^{18}F-FDG PET/CT imaging. Additionally, *in vivo* EpCAM-AF680 NIRF imaging accurately depicted a non-significant therapeutic response following treatment with paclitaxel or trastuzumab in an orthotopic PDX model of endometrial carcinoma. (**Paper II**).

Low ASRGL1 protein expression in endometrial carcinoma hysterectomy samples was validated as a strong prognostic biomarker with independent survival impact, both in the whole patient cohort and in patients diagnosed with endometrioid endometrial carcinoma. Low *ASRGL1* mRNA level was found to be significantly associated with poor outcome. ASRGL1 expression was mainly intact in the precursor lesion complex atypical hyperplasia (CAH), while the majority of metastatic lesions had lost ASRGL1 expression (**Paper III**).

Similar expression of ASRGL1 in corresponding curettage and hysterectomy samples were observed in 85% of patients where ASRGL1 status in post-operative specimens was known. Low expression of ASRGL1 in curettage was found to independently

predict poor outcome in the whole patient cohort, as well as in patients with presumed low risk curettage histology. Significant associations between low ASRGL1 expression and preoperatively assessed features of aggressive disease were observed, including high-risk curettage histology, hormone receptor loss in curettage, and large tumor size on MRI. Low ASRGL1 expression in curettage was also found to be an independent predictor of lymph node metastases (**Paper IV**).

Conclusions: We have successfully generated orthotopical mouse models of endometrial carcinoma, including PDXs with different histological backgrounds, and demonstrated that tumor development and response to treatment can be monitored by multiple advanced small animal imaging techniques. Low expression of ASRGL1 in hysterectomy samples has been validated as an independent prognostic biomarker in endometrial carcinoma, and we suggest ASRGL1 expression in curettage as a promising pre-operative biomarker with a potential to improve risk-stratification and surgical planning.

List of publications

I. Haldorsen IS, Popa M*, **Fonnes T***, Brekke N, Kopperud R, Visser NC, Rygh CB, Pavlin T, Salvesen HB, McCormack E, Krakstad C. Multimodal Imaging of Orthotopic Mouse Model of Endometrial Carcinoma. *PLoS One. 2015 Aug 7;10(8):e0135220. doi: 10.1371/journal.pone.0135220.*

II. **Fonnes T**, Strand E, Fasmer KE, Berg HF, Espedal H, Sortland K, Haldorsen IS, Krakstad C, McCormack E. Near-infrared fluorescent imaging targeting epithelial cell adhesion molecule: a novel approach to in vivo imaging in orthotopic endometrial carcinoma mouse models. *Manuscript*

III. **Fonnes, T**, Berg HF, Bredholt T, Edqvist PD, Sortland K, Berg A, Salvesen HB, Akslen LA, Werner HMJ, Trovik J, Tangen ILT, Krakstad C. Asparaginase-like protein 1 is an independent prognostic marker in primary endometrial cancer, and is frequently lost in metastatic lesions. *Gynecol Oncol. 2018 Jan;148(1):197-203. doi: 10.1016/j.ygyno.2017.10.025.*

IV. **Fonnes T**, Trovik J, Edqvist PHD, Fasmer KE, Marcickiewicz J, Tingulstad S, Staff AC, Bjørge L, Amant F, Haldorsen IS, Werner HMJ, Akslen LA, Tangen ILT, Krakstad C. Asparaginase-like protein 1 expression in curettage independently predicts lymph node metastasis in endometrial carcinoma: a multicenter study. *BJOG. 2018 Jul 10. doi: 10.1111/1471-0528.15403.*

*Authors contributed equally

Contents

1. Introduction

1.1 Endometrial carcinoma

The uterus is the major component of the female reproductive system, and consists of three distinct layers; an outer layer of peritoneum (serosa), a thick muscular layer (myometrium), and an inner mucosal lining (endometrium) including glands and stromal cells. Endometrial carcinomas originate from epithelial cells in the endometrium, and may potentially invade the surrounding myometrium and metastasize to local and distant sites (1). Despite the high number of patients diagnosed with endometrial carcinoma worldwide, there has been less research focusing on this malignancy compared to several other cancers (i.e. breast cancer). The mechanisms of endometrial carcinoma establishment and progression are yet not fully understood, and increasing this knowledge would be beneficial. Another problem is that current disease classification systems are suboptimal, thus making risk-stratification and planning of treatment difficult. Additionally, there is a dire need of better treatment strategies for patients with advanced and recurrent disease. More high-quality research is thus needed to help solve these issues and to improve the treatment of endometrial carcinoma in the future.

1.1.1 Epidemiology

Incidence

Endometrial carcinoma has the 6th highest cancer incidence in women worldwide, and is the 4th most common female cancer in Europe after breast, colorectal, and lung cancer (2). Endometrial carcinoma is not as common in less developed countries, indicating that environmental factors contribute to disease development. In Norway, 774 new cases of endometrial carcinoma were recorded in 2016 (3). An increasing incidence of endometrial carcinoma has been observed over the last decades (Figure 1), and can be explained by several factors, including higher life-expectancy and an increasing rate of obesity. It is estimated that 1 in 40 women will develop endometrial

carcinoma during their lifetime, and prognostic models suggest that between 1016-1257 new cases of endometrial carcinoma will be diagnosed annually in Norway in 2025 (4).

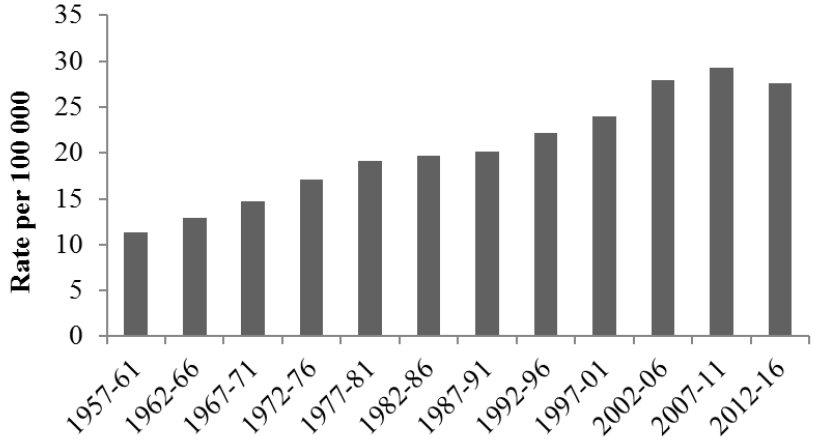

Figure 1. Age standardized incidence rates of endometrial carcinoma in Norway per 100 000 person-years by 5-year period, 1957-2016 (3).

Mortality

Worldwide it is estimated that endometrial carcinoma accounts for approximately 76 000 deaths each year (5). Although being a common type of cancer, prognosis is usually good and mortality rates are low. In 2015 there were 67 deaths due to endometrial carcinoma in Norway. Survival is highly dependent on disease stage, and the 5-year relative survival for endometrial carcinoma is 95.7% for patients with localized disease, 61% with regional disease, and 38.1% for distant metastatic disease. Overall, there has been a slight improvement in survival over the last decades (Figure 2) (3).

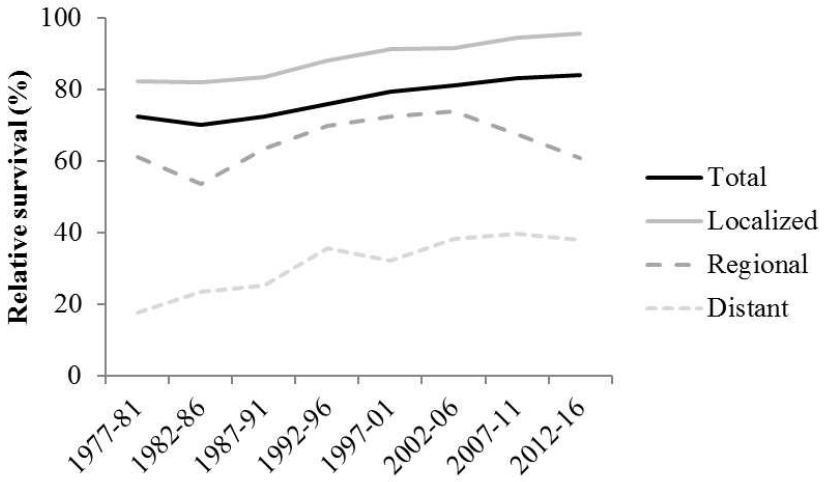

Figure 2. Five-year relative survival from endometrial carcinoma in Norway stratified by disease stage, 1977-2016 (3).

1.1.2 Clinical aspects

Risk factors

Most cases of endometrial carcinoma occur spontaneously. Several factors are reported to associate with increased risk of developing endometrial carcinoma, including nulliparity, early menarche and conditions causing metabolic disturbances such as polycystic ovary syndrome and diabetes mellitus (1, 6, 7). For endometrioid endometrial carcinoma, which is the most common subtype, unopposed estrogen exposure is a crucial risk factor (8). Exposure to estrogen stimulates cell proliferation, and may cause endometrial hyperplasia, cellular atypia, and development of endometrial carcinoma (9). Obesity is an important risk factor, most likely due to enzymatic production of estrogen in adipose tissue (9, 10). The degree of overweight is also of significance, as an increasing body mass index leads to higher risk of developing endometrial carcinoma (10). The growing rate of obesity amongst women is believed to be the cause of more than half the endometrial carcinoma cases worldwide, and is expected to contribute to an increasing incidence of endometrial carcinoma in the future (11). In contrast, multiparity, short pre-menopausal delivery-

free period, and long term use of oral contraceptives are factors considered to reduce the risk of developing endometrial carcinoma (1, 6, 7).

Some hereditary disorders are associated with higher risk of developing endometrial carcinoma, and are believed to account for approximately 5% of cases (6, 12, 13). Lynch syndrome is the most common hereditary genetic predisposition, characterized by germline mutations in deoxyribonucleic acid (DNA) mismatch repair (MMR) genes which lead to increased risk of developing several cancers - including endometrial carcinoma and colorectal cancer. The lifetime risk of endometrial carcinoma in women with Lynch syndrome is 40-60% (12). Other rare hereditary conditions associated with higher risk for endometrial carcinoma includes Cowden syndrome, where patients have germline mutations in the tumor supressor gene Phosphatase and Tensin homolog (PTEN) (13).

Clinical symptoms

Most women are diagnosed with endometrial carcinoma after menopause, and the classical presenting symptom is abnormal uterine bleeding (10). Patients with advanced disease may also experience abdominal distention, pelvic or abdominal pain, or changes in bowel and/or bladder function (6). As unexpected vaginal bleeding urges most women to visit their doctor, the majority of patients are diagnosed at an early stage. Only 5-10% of patients presenting with abnormal vaginal bleeding actually have endometrial carcinoma, although the chance is higher with increasing age and presence of risk factors (10). Currently there is no evidence supporting screening for endometrial carcinoma in the general population, and screening is not believed to reduce mortality rates (10, 14).

Preoperative histology

When suspecting endometrial carcinoma, histologic evaluation of the endometrium is performed as part of diagnosis and pre-operative risk-stratification. Several procedures can be performed to obtain specimens for histological assessment,

including pipelle, curettage, and endometrial biopsies. An endometrial curettage is performed by inserting an instrument through the cervical canal and into the uterine cavity to scrape off the endometrium. Positive findings in pre-operative curettage are reported to accurately diagnose endometrial carcinoma, but a negative curettage may not be sufficient to rule out malignant disease (15). If cancer is diagnosed in curettage specimen, determination of histological type and grade is important for risk-evaluation and surgical planning.

Histological assessment of pre-operative and hysterectomy samples is reported to be divergent in 10 – 33% of cases (16-22), indicating that this pre-operative evaluation is suboptimal as a stand-alone parameter for risk stratification and planning of therapeutic approach (23). Disagreement in histological classification between pre- and postoperative samples can be caused by several factors, including limited collection of tissue during pre-operative sampling, tissue in preoperative specimens only representing superficial areas of tumor, high degree of tumor heterogeneity, and poor inter-observer agreement between pathologists (20). Failure to recognize high-risk disease from pre-operative specimens is reported to associate with poor outcome, most likely because patients are scheduled for less extensive surgery (16). Likewise, patients with pre-operative high risk and post-operative low risk classification have worse survival compared to those with concordant pre- and post-operative low risk histology. This could be due to tumor heterogeneity, and these patients may benefit from adjuvant treatment (22).

Preoperative imaging

Preoperative imaging is a valuable tool in planning of surgical procedures, especially for identification of deep myometrial invasion, cervical stroma invasion and evaluation of metastatic spread. However, there is no consensus on how to best apply imaging in order to identify high-risk cases prior to surgery, and there is a large variation in clinical routines both between hospitals and countries (24, 25). MRI and/or vaginal/transrectal ultrasound is normally recommended for local staging, whereas CT and/or PET are better to assess lymph node metastases and systemic

spread as they allow visualization of the entire pelvis, abdomen and thorax (24). Further information regarding the various modalities used in clinical imaging can be found in section 1.5.

Staging, histopathologic typing and grading

Endometrial carcinoma is a surgically staged disease, and myometrial invasion, metastatic spread, and lymph node involvement are assessed during the procedure. In 2009 the International Federation of Gynecology and Obstetrics (FIGO) Committee on Gynecologic Oncology published their latest review on staging criteria for carcinoma of the vulva, cervix, and endometrium (26). Complete surgical staging includes sampling of pelvic and para-aortic lymph nodes, but in most hospitals this is not routinely performed in all patients. Table 1 describes the different stages of endometrial carcinoma according to the FIGO 2009 classification system.

Table 1. FIGO staging system for endometrial cancer, according to 2009 criteria.

Stage	Description [26]
I	
IA	Myometrial invasion <50%
IB	Myometrial invasion ≥50%
II	Tumor is invading the cervical stroma, but does not extend beyond the uterus.
III	
IIIA	Tumor is invading the serosa of the corpus uteri, and/or adnexa
IIIB	Vaginal and/or parametrial involvement
IIIC	Involvement of specific lymph nodes
IIIC1	Pelvic lymph nodes affected
IIIC2	Para-aortic +/- pelvic lymph nodes affected
IV	
IVA	Tumor invasion of the bladder and/or the bowel mucosa
IVB	Metastases to distant locations, including intra-abdominal metastases and/or inguinal lymph node affection

Endometrial tumors are also classified according to their histological appearances regardless of FIGO stage. Endometrioid adenocarcinoma is the most common type (≈ 80% of endometrial carcinomas), and is characterized by the presence of endometrial glands with varying degree of differentiation. Endometrioid endometrial carcinomas are often associated with high levels of estrogen, and patients may have a history of endometrial hyperplasia (1, 10). Several less common types of endometrial carcinoma are collectively referred to as non-endometrioid tumors, with serous adenocarcinoma and clear cell adenocarcinomas being the most frequent. Serous adenocarcinomas are often characterized by a papillary architecture with poorly differentiated nuclei, while clear cell adenocarcinomas are characterized by the presence of clear glycogen-filled cells. The growth pattern of the tumor can be tubular, papillary, tubulocystic, solid or a mixture of these patterns (1).

In addition to histological type, endometrial carcinomas are also graded based on the amount of solid growth in the glandular parts of the tumor. Higher histological grade indicates less differentiation of tumor, observed as solid nests and sheets of cells replacing the normal glandular appearance (1). Non-endometrioid endometrial carcinomas are by definition considered high grade (1). Grading of endometrioid tumors is performed as described below, and has prognostic relevance. The majority of endometrioid tumors are low grade (1-2), usually associated with a favorable outcome if restricted to the uterus, while grade 3 endometrioid tumors are classified as high-risk (27).

Grade 1: Less than 5% solid growth and a well-defined glandular appearance
Grade 2: 6 - 50% solid growth and a less preserved glandular pattern
Grade 3: More than 50% solid growth and hardly recognizable glands

A major challenge in the histopathological classification of endometrial carcinomas is tumor heterogeneity, where different morphologic characteristics are found within the same tumor. The degree of heterogeneity can vary from subtle variations in cytology to mixed tumors with two distinctly different histological types. Tumor heterogeneity may have a large clinical impact, as failure to identify small populations of cells with aggressive features may cause wrongful assessment of prognosis and suboptimal treatment. Integration of molecular biomarkers may add valuable information to the standard histopathological evaluation, and potentially improve risk-stratification and management of endometrial carcinoma (27).

1.1.3 Treatment

Treatment recommendations for endometrial carcinoma differ between disease subgroups, and large variations in clinical practice exist between countries. In Norway the treatment of endometrial carcinoma has changed somewhat since the early 1980's, favouring more extensive surgery and increased amount of lymph node sampling over the last period. Chemotherapy was implemented as adjuvant treatment during this time period, and the amount of patients receiving chemotherapy increased from 0% in 1981-1990 to 9% in 2001-2010. Conversely, the proportion of patients undergoing adjuvant radiotherapy was dramatically reduced from 75% to 12% during the same time period (28).

Pre-operative risk-assessment of patients is performed in order to plan the surgical approach, and is based on clinical findings, histopathological evaluation of pipelle or curettage samples, and pre-operative imaging. The histological classification of low risk disease includes grade 1 and 2 endometrioid tumors with <50% myometrial invasion, while deeply infiltrating grade 1 and 2 endometrioid tumors, as well as grade 3 endometrioid tumors with <50% myometrial invasion, are referred to as intermediate risk. High risk endometrial carcinoma is defined as grade 3 endometrioid adenocarcinomas with >50% myometrial infiltration as well as non-endometrioid histology (8, 29, 30).

Surgery

The primary treatment for endometrial carcinoma is surgery, and the standard procedure is hysterectomy with bilateral salpingo-oophorectomy (14). For patients with intermediate or high-risk disease more radical surgery might be advised, including pelvic and para-aortic lymphadenectomy, removal of paracervical and parametrial structures and omentectomy (23, 29, 31). Standardized criteria for selection of patients to undergo lymphadenectomy have not been established, and the current practice varies greatly between countries (32). The clinical benefit of lymphadenectomy has also been debated, due to the side effects associated with the

procedure and the lack of agreement regarding the therapeutic value of lymph node removal. However, intermediate- and high-risk patients are often routinely subjected to staging lymphadenectomy in order to improve post-operative risk-stratification (6, 8, 23, 29, 31). Sentinel lymph node mapping is an intraoperative procedure, where the primary draining lymph nodes (which are most likely to harbor metastatic lesions) are identified and removed. This approach reduces the extent of surgery and long-term side effects compared to more extensive lymph node removal, and may represent a good alternative to full lymphadenectomy in patients where assessment of nodal status is required (33-35).

Primary surgical treatment is curative in most cases, however 15-20% of patients experience disease relapse within few years (8, 36). Recurrent endometrial carcinoma is associated with a poor prognosis, especially in patients with distant metastatic disease (36). A key challenge in endometrial carcinoma is thus early identification of patients that are likely to suffer a relapse, in order to consider adjuvant treatment.

Adjuvant therapy

Adjuvant therapy is considered for patients with intermediate or high-risk disease to eliminate disseminated cancer cells or potential residual disease after primary surgery. Traditionally, hormonal treatment, radiation treatment and chemotherapy have been the available alternatives, while immunotherapy and targeted therapies recently have emerged as new cancer treatment strategies (37).

Hormonal treatment can be applied as adjuvant treatment in endometrial carcinoma patients who are ineligible for chemotherapy (38). Several substances are available (including tamoxifen and aromatase inhibitors), but the most commonly used are progestins. Use of hormonal therapy as single agent or combinational therapy has not been found to improve survival in women with advanced or recurrent endometrial carcinoma (39). However; checking the hormone receptor status of patients prior to

applying hormonal treatment is not standard procedure in all hospitals, and this may partially explain the lack of survival benefits.

Radiation treatment consists of local ionizing radiation applied directly at the tumor, and can be performed as vaginal brachytherapy or external beam radiotherapy (EBRT). Vaginal brachytherapy is reported to be effective in preventing local recurrence, and is associated with fewer side-effects than EBRT (40). No survival benefit has been found from treating endometrial carcinoma patients with adjuvant radiotherapy, although radiation is found to reduce locoregional recurrence. Radiation treatment is thus not recommended for low-risk endometrial carcinoma, but may be considered in intermediate- and high risk cases (41-44).

Conventional chemotherapeutics are systemically administered drugs that target rapidly dividing cells by interfering with one or more phases in the cell cycle, potentially eliminating residual cancer cells. Unfortunately, these drugs also exert cytotoxic effects on cells with a natural high turnover (epithelial cells, bone marrow cells, etc.), causing side effects such as hair loss, diarrhea, nausea and immunodepression which can be damaging to elderly and co-morbid patients (37). Response rates of chemotherapeutic treatment in endometrial carcinoma are usually modest, with short progression-free intervals of 4-6 months. The effect on survival is also limited, with median overall survival of 7 to 12 months (38). Anthracyclines, platinum compounds and taxanes are amongst the most heavily used drugs in endometrial carcinoma, with relatively poor response rates. Better response is observed with use of combined chemotherapeutic drugs than single agents alone (38). Commonly applied first-line adjuvant chemotherapeutic regimens include paclitaxel and carboplatin (14, 32), however the most optimal regimen has not yet been defined (45).

Genetic characterization of tumors has revealed several cancer-specific molecular pathways that potentially can be targeted through adjuvant treatment. As targeted therapies intervene with specific molecular mechanisms in cancer cells it is believed

that this approach may be more efficient than traditional drugs, while simultaneously reducing the damaging effect on normal tissue (38). The most common types of targeted therapies are small molecule inhibitors and monoclonal antibodies. Several of these drugs have been approved for clinical use, including bevacizumab for treatment of colorectal cancer and non-small cell lung cancer (46-48), temsirolimus for advanced renal cell carcinoma (49) and trastuzumab for human epidermal growth factor 2 (HER2) positive breast cancer (37). Currently there are no targeted therapies specifically approved for endometrial carcinoma (8, 50) but several candidates have been and are being explored in clinical trials, including phosphatidylinositol-4,5-biphosphate 3-kinase (PI3K)- and mammalian target of rapamycin (mTOR) inhibitors (51).

The ability of cells to avoid destruction by the immune system is important for formation of tumors, and is considered an emerging hallmark of cancer (52). Several clinical trials evaluating immunotherapeutic drugs in patients diagnosed with endometrial carcinoma are ongoing, including studies of the immune checkpoint inhibitor pembrolizumab (NCT02549209, NCT02630823, NCT02054806 (53)). Pembrolizumab was recently approved by the United States Food and Drug Administration for use in solid tumors with MMR deficiencies, and may thus be used to treat selected endometrial carcinoma patients where such aberrations have been confirmed (54).

1.1.4 Personalized medicine

Cancer has traditionally been treated with standardized protocols for all patients with similar diagnosis, a “one size fits all” approach which takes little consideration of disease heterogeneity and individual variations. Personalized oncology aims to select optimal therapeutic and preventive protocols for individual patients based on their specific molecular and genetic sequence variants – the right treatment for the right patient at the right time. However, in order to incorporate these principles into clinical practice it is necessary to identify specific biomarkers for disease characterization and for tailoring targeted therapies.

1.2 Cancer genetics and signaling pathways

1.2.1 Genetic alterations

Cancer is a genomic disease where changes in gene expression caused by molecular events such as mutations, gene amplifications, chromosomal rearrangements etc. may alter the genetic landscape of a cell. Tumor development is a dynamic, multistep process that is largely shaped by underlying mechanisms such as genomic instability. The genetic heterogeneity that follows is favourable for cancer evolution as it increases the chance that premalignant cells become malignant, and that some cancer cell clones survive the selection pressure in the microenvironment (52, 55). Heterogeneity exists between subclones of cells within a specific tumor (intratumor heterogeneity), but also between similar tumors from different patients as well as between different types of tumors (intertumor heterogeneity) (56). Additionally, as most tumors are capable of continuous evolution, the genetic landscape of metastatic lesions does not necessarily equal that of the primary tumor. Heterogeneity represents a major challenge for diagnosis, therapy and for development of new drugs, and longitudinal sampling and multiple sampling sites may thus be vital in order to better

understand the biology of tumors - including drug sensitivity and development of therapeutic resistance (57).

Several genomic cancer platforms (including The Cancer Genome Atlas (TCGA)) have been established in order to reveal the genetic landscape of different tumor types. In addition to profiling genetic aberrations in specific cancers, efforts are made to compare data from different cancer types in pan-cancer projects (58). Genomic analyses have revealed that some genes, including *Tumor protein 53* (*TP53), PTEN* and *Phosphatidylinositol-4,5 biphosphate 3 kinase catalytic subunit alpha (PIK3CA),* are commonly mutated in several tumor types, whereas others are specific for single cancers (59). Endometrial carcinoma has been classified into four distinct subgroups by the TCGA research network based on their genetic characteristics; Polymerase ε (POLE) ultramutated, microsatellite instability (MSI) hypermutated, copy number high, and copy number low (Table 2) (60). As the individual subgroups are associated with differences in survival and may be linked to treatment response, molecular subtyping should be considered in endometrial carcinoma patients. However, extensive genetic analyses are expensive and identification of surrogate markers (i.e mutS homolog 6 (MSH6) and mismatch repair endonuclease PMS2 (PMS2) for identification of patients with MMR deficiencies in the MSI subgroup) may facilitate the integration of molecular classification into clinical practice (27, 61, 62).

Table 2: TCGA classification of endometrial carcinomas

Subgroup:	Selected characteristics [60]:
POLE	- Very high number of mutations - Favorable PFS - Frequent mutations in *PTEN*, *PIK3CA* and *KRAS*
MSI	- High degree of mutations - Frequent *MLH1* promoter methylation - Low number of SCNAs - Few mutations in *TP53*
Copy number high	- High number of SCNAs - Frequent *TP53* mutations - Low degree of MSI - Poor PFS
Copy number low	- Low mutation rate - Microsatellite stable

KRAS proto-oncogene (KRAS), MutL homolog 1 (MLH1), Microsatellite instability (MSI), Progression-free survival (PFS), Phosphatidylinositol-4,5 bisphosphate 3-kinase catalytic subunit alpha (PIK3CA), Polymerase ε (POLE), Phosphatase and Tensin homolog (PTEN), Somatic copy number alterations (SCNA), Tumor protein p53 (TP53)

1.2.2 Signaling pathways

Cells can receive several types of stimuli through direct contact with neighbouring cells, from local mediators (paracrine signaling), hormones (endocrine signaling), or by self-stimulation (autocrine signaling). Activation of various extra- or intracellular receptors generates a non-linear signaling cascade that ultimately may affect several cellular processes, including proliferation, growth, metabolism and apoptosis (52, 55). Highly controlled transmission of signals is essential for normal cell function and for cells to respond appropriately to specific stimuli. Signaling pathway aberrations contribute to several of the “hallmarks of cancer” including self-sufficiency in growth

signals and insensitivity to anti-growth signals (52, 55). A variety of signaling routes are known to be dysregulated in cancer, including the PI3K/Protein kinase B (AKT)/mTOR pathway. When activated, this pathway leads to an increase in cell growth, protein synthesis and angiogenesis as well as inhibition of apoptosis (63). The tumor suppressor protein PTEN is a negative regulator of the PI3K/AKT/mTOR pathway. As a high number of patients with endometrial carcinoma (particularly endometrioid) have lost expression of PTEN, the PI3K/AKT/mTOR cascade is amongst the most commonly dysregulated signaling pathway in this type of cancer (54, 63). Other known signaling aberrations in endometrial carcinoma include overexpression of HER2 and dysregulation of the RAS/RAF/mitogen-activated protein kinase kinase (MEK) pathway (54, 63, 64).

1.3 Biomarkers

A biomarker is often defined as "a characteristic that is objectively measured and evaluated as an indicator of normal biologic processes, pathogenic processes, or pharmacologic responses to a therapeutic intervention" (65). Using biomarkers to identify high-risk disease and stratify patients to specific treatments may improve response rates and survival for a large number of cancer victims (8). However, the translation process from bench to bedside is both long and cumbersome, and only a limited number of biomarkers have been successfully implemented into clinical practice (66, 67). This is also the case in endometrial carcinoma (68).

Prognostic biomarkers

A prognostic biomarker predicts the natural course of disease, distinguishing tumors associated with a good outcome from those with a poor outcome irrespective of treatment. Although prognostic biomarkers are unable to predict the response to a specific therapy, they can be useful to identify high-risk patients that, in general, might benefit from more aggressive treatment (66, 69). Prognostic biomarkers may reduce overtreatment of patients with low-risk tumors who do not have added benefit

from extensive treatment, and also under-treatment of patients who otherwise would receive only standard care (66). Examples of prognostic biomarkers currently used in clinical diagnosis of cancer includes prostate-specific antigen (PSA) levels in serum of patients with prostate cancer and elevated serum CA125 level in ovarian cancer (70, 71). Although lagging behind other cancer types when it comes to clinical implementation of biomarkers, several prognostic markers have been rigorously investigated in endometrial carcinoma, including p53 (72), DNA ploidy (73-75), and the hormone receptors estrogen receptor α (ERα) (76-78) and progesterone receptor (PR) (78, 79). Additionally, new, potential prognostic markers such as L1 cell adhesion molecule (L1CAM) (80-84) are emerging.

Predictive biomarkers

Predictive biomarkers forecast the likely response to a specific therapeutic intervention. Such markers can be used to select which patients should receive a particular drug, or they can be applied in early stages of therapy to predict therapeutic response (69). Predictive biomarkers are implemented in several cancer types, including HER2 overexpression for allocation of trastuzumab in breast cancer, presence of the fusion gene *BCR-ABL* for assigning imatinib treatment in chronic myeloid leukaemia and *KRAS* mutational status for selecting patients eligible for epidermal growth factor receptor (EGFR) targeting drugs in colorectal cancer (70, 85). No biomarkers are currently clinically applied to predict the response to specific treatments in endometrial carcinoma, and identifying markers that can select the right patients and monitor their response would potentially increase the response rates of both new and existing drugs (86). Candidate markers include mutated PTEN for assignment of mTOR inhibitors and ERα/PR status for allocation of hormonal therapy (54).

Imaging biomarkers

Imaging biomarkers can be used for non-invasive monitoring of tumors to provide both anatomical and functional information, and can also be used to evaluate treatment response (69). Several imaging parameters have been reported as potential preoperative biomarkers in endometrial carcinoma, including tumor size, ultrasound echogenicity and vascularization, functional MRI parameters (i.e. apparent diffusion coefficient (ADC) -value and blood flow) and metabolic PET/CT parameters such as metabolic tumor volume (MTV) and total lesion glycolysis (TLG) (25, 87-90).

1.4 Preclinical cancer models

Preclinical research is a wide term, including a variety of techniques and model systems that can be applied to study specific hypotheses prior to testing in clinical trials. The development of cancer models is a dynamic process, involving a series of steps where the model system is defined, generated and improved based on the outcome of initial testing (91). The most common preclinical research systems are *in vitro* and *in vivo* models, where specific events are studied in laboratory- or animal studies. Computational *in silico* models are also of increasing interest, and can be used to generate predictions and hypotheses. There are many advantages with a computational approach, including low costs, high accuracy, and rapid estimation of specific interventions on a range of different parameters. Still, these model systems are developed from pre-existing data which often have been generated through multiple experiments and under different conditions (92). Hypotheses must therefore be validated experimentally.

1.4.1 *In vitro* models

In vitro experiments are typically performed in test tubes or cell cultures, and have been important model systems in preclinical cancer research for decades. Major advantages of *in vitro* models are that they provide a controlled system that is feasible for studies of molecular mechanisms, they are cheap and data can be acquired rapidly. However, there are several limitations. Cell cultures are often criticized for lacking stromal interactions, accumulating mutations, adapting to *in vitro* conditions, and failing to recapitulate the heterogeneity found in tumors *in vivo* (93, 94). Additionally, performing studies on single cell lines may lead to wrongful interpretation of data, as the response in individual cell lines could represent only a subgroup of tumors (or a subpopulation of cells within a tumor) and not the entire patient population. High-throughput screening of multiple cell lines may thus improve the comparability of results in *in vitro* experiments and clinical trials (94). Still, prior to clinical testing hypotheses generated from *in vitro* experiments should be validated in *in vivo* preclinical models.

1.4.2 In vivo models

Animal models are commonly used to generate hypotheses and perform initial studies before proceeding to testing in human patients. Compared to *in vitro* models, animal models provide a more natural environment for tumor establishment and disease evolvement. Cells grown *in vivo* are able to interact with normal tissue cells and components, and to undergo disease related events such as invasion, migration and dissemination. Additionally, many molecular and physiologic processes are similar in animals and humans (95). Animal models are amongst the best currently available systems for studies of human cancer. Still, results from preclinical experiments are often not reproducible in subsequent clinical trials (86, 96). It is thus important to establish clinically relevant animal models to explore the mechanisms of development, progression, invasion and metastasis of cancer in a systemic setting, and for preclinical studies of biomarkers and therapeutic response (97, 98).

1.4.3 Mouse models

The use of laboratory mice has a long tradition in medical research. Mice are small of size, easy to breed and have a short life-span, which makes them easy and relatively cheap to house, feed and handle (95, 99). In addition there is a high degree of similarities between the human and mouse genome which improves their suitability as model animals for human disease. Many different mouse models exist; however, not all models are equally applicable for all types of preclinical studies. Genetically engineered models (GEM) can be used to study genomic mutations in a systemic setting, and mutations that cause tumor development can be induced in germline cells by embryonic engineering or be selectively expressed in specific cells and tissues (95, 99-101). Isograft models are established by transplantation of cells or tissue between animals with the same genetic background, so there is no need to compromise the host immune system to enable tumor engraftment. Although a vast number of mechanisms involved in cancer establishment and progression can be studied using GEM and isografts, both tumor and stromal cells are of mouse origin - making them less optimal models for human tumor biology (99). Xenograft models are generated by transplantation of cells or tissue between individuals of different species, and thus allows for human material to grow in a murine host. Due to the human origin of xenografts, these models may be more representative of human cancer than GEMs and isografts.

The most commonly used xenograft models are derived from immortalized human cancer cell lines. However, long time culturing of cell lines *in vitro* may alter their genetic and functional characteristics, making cell line based mouse models less representative of clinical disease (86). PDX models are established by implantation of cell suspension or small pieces of tissue from a patient biopsy, and are believed to mimic human clinical cancer more closely than cell line based models because molecular and histologic characteristics of the human tumor are better preserved (86, 97, 102, 103). In spite of their advantages, PDX models are still not very widely used.

They are often time-consuming to establish (causing housing and keeping of PDX-models to be more costly), and requires more time spent on handling and observation compared to several other available preclinical models (103). Not all primary cells form tumors in mice, and cells that engraft may harbour more aggressive features than the cells that do not. PDX models have been generated for a variety of cancers, including breast, colorectal and renal cell cancer (86). It has been demonstrated that drug response (including both standard chemotherapeutic and targeted treatments) in PDX models is similar to the response in the corresponding human donor (86, 104), suggesting that the use of PDX models may improve the translational value between preclinical studies and clinical trials. Several mouse models of endometrial carcinoma have been generated (97, 105-110), including PDXs (111-113). In addition to primary tumors, endometrial carcinoma xenografts have also been established from both metastatic and recurrent lesions (111).

Xenograft models can be generated through implantation of tumor cells under the skin (subcutaneously) or in the organ of origin (orthotopically). The subcutaneous method is commonly applied as it is low cost, little time consuming, does not require surgical training, and tumor development is easy to monitor and measure (98, 102). Still, subcutaneous tumors are surrounded by a completely different microenvironment than the organ they usually would inhabit, and are not necessarily representative for tumors in the primary site. Tumors grown in such models will often lack infiltrative behavior, are less likely to metastasize, and may respond completely different to chemotherapy than tumors found in their original milieu (97, 98, 105, 114). In orthotopic models cancer cells are allowed to grow and metastasize under conditions more similar to those of the primary tumor, making it a more clinically relevant model (98, 102, 105, 114). However, generation of orthotopic models often requires surgical expertise, and monitoring of tumor development is more challenging in orthotopic compared to subcutaneous models (86, 98, 115). The latter problem can be overcome through use of *in vivo* imaging.

1.5 Advanced imaging modalities

Imaging can be used for non-invasive collection of information on the anatomy and physiology of tumors, and is applied in the diagnosis and follow-up of multiple cancer types; including gynaecological cancers. Although several hospitals have included imaging as part of the preoperative diagnostic work-up in endometrial carcinoma there is little agreement on when and how to use these imaging techniques, and different institutions and countries have varying practices (24, 25). Imaging of preclinical cancer models is also of great importance; especially as such models are becoming continuously more complex. The most common imaging alternatives available for clinical and preclinical purposes will be presented over the next sections, with a particular focus on imaging modalities relevant for endometrial carcinoma. Strengths and weaknesses of different imaging modalities are summarized in Table 3.

Table 3. Strengths and limitations of selected imaging modalities

Modality	Strengths	Limitations
US [116]	- Inexpensive - Fast - Doppler visualizes blood flow - Accurate measurement of tumor size	- Operator variability - Unsuited for brain and bone tumors - Difficult to detect metastatic disease
MRI [116, 117]	- High spatial resolution - Excellent soft tissue contrast - DCE-MRI provides information on microvasculature and circulation - No radiation	- Long acquisition time - High equipment costs

CT [116]	- High contrast - Good anatomical visualization	- Poor soft tissue contrast - Radiation
PET [116-118]	- High sensitivity, irrespective of depth - Functional imaging - Several available tracers	- High demands to facilities - Radiation - Expensive - Low spatial resolution - Little anatomical information
BLI* [116, 119, 120]	- Cost efficient - High throughput - High signal-to-noise ratio	- Requires reporter genes - No anatomical information - Semi-quantitative
NIRF* [121]	- Reporter genes not required - High throughput - Targeted fluorophore probes	- Tissue autofluorescence - Low signal-to-noise ratio - Limited penetration of tissue (≈ 1 cm)

Bioluminescent imaging (BLI), Computed tomography (CT), Dynamic contrast enhanced (DCE), Magnetic resonance imaging (MRI), Near-infrared fluorescent imaging (NIFR), Positron emission tomography (PET), Ultrasound (US). *Preclinical imaging only.

Ultrasound

Transvaginal ultrasound is commonly used in the initial diagnosis of endometrial carcinoma (24, 25). In ultrasound, sound waves over 20 MHz are generated by a transducer and directed towards the tumor and surrounding tissue. When hitting borders between tissues with different acoustic impedance, sound waves are reflected and the echo is used to generate a grayscale image (116). There are several advantages with ultrasound as it is a rapid, low-cost and minimally invasive procedure. Challenges include interobserver variation, poor image quality in obese

patients due to excess amounts of fatty tissue and difficulties in evaluation of disseminated disease. To the best of the author's knowledge, ultrasound has so far not been used to evaluate endometrial carcinoma in preclinical models.

Magnetic resonance imaging

MRI machines use superconducting magnets to generate a constant external magnetic field that affects the alignment of protons in the patient body. Radiofrequent pulses are turned on and off to interfere with the protons, and this activity results in an alternating electrical current that can be registered as an MR-signal. MRI is highly feasible for visualization of soft tissue, offering high resolution and excellent contrast in fat rich and water rich tissues (122). The main limitations of the MRI technique are that patients with metal implants or electronic medical implants (i.e. pacemakers) cannot be scanned due to the strong magnetic field, that scan-time is relatively long, and that the instrumentation is costly and requires high technical expertise (122). In endometrial carcinoma MRI is often considered to be the preferred pre-operative imaging method, and is performed to assess the depth of myometrial infiltration and invasion of cervical stroma (123). Standard MRI can also be used to estimate tumor size and to identify suspicious lymph nodes (123, 124). Paramagnetic substances (i.e. gadolinium) can be injected intravenously to enhance contrast (122), and is used to better delineate the tumor from the myometrium in endometrial carcinoma patients (24). Functional MRI techniques are increasingly explored, and may add valuable information regarding the physiological properties of a tumor. Dynamic contrast enhanced (DCE) MRI enables characterization of tumor microvasculature (123, 124), while diffusion weighted images (DWI) visualizes differences in tissue water diffusion as a measure of tissue cellularity which can be used to differentiate tumor from normal tissue (123). DCE-MRI and DWI parameters (low blood flow, low ADC-values, etc.) are reported to associate with features of aggressive endometrial carcinoma and reduced survival, and may serve as potential imaging biomarkers (125). The ability of MRI to detect tumor in preclinical models has been demonstrated in several cancers, including non-small-cell lung cancer (126). As far as

the author is aware, MRI has not previously been used for tumor imaging in endometrial carcinoma xenograft models.

Computed tomography

CT is an imaging technique using several narrow x-ray beams, which can be reconstructed into a three-dimensional image of patient anatomy (127). Images are created based on differences in x-ray absorption, illustrating different tissues by various shades of grey. Advantages of CT-technology include that it is relatively quick to acquire images compared to other modalities, it is applicable for most body systems, and it provides more details in deep tissues that may be less accessible by e.g. transabdominal ultrasound. CT also offers high resolution in tissues with good contrast, such as bone and lungs. The main disadvantages are that patients are exposed to radiation, and that intrinsic contrast in soft tissue is limited (116). CT is not commonly utilized as a single imaging modality in endometrial carcinoma due to poor diagnostic performance for local staging. However, CT is widely used to assess lymph node metastases or distant spread, either alone or combined with PET imaging allowing for attenuation correction and anatomical correlation in both clinical and preclinical applications.

Positron emission tomography

PET imaging is based on intravenous injection of short-lived radionuclides linked to biologically active elements, and the physiological information from the PET-scan can be combined with the anatomical information from CT or MRI-scans to create a fusion image (128, 129). PET may also be a valuable tool for assessment of adjuvant treatment effects, as metabolic changes in tumor tissue may be evident at an earlier stage than alterations in tumor volume (118, 129-131). However, PET images may be affected by factors such as signal spilling, non-tumor activity (i.e. signal from urinary system or intestine) and scanner properties that potentially may lead to over-or underestimation of tumor size and metabolic activity (131). Additionally, PET imaging is expensive, exposes the patient to radiation, and poses high demands to

facilities and staff. Several PET-tracers exist, each with specialized properties which make them feasible for different types of investigations. One of the most commonly used PET-tracers is ^{18}F- FDG. ^{18}F-FDG is imported into cells by glucose transporting molecules and phosphorylated by hexokinase, thereby trapping it inside the cell (118). High glucose uptake is a common feature of cancer cells, which makes ^{18}F-FDG a feasible tracer for both qualitative and quantitative measures. Another available PET-tracer is ^{18}F- FLT. ^{18}F- FLT enters the cell by both passive diffusion and active nucleoside transporters, and gets trapped intracellularly after being phosphorylated by thymidine kinase 1 during cell cycle S-phase (132). ^{18}F- FLT PET takes advantage of the increased cell proliferation that is characteristic of many cancers. Several molecular parameters can be evaluated based on PET scans to elucidate inherent properties of the tumor. Standard uptake value (SUV) is the measured activity in tissue divided by injected activity per unit body weight, and describes the uptake of tracer in tumor. Measures of metabolic tumor burden includes MTV and TLG (133). In endometrial carcinoma, PET/CT imaging using ^{18}F-FDG as tracer is reported to be a valuable tool both for detection of metastatic lymph nodes prior to surgery and for identification of recurrent disease (134). PET/CT may also be used in preclinical applications, and has been successfully employed in studies of lung cancer and melanoma models (135, 136) . However, there are no previous reports of PET/CT imaging of endometrial carcinoma models.

Optical molecular imaging

OMI is applicable for real-time visualization of tumor growth and metastasis, as well as observation of treatment effects *in vivo* (121, 137). The technique is non-invasive, does not require radiant substances, is relatively low cost and the equipment is easy to operate. However, there are also some disadvantages with OMI. Due to the poor penetration of photons in tissue there is a depth restriction which makes it less applicable in deep viscera. Spatial resolution is low due to the amount of light scattering in biological tissue (121), and the anatomy is difficult to comprehend. One

OMI modality commonly used for research purposes is BLI. The firefly luciferase enzyme catalyzes the transformation of D-luciferin to oxyluciferin in the presence of O_2, Mg^{2+}, and adenosine triphosphate, yielding the emission of light as well as byproducts such as adenosine monophosphate, CO_2, and pyrophosphate (138, 139). BLI is a high-throughput technique that is relatively easy to conduct. As normal mammalian cells do not express luciferase, BLI offers a high signal-to-noise ratio and excellent sensitivity (120, 121). The major limitation is that cells need to be transfected with a luciferase expressing vector for BLI to be eligible (139), and this imaging technique is thus not applicable for clinical use. However, BLI has been demonstrated as a valuable tool for visualization of luciferase positive tumor cells in several cancer models, including endometrial carcinoma (97, 107, 110).

Another OMI modality that is feasible for *in vivo* studies is NIRF. Fluorescent molecules are excited by light of specific wavelengths, and emit light with a different wavelength when returning to their ground state (137, 139, 140). NIRF is not visible to the human eye, and highly sensitive cameras or detectors are needed to register the emitted light. Fluorescent *in vivo* imaging can be challenging due to high degree of tissue autofluorescence and low signal-to-background ratios (121). Photons can be scattered or absorbed by surrounding tissue, reducing the amount of signal that is received by the detector. Light with wavelengths above 1100 nm will be almost completely absorbed by water (which is abundant in most tissue), while light with wavelengths in the range of 400-500 nm will be absorbed by molecules such as hemoglobin and melanin. By using fluorescent molecules that emit light in the near-infrared range (700-900 nm) some of these challenges can be overcome, as infrared light is less absorbed and enables better tissue penetration (121, 139-141). Although there is currently little tradition for using optical imaging in clinical settings, image-guided surgery using fluorescent dyes (i.e. indocyanine green) is now being explored and represents a promising tool for detection of sentinel lymph nodes in several gynecological cancers – including endometrial carcinoma (142). NIRF imaging has been demonstrated to visualize tumor in preclinical models of several cancers,

including acute myeloid leukemia (AML) and epithelial ovarian cancer (143, 144). NIRF imaging of endometrial cancer mouse models has not yet been reported.

2. Aims of the project

2.1 Background

Endometrial carcinoma is the most common pelvic gynaecologic malignancy, and the incidence is expected to increase in the future due to an ageing and more obese population. Prognosis is good for most patients, but for those who experience recurrent disease the outcome is often poor. There is a need for identification and validation of new biomarkers for endometrial carcinoma, both to improve risk-stratification and to tailor treatment for individual patients. Establishment of robust and clinically relevant preclinical models is essential in order to increase the translational success rate from preclinical research to clinical trials. Implementation of non-invasive small animal imaging techniques is also vital, as these methods allow continuous monitoring of disease development and response to treatment *in vivo*.

2.2 Overall aim

The overall aim of this project was to explore potential biomarkers in endometrial carcinoma, and to develop relevant preclinical model systems that may be used for studies of new biomarkers and anti-cancer therapies.

2.3 Specific aims

Paper I: The aim of this study was to establish cell line based and patient derived orthotopic mouse models of endometrial carcinoma, and to evaluate the feasibility of selected small animal imaging modalities with regards to monitoring of tumor growth and metastatic spread.

Paper II: We aimed to develop an NIRF imaging protocol that can be used for longitudinal monitoring of tumor growth and treatment response in orthotopic endometrial carcinoma PDX models.

Paper III: The aim of this study was to validate ASRGL1 as a postoperative prognostic biomarker in endometrial carcinoma, and to explore the expression of ASRGL1 in precursor lesions, primary tumors and metastases.

Paper IV: We aimed to evaluate the ability of ASRGL1 protein expression in preoperative samples to identify endometrial carcinoma patients with high risk of aggressive disease and poor survival prior to surgery.

3. Material and methodological conciderations

3.1 Patients and clinical samples

3.1.1 Patient series

Patients treated for endometrial carcinoma at HUS were prospectively included between March 2001 and October 2015. HUS is the referral hospital for Hordaland County, covering approximately 10% of the Norwegian population. The HUS cohort is regarded a population-based patient series as both incidence rates, patient- and disease characteristics for this region are representative compared to the entire population in Norway (3). In addition to the patients collected at HUS, nine other hospitals in Norway, Sweden and Belgium have contributed with samples and data from prospectively included endometrial carcinoma patients in the Molecular Markers in Treatment of Endometrial Cancer study (MoMaTEC, NCT0059884). All patients have given written informed consent prior to inclusion, and biological samples, clinicopathological information and follow-up data have been collected at the respective centres. The biobank contains tissue samples from preoperative curettage, hysterectomy specimens, and metastatic lesions, and tissue samples were snap-frozen in liquid nitrogen and/or fixed in formalin. Clinicopathological information including age, histological type, histological grade and follow-up data was retrieved from medical records. A series of patients diagnosed with CAH has also been collected and clinical information retrieved as for endometrial carcinoma patients. As surgical treatment of CAH is presumed to be curative, these patients have no follow-up data. An overview of biological samples and applied methods is shown in Figure 3.

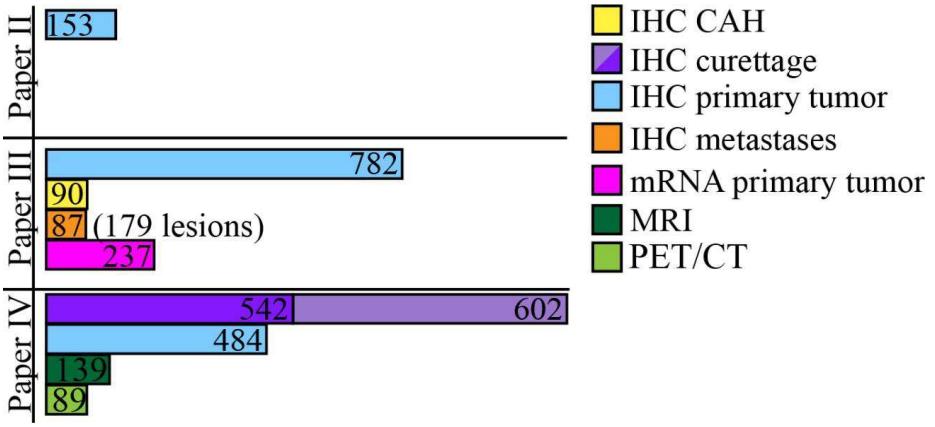

Figure 3. Overview of patient samples and methods used in **papers II**- **IV**. Numbers in bars represent included patients for each analysis. Dark purple: curettage samples from patients treated at Haukeland University Hospital. Light purple: curettage samples from patients treated at other hospitals. Abbreviations: complex atypical hyperplasia (CAH), immunohistochemistry (IHC), magnetic resonance imaging (MRI), positron emission tomography/computed tomography (PET/CT).

3.1.2 Tissue microarrays

Formalin fixed paraffin embedded (FFPE) tissue was used to generate tissue microarrays (TMA). The area with the highest tumor cell content was identified on hematoxylin and eosin stained slides by an experienced gynecologic oncologist, and a custom made precision instrument (Beecher instruments, Silver Spring, MD, USA) was used to punch out tissue cylinders (0.6 mm) from the donor block before mounting in a recipient paraffin block (145). Three tissue cylinders were collected from CAHs, curettage specimens and primary tumors, and one tissue cylinder from metastatic lesions. For patients treated at other centers than HUS, only tissue from curettage samples was available for TMA processing.

3.1.3 Immunohistochemistry

In this project we used IHC to evaluate protein expression in FFPE tissue collected from endometrial carcinoma patients and xenograft models. With the exception of ASRGL1 staining, which was performed by automated IHC using a LabVision Autostainer 480S (Thermo Fisher Scientific, Runcorn, UK), all immunohistochemical staining was performed at our facility using a standardized protocol. Tissue sections were dewaxed in xylene and rehydrated in graded ethanol series prior to microwave boiling for 15 minutes in target retrieval buffer (Tris EDTA – pH 9 or Citrate – pH 6). Slides were covered with peroxidase block for 8 minutes before application of primary antibody. Specifications for the different primary antibodies are listed in Table 4. For all antibodies a secondary horse radish peroxidase conjugated agent (anti-mouse or anti-rabbit) was added for 30 minutes and diaminobenzidine applied for 8 – 10 minutes before counterstaining with hematoxylin.

Table 4: Antibodies used for immunohistochemistry

Target	Primary antibody	Buffer	Dilution	Incubation
ASRGL1	HPA029725 [146, 147] *Atlas antibodies, Sweden*	Citrate pH 6	1:375	30 min
	AMAb90907 *Atlas antibodies, Sweden*	Citrate pH 6	1:1000	30 min
EpCAM	D9S3P *CST, USA*	Citrate pH 6	1:200	60 min
ERα	HC-20* *Santa Cruz, USA*	Tris EDTA pH 9	1:400	60 min
	SP-1* *Thermo Scientific, USA*	Tris EDTA pH 9	1:400	60 min
	M7047 [77, 148] *Dako, Denmark*	Tris EDTA pH 9	1:50	30 min
PR	M3569 [79] *Dako, Denmark*	Tris EDTA pH 9	1:150	30 min

*Used to stain tissue samples from mice xenografted with human endometrial carcinoma cells. *Asparaginase-like protein 1 (ASRGL1), Cell signalling technology (CST), Epithelial cell adhesion molecule (EpCAM), Estrogen receptor alpha (ERα), Ethylenediaminetetraacetic acid (EDTA), Progesterone receptor (PR)*

IHC staining of slides was assessed by standard light microscopy, evaluating the staining of epithelial tumor cells. For each patient a staining index (SI) was calculated by multiplying staining intensity (0-3) and area of positive stained tumor cells (1 = <

10%, 2 = 10 – 50%, 3 = > 50%). Cases were ranked based on SI for statistical analyses, and categorized into tertile/quartile groups according to frequency distribution and subgroup size. Groups with similar survival were combined. Table 5 lists the cut-offs for IHC biomarkers included in this project.

Table 5: Biomarker cut-off, immunohistochemistry

	SI defined as loss/low expression	**SI defined as high expression**
ASRGL1	0 – 1	2 – 9
EpCAM	0 – 4	6 – 9
ERα	0 – 3	4 – 9
PR	0	1 – 9

Asparaginase-like protein 1 (ASRGL1), Epithelial cell adhesion molecule (EpCAM), Estrogen receptor alpha (ERα), Progesterone receptor (PR), Staining index (SI)

3.1.4 Ribonucleic acid (RNA) microarray analysis

Tissue samples were collected during surgery, snap-frozen in liquid nitrogen and stored at -80°C. Hematoxylin and eosin stained slides were used to identify areas with high tumor cell content (preferably > 80%, minimum 50% tumor purity). Extraction of RNA was performed using the RNeasy Mini Kit (Qiagen, Hilden, Germany). The quality of RNA extracts was assessed using a Nanodrop 1000 spectrophotometer (Thermo Scientific, Waltham, MA, USA) and an Agilent 2100 Bioanalyzer (Agilent, Santa Clara, CA, USA). Samples were hybridized to Agilent Whole Human Genome Microarrays 44k according to the manufacturers' instructions, and subsequently scanned by the Agilent Microarray Scanner Bundle. Log 2 transformation and quantile normalization of data was performed. Expression data was analysed using the J-Express software (Molmine, Bergen, Norway). In **paper III** patients were ranked by *ASRGL1* mRNA expression and grouped in quartiles. The lowest quartile of patients was used as cut-off for survival analyses.

3.1.5 Approvals

This study has been approved according to Norwegian legislation, including the Norwegian Data Inspectorate, Norwegian Social Sciences Data Services and Western Regional Committee for Medical and Health Research Ethics (REK 2009/2315, REK 2014/1907, REK 2018/594).

3.2 Pre-operative imaging

Preoperative MRI and ^{18}F-FDG PET/CT have been routinely performed in endometrial carcinoma patients treated at HUS since 2009 and 2011, respectively. In **paper IV** selected MRI and ^{18}F-FDG PET parameters were related to ASRGL1 expression in pre-operative curettage.

3.2.1 Magnetic resonance imaging

MRI of patients was performed according to a standardized protocol, using a whole-body 1.5-T MRI system (Siemens Avanto running Syngo v. B17, Erlangen, Germany) with a six-channel body coil (149, 150). The largest tumor diameter was identified and measured in three planes (a, b, c). Tumor volume was estimated as following: Tumor volume = (a x b x c)/2 (151). T1-weighted images were acquired before and after intravenous injection of contrast (Dotarem, Guerbet, 0.1 mmol gadolinium/kg bodyweight). DWI of the pelvis was performed by an axial two-dimensional echo planar imaging sequence with b-values of 0 and 1000 s/mm^2, and used for generation of ADC-maps. DCE-MRI was acquired with 12 axial slices and a temporal resolution of 2.5 s Blood flow and transfer constant from extravascular extracellular space to blood were calculated using the extended Tofts kinetic model with a standardized arterial input function (125)

3.2.2 PET/CT imaging

Patients were fasting 6 hours prior to PET/CT scan. PET/CT images were acquired using a Biograph 40 True Point scanner (Siemens, Erlangen, Germany), covering an area from the meatus of the ear to the proximal thigh. ^{18}F-FDG was injected intravenously 60-120 minutes before starting the CT scan. Low-dose CT (120 kV, 50 reference mAs) was performed for attenuation correction, and static PET images were collected at intervals of 3 minutes per bed position. Maximum standard uptake value ($SUV_{max)}$ was measured in the tumor, and a volume of interest (VOI) was generated including voxels with SUV > 2.5. The VOI was used to estimate mean standard uptake value (SUV_{mean}) and MTV. TLG was calculated as following; TLG = SUV_{mean} x MTV (133, 152).

3.3 Cell studies

In this PhD-project we have used endometrial carcinoma cell lines and primary tumor cells to explore the expression of potential biomarkers and to establish orthotopic mouse models (**paper I** and **II**).

3.3.1 Maintainance of cell cultures

Endometrial carcinoma cell lines were grown at 37°C in a humidified atmosphere, with 5% CO_2. Table 6 contains an overview of growth mediums and supplements used to maintain cell cultures in the different studies.

Table 6: Medium and supplements for cell cultures

Cell line	Paper	Growth medium	FBS%	Supplements
AN3CA *ATCC, USA*	II	EMEM *Lonza, Switzerland*	10	100 IU/ml penicillin 100 µg/ml streptomycin 2 mM L-glutamine
Hec1B *ATCC, USA*	II	EMEM *Lonza, Switzerland*	10	100 IU/ml penicillin 100 µg/ml streptomycin 2 mM L-glutamine
Ishikawa *Sigma-Aldrich, USA*	I, II	EMEM *Lonza, Switzerland*	5	100 IU/ml penicillin 100 µg/ml streptomycin 2 mM L-glutamine 1% non-essential amino acids
RL95-2 *ATCC, USA*	II	DMEM Ham's F-12 (1:1)	10	100 IU/ml penicillin 100 µg/ml streptomycin 2 mM L-glutamine 2.0 g/L sodium bicarbonate 0.005 mg/ml insulin 1% Hepes
Primary tumor cells	I, II	EMEM *Lonza, Switzerland*	10	100 IU/ml penicillin 100 µg/ml streptomycin

American type culture collection (ATCC), Dulbecco's modified Eagle medium (DMEM), Eagle's minimum essential medium (EMEM), Fetal bovine serum (FBS), International units (IU),

3.3.2 Cell transfection

Transfection refers to the introduction of exogenous DNA into a cell. Transfection can be transient, or it can be stable by incorporating the new DNA into the recipient's genome. It is common for the transferred DNA-sequence to contain a selection marker, such as an antibiotic resistance gene, or a reporter gene (i.e. green fluorescent protein) to be able to distinguish successfully transfected cells from wild type cells. In our studies we have used Ishikawa (**paper I** and **II**) and Hec1B cells (**paper II**) that have been stably transfected with a luciferase expressing (luc+) vector (153, 154). Transfected cells ($Hec1B^{luc+}$ and $Ishikawa^{luc+}$) were selected using 1 μg/ml puromycin (Sigma-Aldrich, St. Louis, MO, USA). Luciferase activity was confirmed by *in vitro* BLI using an Optix MX3 Time-Domain Optical Imager (ART Inc. Saint-Laurent, QC, Canada) 10 minutes after addition of 2.5 mg/ml D-luciferin (Promega, Madison, WI, USA).

3.3.3 Flow cytometry

Flow cytometry is a technology that allows simultaneous measurement of multiple physical characteristics of cells, such as size, granularity, or expression of proteins. In **paper II** the expression of four potential NIRF-imaging targets was explored in four endometrial carcinoma cell lines (AN3CA, Hec1B, Ishikawa and RL95-2) by flow cytometry. These four proteins (Activated leukocyte cell adhesion molecule (ALCAM), EpCAM, Insulin-like growth factor 1 receptor alpha (IGF1Rα), and L1CAM, Table 7) were all reported to be overexpressed or associated with poor prognosis in patients diagnosed with endometrial cancer (82, 84, 155-160). Cells were washed twice with 1% bovine serum albumin (BSA)/phosphate buffered saline (PBS) before incubation with antibody for 30 minutes on ice protected from light. Cells were washed again, and resuspended in PBS. Samples were analyzed using an Accuri™ C6 (BD Biosciences, San Jose, CA, USA) flow cytometry system, and results were processed using CFlow Sampler Analysis 1.0 software.

Table 7. Specifications of antibodies used for flow cytometry in paper II.

Target	Clone	Conjugate
ALCAM	3A6 *BD Biosciences, USA*	PE
EpCAM	EBA-1 *BD Biosciences, USA*	PE
IGF1Rα	1H7 *BD Biosciences, USA*	PE
L1CAM	03 *Sino Biological Inc., China*	PE

Activated leukocyte cell adhesion molecule (ALCAM), Epithelial cell adhesion molecule (EpCAM), Insulin-like growth factor 1 receptor alpha (IGF1Rα), L1 cell adhesion molecule (L1CAM), phycoerythrin (PE).

3.3.4 Antibody conjugation

For *in vivo* fluorescence imaging in **paper II** an anti-human EpCAM antibody (MCA1870EL, clone VU-1D9; BioRad, Hercules, CA, USA) was conjugated to AF680 using the SAIVI Rapid Antibodies Labeling Kit (Invitrogen, Waltham, MA, USA) as described by the supplier. Protein concentrations and degree of labeling was determined using a Nanodrop 1000 spectrophotometer (Thermo Scientific, Waltham, MA, USA).

3.3.5 Proliferation and viability assays

In **paper II**, proliferation and viability of wild type cells and cells exposed to an anti-EpCAM antibody (MCA1870EL) was compared. Cell proliferation was assessed

using the CellTiter 96® AQueous One Solution Cell Proliferation Assay (Promega, Madison, USA) as described by the supplier. All experiments were performed in triplicates. Proliferation was assessed by measuring absorbance at 490 nm one hour after addition of 20 µl of substrate. Absorbance was recorded using a TECAN Magellan Sunrise plate reader and TECAN Magellan software version 6.3 (both Tecan; Männedorf, Switzerland). Apoptosis was evaluated by flow cytometry following 15 minutes of Annexin V/propium iodine staining (Thermo Fisher Scientific, Waltham, MA, USA).

3.4 Animal studies

All animal studies have been approved by the Norwegian State Commission for Laboratory Animals (FOTS ID 4036 - **Paper I** and FOTS ID 6735 - **Paper II**) and have been conducted according to the European Convention for the Protection of Vertebrates Used for Scientific Purposes. Female non-obese diabetic severe combined immune deficiency gamma (NOD/SCID IL2rγ^{null} (NSG)) mice were used for all animal studies. Mice were kept under pathogen-free conditions in individually ventilated cages, with a maximum of 5 animals per cage. Environmental conditions were highly controlled, with constant temperature of 21°C, 50% relative humidity, and 12 hours day/night schedule. Animals had *ad libitum* access to food and water. In **Paper II** animals were fed a chlorophyll-free diet (2018S Teklad Global 18% Protein Rodent Diet, Envigo, Cambridgeshire, UK or D10001, Research Diets Inc., New Brunswick, NJ, USA) to reduce background signal in fluorescent images. When developing clinical signs of disease, manifested by 10-15% weight loss, abdominal distention, lethargy or ruffled fur, animals were anesthetized and sacrificed by cervical dislocation. Tissue samples were collected during necropsy, and fixed in formalin or snap-frozen in liquid nitrogen. Full sections were prepared from FFPE-tissue and stained with hematoxylin and eosin for histological examination.

3.4.1 Generation of orthotopic xenograft models

Mice were anesthetized by i.p. injection of tribromoethanol (250 mg/kg) dissolved in 2 methyl-2 butanol and diluted in sterile water to a final concentration of 12.5 mg/ml. Prior to surgery 0.1 mg/kg buprenorphine was injected s.c. for analgesia. Abdominal fur was removed and the skin disinfected before placing the animal in dorsal recumbency on a heating pad. A 1 cm long incision was made in the caudal abdomen, and the left uterine horn exteriorized. The uterine lumen was sealed by a temporary ligature to prevent vaginal leakage prior to injection of tumor cells (typically 10^6 cells per mice) suspended in BD Matrigel Basement Membrane Matrix (BD Biosciences, San Jose, USA) as demonstrated in Figure 4. After the cell suspension polymerized, the ligature was removed and the uterine horn replaced. Skin and musculature were closed separately using absorbable sutures. Animals were rehydrated by s.c. injection of saline before being placed under a heating lamp and observed until full recovery. Buprenorphine was administered s.c. for post-operative analgesia.

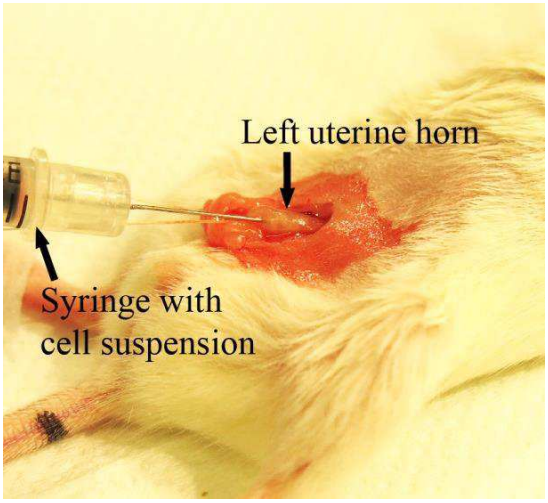

Figure 4. Generation of orthotopic endometrial carcinoma xenograft. The left uterine horn was exteriorized and sealed off by a temporary ligature. A needle was inserted through the uterine wall, and cell suspension injected into the uterine lumen.

In **Paper I** the human origin of uterine xenograft tumors was confirmed by IHC. 4 µm thick full sections were made from FFPE-tissue and stained for human ERα (SP-1). Species specificity of the antibody was validated by comparison with sections stained with a non-species specific ERα antibody (HC-20). IHC staining was performed as described in section 3.1.3 and Table 4.

3.4.2 Patient derived xenografts

Fresh tumor tissue was collected during hysterectomy of endometrial carcinoma patients treated at HUS, and kept on ice until further processing. Tissue samples were manually dissociated and filtered through a 40 µm pore filter (Fisher Scientific, Hampton, NH, USA). Cells were centrifuged at 900 rpm for 4 minutes, before resuspension in BD Matrigel Basement Membrane Matrix. Orthotopic implantation of cells was performed as described in the previous section. Mice (P0 generation) were euthanized when developing clinical signs of disease, and cell suspension prepared from the uterine tumor before re-implantation in a new generation of mice

(P1). This process was continued in each generation to maintain the PDX models. Information regarding the individual PDX models is found in Table 8.

Table 8. Background of endometrial carcinoma PDX-models

PDX nr	Patient age (yrs)	Histologic subtype/grade (donor tumor)	Paper	Generation (P)
1	69	Grade 3 endometrioid endometrial carcinoma	I, II	P0-P2
2	75	Serous endometrial carcinoma	II	P1
3	65	Grade 1 endometrioid endometrial carcinoma	II	P1
4	58	Grade 3 endometrioid endometrial carcinoma	II	P0

3.4.3 *In vivo* treatment study

In **paper II** 24 mice were orthotopically implanted with short-term cultured primary tumor cells (PDX 4, Table 8). After four weeks (day 28), treatment with paclitaxel (12 mg/kg i.p. twice weekly, n = 8 mice), trastuzumab (10 mg/kg i.p. once weekly, n = 8 mice) or vehicle (n = 8 mice) was initiated. *In vivo* tumor growth was monitored using EpCAM-AF680 NIRF imaging pre- (day 26) and post treatment (day 55). ^{18}F-FDG PET/CT imaging was performed on day 47. Animals were euthanized on day 57 or prior to this if developing clinical signs of disease. After euthanasia, uterine tumors were weighed and tissue samples collected and fixed in formalin.

3.5 Small animal imaging

Several small animal imaging modalities exist, and we have used BLI, NIRF, MRI and PET-CT to detect and monitor tumor growth in our endometrial carcinoma xenograft models. Figure 5 demonstrates the different imaging techniques used in this PhD-project.

3.5.1 Optical imaging

Bioluminescence

BLI was performed to monitor tumor growth in mice orthotopically implanted with endometrial carcinoma cell lines (Ishikawa^{luc+} – **Paper I** and **II** or Hec1B^{luc+} – **Paper II**). Images were obtained using an In-Vivo FX PRO molecular imaging system (Carestream Health Inc., Rochester, NY, USA, **Paper I**) or an Optix MX3 Small Animal Molecular Imager (ART Inc., Saint-Laurent, QC, Canada, **Paper II**). Independent of the type of scanner, mice were injected i.p. with D-luciferin (150 mg/kg) 10 minutes prior to imaging. Animals were anesthetized with 3% isoflurane (IsoFlo vet.; Zoetis, Helsinki, Finland) for induction and 1-2 % for maintenance. BLI was performed weekly, and images were analyzed using Carestream MI software (Standard Edition, v.5.0.6.20, Carestream Health Inc., **Paper I**) or Optix OptiView software (**Paper II**), and total bioluminescent signal was measured after manually defining a region of interest (ROI) of the abdomen and thorax. Mice that failed to develop bioluminescent signal were excluded from the studies. *Ex vivo* imaging of organs was performed to confirm the origin of the bioluminescent signal.

Near Infrared Fluorecent Imaging

NIRF imaging was applied to monitor disease progression and therapeutic response in endometrial carcinoma mouse models in **Paper II**. Mice were injected intravenously with 50 – 75 µg EpCAM-AF680 24 hours before imaging. Fur was

removed immediately prior to imaging, and the bladder was manually emptied. NIRF imaging was performed using the Optix MX3 Time-Domain Optical Imager (ART Inc., Saint-Laurent, QC, Canada), λ_{ex} = 670 nm, λ_{em} = 700 LP, raster scan points 1.5 mm apart. In the cell line based model ROIs containing the abdomen and thorax were used for measuring of fluorescent signal in *in vivo* images, and ROIs surrounding each organ in *ex vivo* images. For measurement of fluorescent signal in PDX models the image with the largest tumor area was identified for each mouse. A ROI was drawn around the tumor, and subsequently applied to all individual images from the same mice. Imaging data was analysed using the Optix OptiView software (version 2.02; ART Inc., Saint-Laurent, QC, Canada). A tumor-free mouse injected with a corresponding dose of EpCAM-AF680 was imaged as control.

3.5.2 Magnetic resonance imaging

In **Paper I** MRI was used to visualize uterine tumor in the cell line based orthotopic endometrial carcinoma mouse model (Ishikawa^{luc+}). Images were obtained by a 7T horizontal-bore preclinical scanner (Pharmascan 70/16, Bruker Corporation, Germany), using a 40 mm mouse body quadrature volume resonator in a single-coil configuration. 3% sevoflurane was used for anesthesia during imaging. A T_2-weighted rapid acquisition with relaxation enhancement (RARE) sequence (Echo time/repetition time (TE/TR) = 36/4300 ms, 2 averages, matrix 256 x 256, field of view (FOV) 3.2 x 3.2, 1 mm slice thickness) was used for tumor identification and estimation of tumor size. T_1-weighted RARE sequences (TE/TR = 9/1000 ms, 4 averages, matrix 256 x 256, FOV 3.2 x 3.2 cm, 1 mm slice thickness) were employed to obtain images before and after i.v. injection of a gadolinium based contrast agent (Dotarem, Guerbet, USA)(0.1 mmol/kg). DWI (TE/TR = 24.6/3100 ms, 2 averages, matrix 128 x 128, FOV 3.2 x 3.2 cm, 1 mm slice thickness, and 3 diffusion directions with b-values of 100, 200, 400, 600, 800 and 1000 s/mm^2) were used to generate ADC-maps.

3.5.3 PET/CT imaging

Both cell line based- and PDX-models were monitored by PET/CT during disease progression and/or when developing signs of clinical disease. ^{18}F-FLT (**Paper I**) or ^{18}F-FDG (**Paper I** and **II**) were used as tracers. Integrated PET/CT whole-body images were collected using a nanoScan PC PET/CT (Mediso Medical Imaging Systems Ltd, Budapest, Hungary), with spatial resolution 800 μm (PET) and 30 μm (CT). PET detectors consisted of LYSO crystals, and acquisition was performed in 1:5 coincidence and normal count mode. With exception of the PDX treatment study in **paper II** where mice were fasted overnight before PET/CT imaging, scans were obtained without prior fasting. Two mice were imaged simultaneously using a dual mouse bed with integrated system for heating and anesthesia. Animals were anesthetized with 3% sevoflurane (SevoFlo vet.; Zoetis, Parsippany, NJ, USA) during imaging. ^{18}F-FDG was injected i.v. when starting the PET-scan. Total acquisition time was 1 hour, and a static image was reconstructed from the last 30 minutes. ^{18}F-FLT was injected i.v. 30 minutes prior to scanning, and the duration of the scan was 30 minutes. In both cases, helical whole-body CT scans (50 kVP tube energy, 300ms exposure time, 720 projections, binning 1:4) were acquired for anatomical orientation and attenuation correction of PET images. Reconstruction of PET images were performed using the Tera-Tomo 3D ordered subset expectation maximization algorithm, correcting for depth-of-interaction, radionuclide decay, randoms, crystal dead time, detector normalization and attenuation. Detector coincidence mode was 1:3, 4 interations and 6 subsets, no filtering. CT images were reconstructed using RamLak filter. Automatic co-registration of PET- and CT images was performed, and voxel size for reconstructed images was 0.25x0.25x0.25 mm^3 for CT and 0.4x0.4x0.4 mm^3 for PET. InterView Fusion software v. 2.02.055.2010 (Mediso Ldt., Budapest, Hungary) was used for further analyses of imaging data. SUV was calculated as: $SUV = C_{PET}(T)/(ID/BW)$, where $C_{PET}(T)$ equals the measured activity in tissue, ID the injected dose (kBq), and BW the body weight of the animal (kg) . A VOI with radius 1.5 mm was defined in the nuchal musculature, and SUV_{mean} of this VOI used as reference tissue to identify presumed tumor tissue with SUV ratios of > 2 (^{18}F-

FLT, **Paper I**) and > 6 (^{18}F-FDG, **Paper I**). In **Paper II** voxels with SUV values > 2.5 were included in measurements of SUV_{mean} and MTV. Semi-automatically VOIs were drawn for both primary uterine tumors and presumed metastases, and MTV and SUV_{mean} calculated. TLG (^{18}F-FDG scans) was estimated as TLG = FDG-SUV_{mean} x MTV, and a similar parameter (FLT-SUV_{mean} x MTV) based on the same equation was calculated for ^{18}F-FLT –scans as a measure of total number of metabolically active tumor cells.

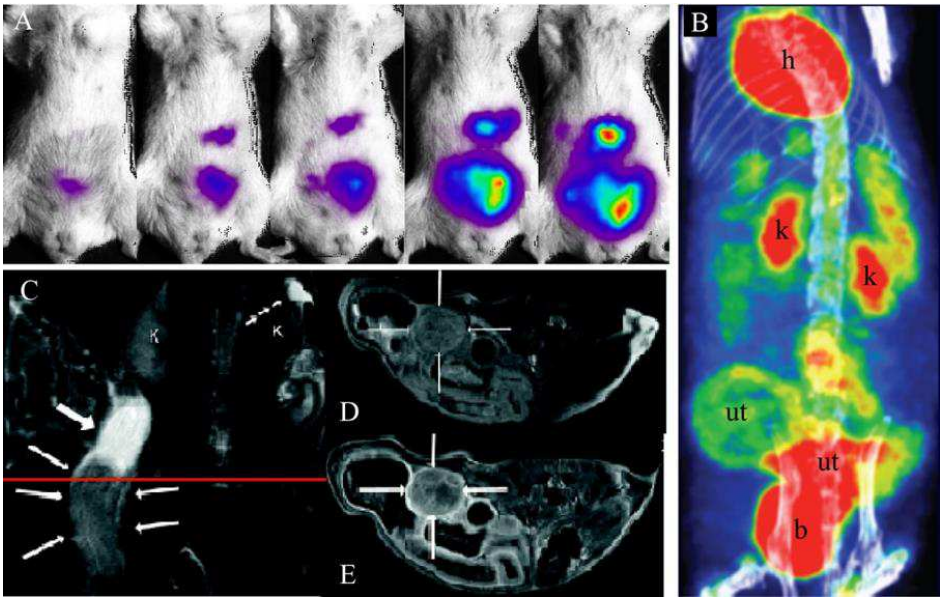

Figure 5. ***In vivo*** **small animal imaging.** Optical imaging enables monitoring of tumor growth over time, here demonstrated by bioluminescent imaging of the same mouse over five consecutive weeks (A). PET/CT visualizes uterine tumors, in this case using ^{18}F-FDG as tracer (B). Uterine tumor is also detectable by MRI, on both T2-weighted (C) and T1-weighted images before (D) and after (E) injection of contrast. Thin arrows point out the uterine tumor, while the thick arrow is directed at intrauterine fluid that has accumulated cranial to the tumor. Bladder (b), heart (h), kidney (k), uterine tumor (ut). Figure adapted from Haldorsen et.al (161).

3.6 Statistics

Categorical variables were analysed using the Pearson χ^2 test or Fisher's exact test, while continuous variables were evaluated using the Mann-Whitney U test. The Kaplan-Meier method was used to generate disease-specific survival curves, and survival between groups was compared using the log-rank test (Mantel-Cox). Date of primary surgery was used as entry date, and time of death due to endometrial carcinoma defined as endpoint. Patients who were alive on the last day of follow-up or died from other causes were censored. In *in vivo* mouse models, time of implantation was used as entry date, and time of sacrifice as endpoint. The prognostic impact of ASRGL1 on survival (corrected for other variables with known prognostic impact) was evaluated by the Cox proportional hazard regression model, and the ability of ASRGL1 to predict lymph node metastasis evaluated by binary logistic regression. Kappa value (κ) or intraclass correlation coefficient (ICC) was calculated to assess interrater reliability of immunohistochemical scoring in biomarker studies. ICC estimates were calculated by a single rater absolute agreement, two-way random effects model. Pearson correlation was used to evaluate the relationship between bioluminescent and fluorescent signal *in vivo*. One-way analysis of variance with Tukey post hoc testing was applied to compare tumor weights, NIRF-signal and MTV values between groups of mice treated with paclitaxel, trastuzumab or saline. Statistical analyses were performed using the software package SPSS (IBM, Armonk, NY, USA) version 24, and P-values < 0.05 were regarded statistically significant.

4. Summary of results

Paper I: We successfully established orthotopic mouse models from both an endometrial carcinoma cell line (Ishikawa^{luc+}) and cells from endometrial carcinoma biopsies. In the cell line model increasing bioluminescent signal was observed over time, along with gradual development from focal towards a more diffuse abdominal signal - indicating tumor growth and metastatic spread. MRI was performed in a mouse from the Ishikawa^{luc+} model, and uterine tumor was detected in both T1- and T2-weighted images. Tumor was observed to moderately enhance in T1-series after i.v. injection of contrast, and ADC-mapping revealed restricted diffusion within tumor tissue. PET/CT imaging of mice in the cell-line based model revealed ^{18}F-FDG/^{18}F-FLT-avid tumor tissue in the uterus of 6 out of 7 mice. Increasing MTV and SUV_{mean} x MTV was observed in both primary tumors and metastases. Although the calculated MTV and SUV_{mean} x MTV values of the different tracers were not directly comparable, both ^{18}F-FDG and ^{18}F-FLT seemed equally able to identify tumor tissue and monitor disease progression. PET/CT and MRI findings in the Ishikawa^{luc+} mouse model were comparable to imaging characteristics of human endometrial carcinoma patients. ^{18}F-FDG and ^{18}F-FLT PET/CT also detected uterine tumors in mice orthotopically implanted with patient-derived tumor cells.

Paper II: When exploring the presence of selected surface proteins (ALCAM, EpCAM, IGF1Rα and L1CAM) in endometrial carcinoma cell lines (AN3CA, Hec1B, Ishikawa and RL95-2) EpCAM was found to have the highest overall expression, and was particularly abundant in the Ishikawa cell line. Positive EpCAM protein expression was found in 98% of hysterectomy samples in a cohort of 153 endometrial carcinoma patients, and the majority of these demonstrated strong positive staining (SI: 6-9). An anti-human anti-EpCAM antibody was conjugated to an AF680 fluorophore, and used to detect EpCAM expression both *in vitro* and *in vivo*. Both BLI and EpCAM-AF680 NIRF imaging enabled visualization of uterine tumors in orthotopic cell line-based models, however; EpCAM-AF680 NIRF imaging

enabled earlier and more precise visualization of metastatic lesions compared to BLI. Signal origin was confirmed by *ex vivo* imaging of organs, using both BLI and EpCAM-AF680 NIRF imaging. EpCAM-AF680 NIRF imaging successfully detected uterine tumors in multiple endometrial carcinoma PDX models, including models with relatively low expression of EpCAM. We found EpCAM-680 NIRF to be superior to ^{18}F-FDG PET/CT in monitoring of PDX tumors, providing better contrast and earlier detection of tumor in most cases. Mice orthotopically implanted with cells from a patient diagnosed with endometrioid grade 3 endometrial carcinoma were treated with vehicle control (n = 8), paclitaxel (n = 8) and trastuzumab (n =8). Animals were monitored *in vivo* using EpCAM-AF680 NIRF and ^{18}F-FDG PET/CT imaging, without observing any effect of treatment based on mean NIRF-signal ($F(2,21) = 1.07$, $p = 0.36$) or MTV ($F(2,14) = 0.76$, $p = 0.49$). This was consistent with post mortem examinations where no significant differences in tumor weights were found between the three groups ($F(2,21) = 0.07$, $p = 0.93$). Presence of tumor cells in the uteri of mice was confirmed by histological examination.

Paper III: We explored the expression of ASRGL1 in tissue samples from a large, prospectively collected patient cohort, and found that 1% of CAHs, 21% of primary endometrial tumors, and 77% of metastatic lesions have low levels of ASRGL1. Antibody validation was performed by staining 607 primary tumors for ASRGL1 using two different antibodies, demonstrating significantly correlating staining indexes ($P < 0.001$) and similar prognostic value. Low expression of ASRGL1 was associated with characteristics of aggressive endometrial carcinoma, including high age, FIGO stage III-IV, high grade and non-endometrioid histology ($P < 0.001$ in all). A significant overlap between *ASRGL1* mRNA and ASRGL1 protein was observed ($P < 0.001$), and low expression of both *ASRGL1* mRNA and protein expression was associated with poor disease specific survival ($P < 0.001$). In multivariate analyses ASRGL1 had independent prognostic value, both in the total patient population (Hazard ratio (HR): 1.53, 95% confidence interval (CI): 1.04 – 2.26, $P = 0.031$) and in patients with endometrioid endometrial carcinoma (HR: 2.64, CI: 1.47 – 4.74, $P = 0.001$). The highest proportion of metastatic lesions with low ASRGL1 expression

(90%) was found in patients with non-endometrioid endometrial carcinoma, compared to endometrioid endometrial carcinoma patients where only 63% of metastases had low levels of ASRGL1. In cases with low ASRGL1 expression in primary tumor, ASRGL1 was most often lost in corresponding metastases. In most patients with multiple metastases, similar expression of ASRGL1 was found in all metastatic lesions from the same individual. ASRGL1 was also more frequently lost in metastases than the hormone receptor ERα.

Paper IV: 20% (*n* = 227) of patients expressed low levels of ASRGL1 in preoperative samples. For 484 patients ASRGL1 status in hysterectomy specimen was known, and similar expression of ASRGL1 in curettage and corresponding hysterectomy sample was observed in 85% (*n* = 413) of cases ($P < 0.001$). Low expression of ASRGL1 was significantly associated with pre-operatively available parameters related to aggressive disease, such as high risk curettage histology ($P < 0.001$), combined ERα/PR loss ($P < 0.001$) and large tumor volume on MRI ($P = 0.026$). Significant associations between low ASRGL1 level and post-operatively assessed features related to aggressive endometrial carcinoma were also observed, including high FIGO stage, non-endometrioid histology, and high grade ($P < 0.001$ for all). ASRGL1 was found to have independent prognostic value in a multivariate survival analysis adjusting for age, FIGO stage, histological type and grade (HR: 1.63, CI: 1.11 – 2.37, $P = 0.012$). Within the subgroup of patients with low risk curettage histology low ASRGL1 expression had an independent impact on survival when adjusted for age and FIGO stage (HR: 2.54, CI: 1.44 – 4.47, $P = 0.001$). Patients with low expression of ASRGL1 had a higher frequency of metastatic lymph nodes compared to patients with high ASRGL1 expression (23% versus 10%, respectively, $P < 0.001$), and low ASRGL1 level independently predicted lymph node metastasis with an adjusted odds ratio (OR) of 2.07 (CI: 1.27 – 3.38, $P = 0.003$).

5. Discussion

5.1 Preclinical models of endometrial carcinoma

5.1.1 *In vitro models*

Preclinical models based on commercially available cell lines have been a cornerstone in cancer research for decades, and have contributed to achieving valuable insights in cancer biology (115, 162, 163). A variety of laboratory methods are available to study different properties of cells *in vitro*, and cell line studies are useful in generation and initial testing of hypotheses. Cell line models are low cost compared to animal models, and results can be retrieved quickly. Although there are many applications where cell line studies can be useful, these models generally fail to reproduce the complex physiological environment of human tumors. Cell lines are typically cultured as monolayers on plastic surfaces, thus preventing the formation of three-dimensional structures. Growth mediums often contain a variety of supplements, and may not be representative of the physiological microenvironment *in vivo*. Overall, these artificial conditions may affect the genetic, morphologic and physiologic properties of the cells (162, 163). Another weakness of cell cultures is that they lack a normal microenvironment and are devoid of stromal cells, immune cells and blood vessels. Additionally, cell lines derived from normal endometrial tissue are seldom available as controls. Combined, these factors contribute to reducing the clinical relevance of cell culture models (115).

One approach to improve the clinical validity of *in vitro* models is to establish short-term cultures of primary tumor cells derived from patient biopsies. Primary cell cultures are suggested to retain genetic and molecular traits of the primary tumor, and thus be more representative cancer models compared to conventional cell lines. However, culturing of primary patient cells is challenging as these often fail to thrive

in vitro. Certain tumors may be more difficult to culture than others, and thus the distribution of subtypes available as *in vitro* models may not be representative of the prevalence of subtypes in the human population. Intratumoral heterogeneity poses another challenge, as the part of the tumor used for generation of primary cell culture may not reflect the characteristics of the entire tumor. Additionally, selection of clones that are more prone to adhere and grow under non-physiological conditions may lead to reduced cellular heterogeneity in the culture compared to the original sample (113). In **paper IV** we established short-time cultures of primary tumor cells to achieve sufficient cell numbers for simultaneous implantation of multiple mice. This represents a potential limitation of our study as *in vitro* propagation of cells, although only for a few passages, may result in phenotypic alterations. However, for endometrial carcinoma it has been reported that patient derived short-time cultures and xenografts maintain the same genomic traits as the corresponding human primary tumor (113). Short-time culturing of cells prior to xenografting may thus be justifiable, however; more research is needed to elucidate the strengths and weaknesses of models that have been generated using this approach.

Recently, generation of organoid cultures has been presented as a novel approach to improve *in vitro* models of human cancer. Organoids are self-organizing 3D cultures containing both stem cells and differentiated cells that mimic the tissue of origin, and can be generated from patient biopsies. Human organoid cultures have been established from both endometrial carcinoma tissue and normal adjacent endometrium, and demonstrated to reproduce the molecular and histological phenotype of the donor tissue (164-166). Organoid cultures can be used as high-throughput systems for developing and studying new therapies, and findings may be validated in a systemic setting *in vivo* by using organoid-derived mouse models. Altogether, organoids and organoid-based animal models may serve as valuable platforms for preclinical research (166, 167).

5.1.2 Orthotopic mouse models

One of the major challenges in cancer research is that the results from preclinical animal studies are difficult to reproduce in human patients (86, 96), and it is reported that less than 8% of new drugs that were efficient in animal models make it through clinical trials (168). The low translational success rate is often attributed to cancer models that poorly simulate the human disease setting, and possible reasons include differences in physiology between species and failure to recapitulate the complexity of the cancer (168). Development of clinically relevant mouse models is thus of the highest importance in order to improve the congruence between preclinical experiments and clinical studies.

Methodological considerations – establishment of in vivo *models*

In **paper I** and **II** we successfully established orthotopic mouse models from both endometrial carcinoma cell lines and patient primary tumors. Generation of uterine xenografts was performed by transmyometrial injection of cancer cells. Transvaginal injection of tumor cells is also possible; however, the transmyometrial approach is reported to have higher engraftment rates (97). Several previously reported orthotopic endometrial carcinoma models have been generated by implanting tumor tissue on the posterior surface of the uterus (105, 106, 109). Although this intraabdominal approach may provide a more appropriate microenvironment compared to subcutaneous tumors, it may not fully recapitulate the conditions of the endometrium *in uteri*. The implantation of cancer cells directly into the uterine lumen may contribute to a more clinically relevant disease progression, as tumor is established in the endometrium before progression towards myometrial infiltration, peritoneal dissemination, and lymphatic and hematogenous spread (97).

In **paper I** and **II** we used NSG mice for orthotopical implantation of human tumor cells in order to facilitate engraftment. In addition to the severe combined immunodeficiency-mutation, NSG mice inhabits an interleukin 2 receptor gamma chain deficiency, lack functional T-cells, B-cells and natural killer cells and have

deficient cytokine signaling (114). NSG mice are reported to have high take rates (towards 95-100%), and are thus highly suitable as xenograft models (169). However, the lack of a functional immune system unavoidably offers a tumor environment that differs from the human setting, and may affect cancer growth. The possibility to study interactions between tumor and the microenvironment is also limited (86, 93, 98, 102). A potential solution to these problems is development of personalized immune animal models, where bone marrow aspirates from a human patient can be injected into the mouse prior to tumor xenografting (86, 98, 170). Still, even though immunocompetent models would be highly valuable in preclinical research, establishment of such models is technically demanding and requires collection of several invasive biopsies from patients (170).

Patient derived xenograft model

Several PDX-models were successfully established during this PhD-project, representing tumors of low- and high grade endometrioid as well as non-endometrioid histologies. The ability to generate mouse models from different types of primary endometrial tumors is highly beneficial, as using multiple xenograft models in testing of hypotheses and evaluation of drug response (similarly to clinical trials) may improve the translational relevance of future preclinical studies (171).

One major threat to the clinical validity of PDX models is intratumor heterogeneity. Xenografts are established from limited amounts of tissue in tumor biopsies, and the heterogeneity of the primary tumor may thus not be fully comprehended in the PDX model. Still, comparative studies of human endometrial tumors and their corresponding xenografts found high degree of genomic and phenotypic preservation (113). Both implantation of tissue pieces (97, 111, 113, 172, 173) and cell suspension (**paper I** and **II**) have been demonstrated to enable endometrial carcinoma engraftment. Most reported endometrial carcinoma models have been established from tissue pieces. This approach is beneficial, as the tissue architecture of the

primary tumor is retained. The weakness of this method is that only small pieces of tumor can be implanted, potentially making the xenograft representative only to minor parts of the primary tumor. Although losing the three-dimensional structure, the advantage of using single cell suspension is that tumor can be dissociated to generate a heterogeneous sample that may represent a larger proportion of the patient's tumor (171). However, processing of tumor biopsies may reduce the amount of viable tumor cells and reduce engraftment rates. Another challenge for PDX models is that human stroma is demonstrated to be replaced by murine stromal cells after xenografting. This could potentially limit the clinical value of these models - especially in studies of tumor/microenvironment interactions and therapies directed towards the stromal compartment (86, 111). In order to address this issue co-implantation of patient-matched stromal cells such as mesenchymal stem cells or cancer associated fibroblasts has been suggested (170).

Although most reported PDX models of endometrial carcinoma have been generated by subcutaneous implantation of tumor cells or tissue, orthotopic models have also been described (97, 113). In **paper I** and **II** we established orthotopic xenografts from several endometrial carcinoma patients. When comparing our cell line based and patient-derived mouse models, a number of features suggest that the PDX-models are superior in resembling clinical endometrial carcinoma. Firstly, several of the mice in our PDX models have displayed vaginal bleeding towards the later stage of disease development. So far we have not observed the same in any of our cell line based models. This similarity in clinical manifestation is interesting, as vaginal bleeding is the most common presenting symptom of endometrial carcinoma in human patients (10). Secondly, while our cell line models usually develop high degree of intraperitoneal tumor dissemination and distant metastases, PDX tumors are more often confined within the uterus. The latter is more comparable to human endometrial carcinoma, where the majority of patients are diagnosed with low stage disease (174).

One important goal in preclinical research is to establish relevant models for studies of therapeutic effect. Treatment studies conducted in PDX models are reported to

have highly similar drug response compared to human clinical trials (171). This is especially observed in one-to-one studies where the treatment responses of PDX models are compared to the response in the corresponding human donor tumor (86). Several *in vivo* drug treatment studies have been conducted in subcutaneous endometrial carcinoma PDX models. Sensitivity to the dual pan-PI3K/mTOR inhibitor NVP-BEZ235 and the MEK-inhibitor AZD6244 was observed in mice with confirmed *KRAS*, *PTEN* and *PIK3CA* mutations in tumor (111), while another study demonstrated that the antibody-drug conjugate IMGN853 had antitumor effects in a PDX model of serous endometrial carcinoma (173). However, subcutaneous tumors may display diverging response to therapy compared to primary uterine tumors due to differences in growth pattern and environmental factors, and orthotopic models may thus be more favorable for evaluation of treatment. In **paper II** we demonstrated an orthotopic PDX model that can be used for therapeutic studies. To evaluate the feasibility of the model, mice were treated with paclitaxel or trastuzumab. Paclitaxel is a cytostatic drug that stimulates microtubule polymerization and mitotic arrest (175) and was chosen as it is commonly applied as first-line adjuvant chemotherapy in treatment of endometrial carcinoma patients (14). Trastuzumab is a HER2-targeting antibody which has been suggested as a candidate drug to treat endometrial carcinoma patients with HER2-positive tumors. The clinical value of this treatment has so far been hampered by poorly understood mechanisms of acquired resistance (64). However, combinational therapy where trastuzumab is added to the standard paclitaxel/carboplatin regimen has been suggested to improve outcome (176). In the current study, trastuzumab was selected based on positive HER2 immunostaining in the primary human tumor. Neither paclitaxel nor trastuzumab treatment demonstrated statistically significant inhibitory effects on tumor growth. Still, this PDX model may have potential value in studies of drug resistance mechanisms as well as in studies of other candidate drugs.

5.1.3 Small animal imaging

The use of small animal imaging in cancer research has increased enormously over the last years, as development of non-invasive longitudinal imaging techniques has allowed for *in vivo* studies of tumor growth, metastatic spread, and evaluation of therapeutic response. Molecular imaging methods reflect specific tumor properties, including glucose metabolism (^{18}FDG-PET), cell division (^{18}FLT-PET) and EpCAM expression (EpCAM-AF680 NIRF). Evaluation of tumors using several modalities may thus provide valuable information on tumor biology beyond anatomical localization and evaluation of size (114, 116, 117). Molecular imaging is particularly interesting as changes in tumor metabolism may be detectable before changes in tumor size, which may be important for early therapeutic evaluation.

Optical imaging is a commonly applied technique for preclinical imaging, and BLI is reported to be an efficient imaging method to detect tumor growth and metastatic dissemination in several cancer models (97, 113, 120, 154). In **paper I** and **II** BLI was applied to visualize tumor development in cell line based orthotopic endometrial carcinoma models. Although being highly specific and with a high signal-to-background ratio, BLI is only applicable in models where luc+ genes have been introduced. This usually limits the area of use to animal models generated from conventional cell lines. Additionally, the process of introducing the reporter gene must be repeated each time new models are established. BLI has been used to follow tumor growth in an orthotopic PDX model generated from luciferase-transfected short-time cultured endometrial carcinoma cells (113). However, transfection of primary patient cells may potentially disturb the tumor genome and result in an altered cell phenotype. In order to avoid this risk we have explored reporter gene-independent imaging alternatives to visualize tumor growth in our PDX models. In **paper II** we identified EpCAM as a candidate target protein for NIRF imaging in orthotopic endometrial carcinoma xenografts. EpCAM is an adhesion molecule located on the basolateral membrane of epithelial cells, and is reported to be highly expressed in several epithelial cancers (177). As EpCAM-AF680 NIRF imaging is an

antibody-based application, the method is easily applicable for *in vivo* imaging in multiple endometrial carcinoma models. We evaluated the performance of BLI and EpCAM-AF680 NIRF imaging in orthotopic cell line-based models (**paper II**). Although BLI and EpCAM-AF680 NIRF produced similar visualization of primary tumors in models derived from Ishikawa^{luc+} or Hec1B^{luc+} cells, EpCAM-AF680 NIRF imaging enabled earlier and better delineation of distant metastases, suggesting that EpCAM-AF680 is highly feasible for evaluation of metastatic disease. However, it is worth noting that the imaging system we are using is optimized for fluorescent imaging, and different results may have been achieved if an imaging system more optimized for BLI had been applied. EpCAM-AF680 was also found to provide excellent visualization of uterine tumors in multiple PDX models representing different histologic types of endometrial carcinoma, and was found to be superior to ^{18}F-FDG PET/CT. Even uterine tumors in PDX models with low expression of EpCAM (PDX 4) were detected by EpCAM-AF680 NIRF imaging, thus highlighting the feasibility of this imaging modality for preclinical applications.

Optical imaging is highly valuable in studies of orthotopic xenograft models. There are however some challenges, and we have addressed these to limit their impact where possible. In **paper I** and **II** we found BLI and EpCAM-AF680 NIRF imaging to be feasible for detection of both primary tumor and metastatic lesions. However, as these methods only provide two-dimensional images we were not able to accurately decide which organ the signal originated from *in vivo*. Also, distinguishing tumor lesions within the parenchyma from lesions in the peripheral margins of an organ was not possible. We thus performed *ex vivo* imaging and histologic evaluation of organs to confirm the anatomical origin of the signal. Limited penetration of signal combined with signal scattering and absorbance in tissue represents another challenge. As photons in the near-infrared spectrum have better tissue penetration compared to photons with wavelengths of below 500 or above 1100 nm (140), we chose to use AF680 to achieve high image quality. NIRF imaging of uterine tumors may be hampered by high background signal due to autofluorescence in the gastrointestinal tract and accumulation of fluorophore in urine. For the experiments in

paper II we attempted to minimize these problems by emptying the bladder prior to imaging and feeding the animals a chlorophyll-free diet.

PET/CT and MRI have been demonstrated to detect tumors and visualize treatment response in several xenograft models, including breast cancer (178), colorectal cancer (179) and Ewing sarcoma (180). Although the basic principles behind these techniques are the same for humans and animals, specialized machines for small animal imaging have been developed due to body size and technical requirements for optimal resolution (116, 117). In **paper I** we demonstrated that PET/CT using ^{18}F-FDG and ^{18}F-FLT as tracers can be used to visualize orthotopic endometrial carcinoma xenografts. These tracers were chosen as they represent different metabolic processes characteristic of cancer cells (increased glucose metabolism and proliferation, respectively). Additionally, ^{18}F-FDG is used for preoperative imaging of endometrial carcinoma patients in several hospitals, and findings in preclinical models may thus have potential translational value. In **paper II** ^{18}F-FDG PET/CT imaging was performed in PDX-models originating from multiple patients with different histologic backgrounds, and also applied to evaluate paclitaxel and trastuzumab treatment in an orthotopic endometrial carcinoma PDX model. One major benefit with PET/CT imaging is that the data from the functional PET scan is merged with the anatomical information from the CT scan. This enables three-dimensional evaluation of tumor lesions and the localization of the tumor can be more precisely pinpointed to a specific organ. However, ^{18}F-FDG has a high background uptake in organs such as brain and kidneys, as well as increased uptake in inflammatory tissue, which can make oncological assessments difficult (129). Signal from small uterine tumors can also be camouflaged by physiological accumulation of tracer in nearby organs such as urinary bladder and intestine. This may partially explain why ^{18}F-FDG PET/CT imaging failed to identify several of the small tumors in our PDX-models. Fasting animals and emptying the bladder prior to scanning may reduce unspecific signal, and improve the delineation of tumor against normal tissue. This was done prior to imaging of mice in the paclitaxel/trastuzumab treatment study (**paper II**), resulting in markedly reduced background signal

compared to previous experiments. MRI is also often applied in preoperative examinations of patients with endometrial carcinoma. *In vivo* MRI imaging of a mouse orthotopically implanted with an endometrial carcinoma cell line demonstrated that the uterine tumors in the xenograft model had hyperintense appearance on T2-weighted images and restricted diffusion on ADC-maps; highly resembling the findings from MRI imaging in endometrial carcinoma patients (**paper I**). Although being a promising modality for imaging of endometrial PDX models, the value of MRI in preclinical studies remains to be confirmed through future *in vivo* experiments.

5.2 Asparaginase-like protein 1

5.2.1 Methodological considerations – biomarker studies

Correct identification of high-risk patients and stratification of patients to appropriate treatment regimens is vital to improve the outcome of endometrial carcinoma. Biomarkers are central in these processes, and new, robust markers are needed. Before clinical implementation, new biomarkers should be validated in independent patient cohorts and their clinical utility should be assessed. Validation studies should include enough patients to provide sufficient statistical power, and should be conducted in patient groups which are representative for the whole population where the biomarker is intended to be used. Our patient series (HUS and MoMaTEC cohorts) contain a large number of patients that have been included prospectively over a long period of time. The comprehensive database of clinical- and follow up information combined with a biobank containing numerous biological samples serves as an excellent research platform, both to identify potential new biomarkers and to validate findings from other biomarker studies.

In **paper III and IV** ASRGL1 protein expression was evaluated by IHC staining of TMAs. This is a high-throughput method where a large number of samples can be evaluated simultaneously. There are several advantages with using TMAs in research

settings, including reduced use of tissue, shorter analysis time and lower reagent costs (181). The ability to stain all samples simultaneously reduces the risk of batch effects and limits variations in staining technique. Selection of tissue for TMA preparation is performed by identifying the most representative areas with highest tumor cell content in FFPE sections, and may not fully comprehend the characteristics of the entire tumor. However, to compensate for the limited amount of tissue collected in a TMA core, three cores are selected from each biopsy. This makes it more likely that the TMA is representative of a larger part of the tumor. The TMA method has been validated in several studies, demonstrating high concordance between TMAs and corresponding full tissue sections (182-184). Still, new biomarkers identified by TMAs, including ASRGL1, should be validated in full sections prior to clinical implementation.

IHC is a valuable tool for detecting molecular and functional properties in tissues, and may aid in stratification of tumors with an otherwise similar histology. Challenges when studying biomarkers include that scoring systems and cut-offs seldom are standardized and that separate institutions may use different protocols. Thorough studies must thus be performed to identify and validate the optimal staining conditions before new biomarkers are introduced in a clinical setting. We have used a semi-quantitative scoring method to evaluate ASRGL1 protein expression (**paper III** and **IV**), where both the intensity and area of tumor with positive staining is assessed. This SI system is a well-established method in our laboratory (148), and has been applied for several antibodies in various tumor types (185-187). ASRGL1 protein expression in tumor cells was scored without considering subcellular localization, as separate evaluation of nuclear and cytoplasmic staining has been reported not to be of additional value (146). Although making it more difficult to compare results between studies, using different scoring methods and cut-offs for validation could potentially also be beneficial in biomarker studies. In **paper III** and **IV** we have used SI: 0-1 as cut-off for low ASRGL1 expression, while others have defined low ASRGL1 as < 75% cells with positive staining without regarding intensity (146, 147). Irrespective of the different cut-offs and scoring systems we

were able to validate the prognostic impact of ASRGL1, supporting that ASRGL1 is a robust biomarker in endometrial carcinoma.

Assessing the reliability of the scoring method is also important in biomarker studies as good reliability is important for clinical use to ensure uniform diagnosis of patients. Interrater reproducibility describes the variation between two or more observers rating the same objects, and can be evaluated in several ways (i.e. ICC). In **paper III**, an ICC of 0.95 was calculated for ASRGL1 score (CI: 0.93 – 0.96), indicating excellent interrater reliability (188).

5.2.2 ASRGL1 as a preoperative prognostic biomarker

Pre-operative evaluation of curettage histology is important for risk stratification and surgical planning in endometrial carcinoma. Still, the histological assessment of pre- and post-surgical samples is reported to be discordant in 10 – 32% of cases (16-19, 22). Clinical implementation of molecular biomarkers may contribute to identification of patients with high risk disease before surgery (189, 190). Several candidates including ERα, PR, p53, Ki-67, and L1CAM have so far been explored (78, 82, 190, 191). With a few exceptions, these markers are yet not clinically applied. However, an ongoing study (MoMaTEC2, NCT02543710) is evaluating the performance of preoperative hormone receptor status (ERα/PR) in selecting endometrial carcinoma patients for lymphadenectomy. As ASRGL1 was validated to be a strong post-operative prognostic marker (**paper III**) we wanted to explore if ASRGL1 also could serve as a potential biomarker in pre-operative samples. Previously, low ASRGL1 expression combined with PR loss in preoperative samples has been reported to be a strong predictor of FIGO stage III-IV disease in endometrioid endometrial carcinoma (147). This is in accordance with our study (**paper IV**) where low expression of ASRGL1 was significantly associated with characteristics of aggressive disease, including high FIGO stage. We also found that low expression of ASRGL1 in pre-operative specimens had independent prognostic

value, both in the whole patient population and in patients with presumed low risk curettage histology. Altogether, this indicates that ASRGL1 status in curettage may be a valuable marker to improve pre-operative risk stratification in endometrial carcinoma. However, as we are the first to report ASRGL1 as an independent biomarker in preoperative samples, these findings remain to be validated.

5.2.3 Preoperative biomarkers vs sentinel lymph node dissection

In **paper IV** we found that patients with low ASRGL1 expression in preoperative samples were more likely to have metastatic lymph nodes at time of surgery compared to patients with high ASRGL1 expression. This was observed both in the whole patient population and in patients with assumed preoperative low risk histology. Low ASRGL1 also independently predicted lymph node metastasis when adjusting for curettage histology risk, suggesting that evaluation of ASRGL1 in preoperative samples may add valuable clinical information. However, the clinical utility of preoperative markers to guide the decision on whether or not to perform lymphadenectomy has been debated, and sentinel lymph node removal has been suggested as a better alternative. Although sentinel lymph node dissection is associated with less post-operative complications than full lymphadenectomy (33-35), it would still lead to prolonged operating time and increased risk of complications compared to no lymph node sampling. As most patients do not have metastatic lymph nodes it could be debated that sentinel lymph node removal is an unnecessary procedure in many cases and that molecular markers could be used to identify patients that may benefit from sentinel lymph node exploration. By only performing sentinel lymph node mapping in selected patients, one could potentially reduce both time and costs associated with surgical treatment of endometrial carcinoma. At the present time, a large proportion of patients with presumed low risk endometrial carcinoma are treated at hospitals without the equipment that is needed for sentinel lymph node mapping. In such settings, preoperative biomarkers could be used to identify patients that may benefit from undergoing more advanced surgical staging and referral to secondary/tertiary hospitals.

5.2.4 ASRGL1 as a post-operative prognostic marker

In **paper III** we found that low expression of ASRGL1 protein in hysterectomy specimens has independent prognostic value in endometrial carcinoma patients, thus validating the findings from a retrospective study where loss of ASRGL1 protein expression was reported to independently predict poor disease specific survival in endometrioid endometrial carcinoma (146). Another study evaluated a set of IHC markers (ASRGL1, ER, HER2, Ki-67, L1CAM, MLH1, PR, p53), and identified low ASRGL1 and abnormal p53 expression as the best combination within this panel to predict disease-free and disease-specific survival (147). We are however the first to demonstrate that ASRGL1 has independent prognostic value in the whole patient population (**paper III**), not only in patients with endometrioid endometrial carcinoma. As there are currently no IHC biomarkers in clinical use to recommend adjuvant chemotherapy in endometrial carcinoma patients (192-194) and risk stratification is based on traditional parameters such as FIGO stage and histological grade (30), assessment of ASRGL1 status in hysterectomy samples could potentially provide clinically relevant information. Patients with grade 1-2 endometrioid endometrial carcinoma are considered to have low risk disease and will usually not receive adjuvant treatment. Some of these patients will however experience disease relapse. In **paper III**, we found that 8% of patients with grade 1-2 endometrioid endometrial carcinoma express low levels of ASRGL1. It would be interesting to explore if these patients could benefit from more extensive treatment. Conversely, adjuvant chemotherapy often results in damaging side-effects and reduced quality of life - especially in elderly and co-morbid patients. Biomarkers identifying patients who do not benefit from additional treatment may both improve these patients quality of life and reduce overall medical costs. We observed that high expression of ASRGL1 was associated with a favourable prognosis, and one could speculate that ASRGL1 may identify patients that could be spared from adjuvant chemotherapy. Still, the clinical utility of ASRGL1 as a prognostic biomarker remains to be established.

Evaluation of mRNA expression may be an alternative approach for assessment of prognosis in gene-based studies. Previously, reduced *ASRGL1* gene expression has been reported as part of a 29 gene signature identifying a cluster of endometrial carcinomas with aggressive disease and poor recurrence-free survival (195, 196). *ASRGL1* has also been identified as one of the 145 most differentially expressed genes between endometrioid and non-endometrioid endometrial carcinoma (197). In that study, *ASRGL1* expression was downregulated in non-endometrioid compared to endometrioid cases, reflecting that low *ASRGL1* is related to aggressive disease. Additionally, gene expression data from the TCGA study has demonstrated that patients with low *ASRGL1* mRNA levels in their tumors have significantly worse overall survival compared to patients with high *ASRGL1* expression levels (198). This supports our findings in **paper III** where low *ASRGL1* mRNA expression is significantly associated with poor disease specific survival. We also find that *ASRGL1* mRNA is significantly correlated with ASRGL1 protein expression, suggesting that both gene- and protein expression is lost as tumors dedifferentiate.

5.2.5 ASRGL1 expression in metastatic lesions

Metastatic disease is estimated to be the cause of up to 90% of cancer related deaths (199), and more research focusing on metastasizing tumors is needed. In **paper III** we observed that most patients with low ASRGL1 expression in their primary tumors also had low ASRGL1 expressing metastases. Heterogeneous expression of proteins is often observed between different metastatic lesions within the same individual, as reported for hormone receptors (200). Interestingly, when evaluating available metastatic lesions and corresponding primary tumors we found that most patients with multiple metastases had similar ASRGL1 expression in all lesions. We are the first to describe ASRGL1 expression in metastatic endometrial carcinoma. Our study includes sampled metastatic lesions with available corresponding primary tumors. The ability to evaluate ASRGL1 staining in paired primary tumors and metastases is a major advantage, as it may add relevant information on biomarker expression

during disease progression. Although based on metastases available for sampling, which may not be fully representative to all metastatic lesions, our findings are interesting and could be explored in future studies to evaluate the clinical importance of ASRGL1 expression in a metastatic setting.

5.2.6 What is the functional role of ASRGL1 in endometrial cancer?

ASRGL1 was first described as a protein that shares 77% of its genetic sequence with a rat sperm autoantigen (201), and it is classified as an enzyme in the N-terminal nucleophile hydrolase family (202). ASRGL1 is demonstrated to have both L-asparaginase and β-aspartyl peptidase activity *in vitro* (202), but the knowledge concerning the functional role of ASRGL1 in normal and cancerous tissue is limited. Considering the above mentioned mechanisms one could speculate that loss of ASRGL1 function could promote cancer by leading to elevated cellular asparagine levels (which is reported to suppress apoptosis (203)) as well as accumulation of dysfunctional proteins due to reduced degradation of isoaspartyl peptides by β-aspartyl peptidases (202, 204).

In some types of cancer, including breast, ovarian and cervical cancer, high levels of ASRGL1 in tumor compared to normal tissue are suggested to associate with poor prognosis and increased cell growth *in vitro* (205-207). This is inconsistent with our findings, where low ASRGL1 protein expression is associated with aggressive disease and poor survival. The reason for these contrasting results is not known. However, we have evaluated ASRGL1 staining in precursor lesions and tumor tissue, and the expression of ASRGL1 in adjacent normal tissue in our patient cohort has not been assessed. Additionally, as the biological function of ASRGL1 in endometrial carcinoma has not been explored, it is likely that the observed differences in ASRGL1 expression between these cancers is caused by involvement of different molecular processes.

ASRGL1 is reported to display L-asparaginase activity (202). L-asparaginase has been used in the treatment of acute lymphoblastic leukemia (ALL) and Non-Hodgkin lymphoma for several decades. This has resulted in increased remission rates and survival - especially in children with ALL (208). The therapeutic potential of L-asparaginase is being explored in several solid tumors, including ovarian cancer and pancreatic adenocarcinoma (209-212). The rationale for treating endometrial carcinoma patients with L-asparaginase might not be the same as for ALL, as ALL tumor cells are unable to synthesize asparagine and thus depend on the extracellular supply of asparagine (208). Still, it is tempting to speculate in a potential treatment effect also for endometrial carcinoma patients. By administering L-asparaginase to patients with low ASRGL1 expression one may hypothesize that asparagine levels are reduced, thus minimizing its anti-apoptotic effects. L-Asparaginase treatment in endometrial carcinoma should be further explored through both *in vivo* and *in vitro* preclinical studies.

6. Conclusions

Overall, this PhD project has focused on molecular biomarkers and orthotopic mouse models of endometrial carcinoma. We have developed orthotopical mouse models and advanced imaging protocols that enables *in vivo* studies of tumor biology, biomarkers and therapeutic strategies. We have also studied the promising prognostic biomarker ASRGL1 in both pre-and postoperative samples.

Paper I: Orthotopic endometrial carcinoma mouse models are successfully established, both from a luciferase positive cell line and from patient-derived primary tumor cells. The small animal imaging modalities BLI, MRI, ^{18}F-FDG PET/CT, and ^{18}F-FLT PET/CT all enable detection and monitoring of tumor progression in the cell line based mouse model. Additionally, PET/CT imaging (using both tracers) is well suitable for visualization of uterine tumor in PDX-models.

Paper II: EpCAM is highly expressed in endometrial carcinoma cell lines and primary tumor tissue. EpCAM-AF680 NIRF imaging enables earlier detection of metastatic lesions compared to BLI in cell line based models of endometrial carcinoma, and is superior to ^{18}F-FDG PET/CT in visualization of uterine PDX tumors. EpCAM-AF680 NIRF also enables *in vivo* evaluation of therapeutic response in orthotopic endometrial carcinoma PDX models.

Paper III: ASRGL1 validates as a strong post-operative prognostic biomarker in endometrial carcinoma. Loss of ASRGL1 in hysterectomy samples is associated with aggressive disease and has independent prognostic value both in the whole patient population and in the endometrioid subgroup. ASRGL1 expression in endometrial

carcinoma metastases is also investigated for the first time, and is found to be low in the majority of metastatic lesions.

Paper IV: Low ASRGL1 expression in curettage is a promising pre-operative biomarker for aggressive endometrial carcinoma, and has independent prognostic value both in the whole population and in the subgroup of patients with assumed low risk curettage histology. Low expression of ASRGL1 in pre-operative samples independently predicts lymph node metastasis, and may potentially be used to recommend full surgical staging.

7. Future aspects

Further improving endometrial carcinoma mouse models

In **paper I** and **II** we successfully developed orthotopic PDX models of endometrial carcinoma; however, further refinement may improve the feasibility of these models for use in preclinical studies. A strategy using organoid cultures for xenografting is suggested to improve the efficiency of PDX engraftment whilst simultaneously reducing the time of expansion (213), and would facilitate experimental evaluation of both biomarkers and targeted therapies in a highly clinically relevant systemic setting. Future work with endometrial carcinoma PDX models should also include thorough characterization of morphological, histological and genomic features to determine the degree of genetic and phenotypic drift from the human donor tumor throughout the following passages in mice.

The orthotopic PDX 4 model (Grade 3 endometrioid endometrial carcinoma, **paper II**) should be utilized in future studies of treatment response and drug resistance, preferably to explore biomarker-guided targeted therapies that may be clinically relevant for tumors with similar characteristics as this model. It would also be interesting to perform gene expression analyses of samples that were collected in the treatment study in **paper II** in order to elucidate potential mechanisms associated with paclitaxel and trastuzumab resistance. To improve the translational value of preclinical studies, validation of findings (both in the current and future experiments) should be performed in several different PDX models. However, establishment of such models is difficult, time-consuming and expensive. Collaboration with other institutions to assemble larger cohorts of PDX-models may provide a more robust platform for preclinical studies of biomarkers and therapies (171), and should be pursued in the future.

The future of preclinical imaging

The infrastructure of preclinical small animal imaging is well developed in Bergen, thus allowing us to explore multimodal imaging approaches. However, this is not the case in many other centres. For research facilities that have to rely on only one imaging modality, optical imaging is an excellent alternative. In **paper I** and **II** we explored several small imaging modalities. However, much research is needed to determine which method (or combination of methods) is most optimal for imaging in the different endometrial carcinoma models. MRI is often applied as part of the pre-operative diagnosis in endometrial carcinoma, and it would be interesting to evaluate the performance of MRI in imaging of orthotopic endometrial carcinoma PDX models - including monitoring of treatment. MRI has excellent soft tissue contrast, and in the future PET/MRI may be a better option for anatomical and functional visualization of endometrial carcinoma models than PET/CT. Ultrasound is another clinically relevant modality that is highly feasible for imaging of soft tissues (121), and the ability of ultrasound to detect and monitor development of uterine tumor should be explored in our *in vivo* mouse models.

In **paper II** we developed a protocol for EpCAM-AF680 NIRF imaging of orthotopic endometrial carcinoma in preclinical mouse models. NIRF imaging is feasible also in clinical settings, such as for intraoperative mapping of sentinel lymph nodes. NIRF probes specifically targeting tumor cells could help visualize tumor infiltrates and metastatic lesions in real-time during surgery, potentially improving tumor resection and/or reducing the amount of healthy tissue that is removed (214). NIRF imaging targeting EpCAM has been demonstrated to detect orthotopic tumors in cell-line based models of head and neck, breast and colorectal cancer, and EpCAM has been suggested as a multi-tumor target for image-guided surgery (215). As endometrial carcinoma primarily is a surgically treated disease, it would be interesting to explore if EpCAM-AF680 could be used for image-guided surgery also in this large patient group. This could initially be tested through preclinical mouse models. Future studies

should also include IHC evaluation of EpCAM expression in metastatic lesions, preferably in a large cohort of endometrial carcinoma patients.

ASRGL1

Thorough preclinical validation of potential biomarkers is crucial before proceeding to clinical trials, both to improve the success rate of translation from bench to bedside and to spare patients from unnecessary distress. Clinical trials should be conducted to assess the utility of ASRGL1 in hysterectomy specimen as a prognostic biomarker (**paper III**). We are the first to describe that ASRGL1 expression in pre-operative curettage independently predicts lymph node metastases (**paper IV**), and this should be validated in independent patient cohorts prior to clinical testing. Additionally, it would be interesting to explore the functional role of ASRGL1 in normal endometrium and endometrial carcinoma through *in vitro,* and potentially also *in vivo,* studies.

8. References

1. Tavassolli A, Devilee P. World Health Organization Classification of Tumours. Pathology and Genetics of Tumours of the Breast and Female Genital Organs. 2003. IARC Press: Lyon. Available from: http://www.iarc.fr/en/publications/pdfs-online/pat-gen/bb4/index.php.
2. J Ferlay, I Soerjomataram, M Ervik, R Dikshit, S Eser, C Mathers, et al. GLOBOCAN 2012 v1.0, Cancer Incidence and Mortality Worldwide: IARC CancerBase No. 11.Lyon, France: International Agency for Research on Cancer 2013 Available from: http://globocan.iarc.fr.
3. Cancer Registry of Norway. Cancer in Norway 2016 - Cancer incidence, mortality, survival and prevalence in Norway. Oslo: Cancer Registry of Norway,. 2017.
4. Lindemann K, Eskild A, Vatten LJ, Bray F. Endometrial cancer incidence trends in Norway during 1953-2007 and predictions for 2008-2027. International journal of cancer Journal international du cancer. 2010;127(11):2661-8.
5. Ferlay J, Soerjomataram I, Dikshit R, Eser S, Mathers C, Rebelo M, et al. Cancer incidence and mortality worldwide: sources, methods and major patterns in GLOBOCAN 2012. International journal of cancer Journal international du cancer. 2015;136(5):E359-86.
6. S. G. O. Clinical Practice Endometrial Cancer Working Group, Burke WM, Orr J, Leitao M, Salom E, Gehrig P, et al. Endometrial cancer: A review and current management strategies: Part I. Gynecologic oncology. 2014.
7. Setiawan VW, Yang HP, Pike MC, McCann SE, Yu H, Xiang YB, et al. Type I and II endometrial cancers: have they different risk factors? Journal of clinical oncology : official journal of the American Society of Clinical Oncology. 2013;31(20):2607-18.
8. Salvesen HB, Haldorsen IS, Trovik J. Markers for individualised therapy in endometrial carcinoma. The lancet oncology. 2012;13(8):e353-61.
9. Bender DBL, KK. Hormones and Receptors in Endometrial Cancer. Proc Obstet Gynecol. 2011;2(25).
10. Amant F, Moerman P, Neven P, Timmerman D, Van Limbergen E, Vergote I. Endometrial cancer. Lancet. 2005;366(9484):491-505.
11. Onstad MA, Schmandt RE, Lu KH. Addressing the Role of Obesity in Endometrial Cancer Risk, Prevention, and Treatment. Journal of clinical oncology : official journal of the American Society of Clinical Oncology. 2016;34(35):4225-30.
12. Meyer LA, Broaddus RR, Lu KH. Endometrial cancer and Lynch syndrome: clinical and pathologic considerations. Cancer Control. 2009;16(1):14-22.
13. Stadler ZK, Robson ME. Inherited predisposition to endometrial cancer: moving beyond Lynch syndrome. Cancer. 2015;121(5):644-7.
14. Dorum A SR, Vereide AB, Tingulstad S, Woie K, Fiane B. Nasjonalt handlingsprogram med retningslinjer for gynekologisk kreft. Helsedirektoratet. 2016.
15. van Hanegem N, Prins MM, Bongers MY, Opmeer BC, Sahota DS, Mol BW, et al. The accuracy of endometrial sampling in women with postmenopausal bleeding: a systematic review and meta-analysis. European journal of obstetrics, gynecology, and reproductive biology. 2016;197:147-55.
16. Di Cello A, Rania E, Zuccala V, Venturella R, Mocciaro R, Zullo F, et al. Failure to recognize preoperatively high-risk endometrial carcinoma is associated with a poor outcome. European journal of obstetrics, gynecology, and reproductive biology. 2015;194:153-60.

17. Werner HM, Trovik J, Marcickiewicz J, Tingulstad S, Staff AC, Engh ME, et al. A discordant histological risk classification in preoperative and operative biopsy in endometrial cancer is reflected in metastatic risk and prognosis. Eur J Cancer. 2013;49(3):625-32.
18. Eltabbakh GH, Shamonki J, Mount SL. Surgical stage, final grade, and survival of women with endometrial carcinoma whose preoperative endometrial biopsy shows well-differentiated tumors. Gynecologic oncology. 2005;99(2):309-12.
19. Frumovitz M, Singh DK, Meyer L, Smith DH, Wertheim I, Resnik E, et al. Predictors of final histology in patients with endometrial cancer. Gynecologic oncology. 2004;95(3):463-8.
20. Visser NCM, Reijnen C, Massuger L, Nagtegaal ID, Bulten J, Pijnenborg JMA. Accuracy of Endometrial Sampling in Endometrial Carcinoma: A Systematic Review and Meta-analysis. Obstet Gynecol. 2017;130(4):803-13.
21. Helpman L, Kupets R, Covens A, Saad RS, Khalifa MA, Ismiil N, et al. Assessment of endometrial sampling as a predictor of final surgical pathology in endometrial cancer. British journal of cancer. 2014;110(3):609-15.
22. Eggink FA, Mom CH, Bouwman K, Boll D, Becker JH, Creutzberg CL, et al. Less-favourable prognosis for low-risk endometrial cancer patients with a discordant pre- versus post-operative risk stratification. Eur J Cancer. 2017;78:82-90.
23. Giede C, Le T, Power P, Le T, Bentley J, Farrell S, et al. The role of surgery in endometrial cancer. Journal of obstetrics and gynaecology Canada : JOGC = Journal d'obstetrique et gynecologie du Canada : JOGC. 2013;35(4):370-4.
24. Epstein E, Blomqvist L. Imaging in endometrial cancer. Best Pract Res Clin Obstet Gynaecol. 2014;28(5):721-39.
25. Haldorsen IS, Salvesen HB. What Is the Best Preoperative Imaging for Endometrial Cancer? Curr Oncol Rep. 2016;18(4):25.
26. Pecorelli S. Revised FIGO staging for carcinoma of the vulva, cervix, and endometrium. International journal of gynaecology and obstetrics: the official organ of the International Federation of Gynaecology and Obstetrics. 2009;105(2):103-4.
27. Piulats JM, Guerra E, Gil-Martin M, Roman-Canal B, Gatius S, Sanz-Pamplona R, et al. Molecular approaches for classifying endometrial carcinoma. Gynecologic oncology. 2017;145(1):200-7.
28. Trovik J, Mauland KK, Werner HM, Wik E, Helland H, Salvesen HB. Improved survival related to changes in endometrial cancer treatment, a 30-year population based perspective. Gynecologic oncology. 2012;125(2):381-7.
29. Amant F, Mirza MR, Creutzberg CL. Cancer of the corpus uteri. International journal of gynaecology and obstetrics: the official organ of the International Federation of Gynaecology and Obstetrics. 2012;119 Suppl 2:S110-7.
30. Matias-Guiu X, Davidson B. Prognostic biomarkers in endometrial and ovarian carcinoma. Virchows Archiv : an international journal of pathology. 2014;464(3):315-31.
31. Gadducci A, Greco C. The evolving role of adjuvant therapy in endometrial cancer. Critical reviews in oncology/hematology. 2011;78(2):79-91.
32. Fotopoulou C, Kraetschell R, Dowdy S, Fujiwara K, Yaegashi N, Larusso D, et al. Surgical and systemic management of endometrial cancer: an international survey. Arch Gynecol Obstet. 2015;291(4):897-905.
33. Bodurtha Smith AJ, Fader AN, Tanner EJ. Sentinel lymph node assessment in endometrial cancer: a systematic review and meta-analysis. Am J Obstet Gynecol. 2017;216(5):459-76 e10.

34. Khoury-Collado F, St Clair C, Abu-Rustum NR. Sentinel Lymph Node Mapping in Endometrial Cancer: An Update. Oncologist. 2016;21(4):461-6.
35. Geppert B, Lonnerfors C, Bollino M, Persson J. Sentinel lymph node biopsy in endometrial cancer-Feasibility, safety and lymphatic complications. Gynecologic oncology. 2017.
36. Bradford LS, Rauh-Hain JA, Schorge J, Birrer MJ, Dizon DS. Advances in the management of recurrent endometrial cancer. Am J Clin Oncol. 2015;38(2):206-12.
37. Baudino TA. Targeted Cancer Therapy: The Next Generation of Cancer Treatment. Curr Drug Discov Technol. 2015;12(1):3-20.
38. Altundag O, Dursun P, Ayhan A. Emerging drugs in endometrial cancers. Expert Opin Emerg Drugs. 2010;15(4):557-68.
39. Kokka F, Brockbank E, Oram D, Gallagher C, Bryant A. Hormonal therapy in advanced or recurrent endometrial cancer. The Cochrane database of systematic reviews. 2010(12):CD007926.
40. Nout RA, Smit VT, Putter H, Jurgenliemk-Schulz IM, Jobsen JJ, Lutgens LC, et al. Vaginal brachytherapy versus pelvic external beam radiotherapy for patients with endometrial cancer of high-intermediate risk (PORTEC-2): an open-label, non-inferiority, randomised trial. Lancet. 2010;375(9717):816-23.
41. Creutzberg CL, van Putten WL, Koper PC, Lybeert ML, Jobsen JJ, Warlam-Rodenhuis CC, et al. Surgery and postoperative radiotherapy versus surgery alone for patients with stage-1 endometrial carcinoma: multicentre randomised trial. PORTEC Study Group. Post Operative Radiation Therapy in Endometrial Carcinoma. Lancet. 2000;355(9213):1404-11.
42. Kong A, Johnson N, Kitchener HC, Lawrie TA. Adjuvant radiotherapy for stage I endometrial cancer: an updated Cochrane systematic review and meta-analysis. Journal of the National Cancer Institute. 2012;104(21):1625-34.
43. Group AES, Blake P, Swart AM, Orton J, Kitchener H, Whelan T, et al. Adjuvant external beam radiotherapy in the treatment of endometrial cancer (MRC ASTEC and NCIC CTG EN.5 randomised trials): pooled trial results, systematic review, and meta-analysis. Lancet. 2009;373(9658):137-46.
44. Keys HM, Roberts JA, Brunetto VL, Zaino RJ, Spirtos NM, Bloss JD, et al. A phase III trial of surgery with or without adjunctive external pelvic radiation therapy in intermediate risk endometrial adenocarcinoma: a Gynecologic Oncology Group study. Gynecologic oncology. 2004;92(3):744-51.
45. Galaal K, Al Moundhri M, Bryant A, Lopes AD, Lawrie TA. Adjuvant chemotherapy for advanced endometrial cancer. The Cochrane database of systematic reviews. 2014;5:CD010681.
46. Rosen LS, Jacobs IA, Burkes RL. Bevacizumab in Colorectal Cancer: Current Role in Treatment and the Potential of Biosimilars. Target Oncol. 2017.
47. Cohen MH, Gootenberg J, Keegan P, Pazdur R. FDA drug approval summary: bevacizumab (Avastin) plus Carboplatin and Paclitaxel as first-line treatment of advanced/metastatic recurrent nonsquamous non-small cell lung cancer. Oncologist. 2007;12(6):713-8.
48. Cohen MH, Gootenberg J, Keegan P, Pazdur R. FDA drug approval summary: bevacizumab plus FOLFOX4 as second-line treatment of colorectal cancer. Oncologist. 2007;12(3):356-61.
49. Kwitkowski VE, Prowell TM, Ibrahim A, Farrell AT, Justice R, Mitchell SS, et al. FDA approval summary: temsirolimus as treatment for advanced renal cell carcinoma. Oncologist. 2010;15(4):428-35.

50. Lheureux S, Wilson M, Mackay HJ. Recent and current Phase II clinical trials in endometrial cancer: review of the state of art. Expert opinion on investigational drugs. 2014;23(6):773-92.
51. Oza AM, Elit L, Tsao MS, Kamel-Reid S, Biagi J, Provencher DM, et al. Phase II study of temsirolimus in women with recurrent or metastatic endometrial cancer: a trial of the NCIC Clinical Trials Group. Journal of clinical oncology : official journal of the American Society of Clinical Oncology. 2011;29(24):3278-85.
52. Hanahan D, Weinberg RA. Hallmarks of cancer: the next generation. Cell. 2011;144(5):646-74.
53. Ott PA, Bang YJ, Berton-Rigaud D, Elez E, Pishvaian MJ, Rugo HS, et al. Safety and Antitumor Activity of Pembrolizumab in Advanced Programmed Death Ligand 1-Positive Endometrial Cancer: Results From the KEYNOTE-028 Study. Journal of clinical oncology : official journal of the American Society of Clinical Oncology. 2017;35(22):2535-41.
54. Arend RC, Jones BA, Martinez A, Goodfellow P. Endometrial cancer: Molecular markers and management of advanced stage disease. Gynecologic oncology. 2018.
55. Hanahan D, Weinberg RA. The hallmarks of cancer. Cell. 2000;100(1):57-70.
56. Burrell RA, McGranahan N, Bartek J, Swanton C. The causes and consequences of genetic heterogeneity in cancer evolution. Nature. 2013;501(7467):338-45.
57. McGranahan N, Swanton C. Clonal Heterogeneity and Tumor Evolution: Past, Present, and the Future. Cell. 2017;168(4):613-28.
58. Cancer Genome Atlas Research N, Weinstein JN, Collisson EA, Mills GB, Shaw KR, Ozenberger BA, et al. The Cancer Genome Atlas Pan-Cancer analysis project. Nat Genet. 2013;45(10):1113-20.
59. Lawrence MS, Stojanov P, Mermel CH, Robinson JT, Garraway LA, Golub TR, et al. Discovery and saturation analysis of cancer genes across 21 tumour types. Nature. 2014;505(7484):495-501.
60. Cancer Genome Atlas Research N, Kandoth C, Schultz N, Cherniack AD, Akbani R, Liu Y, et al. Integrated genomic characterization of endometrial carcinoma. Nature. 2013;497(7447):67-73.
61. Singh N, Gilks CB. The changing landscape of gynaecological cancer diagnosis: implications for histopathological practice in the 21st century. Histopathology. 2017;70(1):56-69.
62. Kommoss S, McConechy MK, Kommoss F, Leung S, Bunz A, Magrill J, et al. Final validation of the ProMisE molecular classifier for endometrial carcinoma in a large population-based case series. Annals of oncology : official journal of the European Society for Medical Oncology / ESMO. 2018;29(5):1180-8.
63. Eritja N, Yeramian A, Chen BJ, Llobet-Navas D, Ortega E, Colas E, et al. Endometrial Carcinoma: Specific Targeted Pathways. Adv Exp Med Biol. 2017;943:149-207.
64. Diver EJ, Foster R, Rueda BR, Growdon WB. The Therapeutic Challenge of Targeting HER2 in Endometrial Cancer. Oncologist. 2015;20(9):1058-68.
65. Biomarkers Definitions Working Group. Biomarkers and surrogate endpoints: preferred definitions and conceptual framework. Clinical pharmacology and therapeutics. 2001;69(3):89-95.
66. Mordente A, Meucci E, Martorana GE, Silvestrini A. Cancer Biomarkers Discovery and Validation: State of the Art, Problems and Future Perspectives. Adv Exp Med Biol. 2015;867:9-26.

67. Duffy MJ, Sturgeon CM, Soletormos G, Barak V, Molina R, Hayes DF, et al. Validation of new cancer biomarkers: a position statement from the European group on tumor markers. Clin Chem. 2015;61(6):809-20.
68. Werner HM, Salvesen HB. Current status of molecular biomarkers in endometrial cancer. Curr Oncol Rep. 2014;16(9):403.
69. Oldenhuis CN, Oosting SF, Gietema JA, de Vries EG. Prognostic versus predictive value of biomarkers in oncology. Eur J Cancer. 2008;44(7):946-53.
70. Nalejska E, Maczynska E, Lewandowska MA. Prognostic and predictive biomarkers: tools in personalized oncology. Mol Diagn Ther. 2014;18(3):273-84.
71. Huang J, Hu W, Sood AK. Prognostic biomarkers in ovarian cancer. Cancer Biomark. 2010;8(4-5):231-51.
72. Engelsen IB, Stefansson I, Akslen LA, Salvesen HB. Pathologic expression of p53 or p16 in preoperative curettage specimens identifies high-risk endometrial carcinomas. Am J Obstet Gynecol. 2006;195(4):979-86.
73. Wik E, Trovik J, Iversen OE, Engelsen IB, Stefansson IM, Vestrheim LC, et al. Deoxyribonucleic acid ploidy in endometrial carcinoma: a reproducible and valid prognostic marker in a routine diagnostic setting. Am J Obstet Gynecol. 2009;201(6):603 e1-7.
74. Mauland KK, Wik E, Salvesen HB. Clinical value of DNA content assessment in endometrial cancer. Cytometry B Clin Cytom. 2014;86(3):154-63.
75. Njolstad TS, Trovik J, Hveem TS, Kjaereng ML, Kildal W, Pradhan M, et al. DNA ploidy in curettage specimens identifies high-risk patients and lymph node metastasis in endometrial cancer. British journal of cancer. 2015;112(10):1656-64.
76. Wik E, Raeder MB, Krakstad C, Trovik J, Birkeland E, Hoivik EA, et al. Lack of estrogen receptor-alpha is associated with epithelial-mesenchymal transition and PI3K alterations in endometrial carcinoma. Clinical cancer research : an official journal of the American Association for Cancer Research. 2013;19(5):1094-105.
77. Krakstad C, Trovik J, Wik E, Engelsen IB, Werner HM, Birkeland E, et al. Loss of GPER identifies new targets for therapy among a subgroup of ERalpha-positive endometrial cancer patients with poor outcome. British journal of cancer. 2012;106(10):1682-8.
78. Trovik J, Wik E, Werner HM, Krakstad C, Helland H, Vandenput I, et al. Hormone receptor loss in endometrial carcinoma curettage predicts lymph node metastasis and poor outcome in prospective multicentre trial. Eur J Cancer. 2013;49(16):3431-41.
79. Tangen IL, Werner HM, Berg A, Halle MK, Kusonmano K, Trovik J, et al. Loss of progesterone receptor links to high proliferation and increases from primary to metastatic endometrial cancer lesions. Eur J Cancer. 2014;50(17):3003-10.
80. Geels YP, Pijnenborg JM, Gordon BB, Fogel M, Altevogt P, Masadah R, et al. L1CAM Expression is Related to Non-Endometrioid Histology, and Prognostic for Poor Outcome in Endometrioid Endometrial Carcinoma. Pathol Oncol Res. 2016;22(4):863-8.
81. Pasanen A, Tuomi T, Isola J, Staff S, Butzow R, Loukovaara M. L1 Cell Adhesion Molecule as a Predictor of Disease-Specific Survival and Patterns of Relapse in Endometrial Cancer. International journal of gynecological cancer : official journal of the International Gynecological Cancer Society. 2016;26(8):1465-71.
82. Tangen IL, Kopperud RK, Visser NC, Staff AC, Tingulstad S, Marcickiewicz J, et al. Expression of L1CAM in curettage or high L1CAM level in preoperative blood samples predicts lymph node metastases and poor outcome in endometrial cancer patients. British journal of cancer. 2017.

83. van der Putten LJ, Visser NC, van de Vijver K, Santacana M, Bronsert P, Bulten J, et al. L1CAM expression in endometrial carcinomas: an ENITEC collaboration study. British journal of cancer. 2016;115(6):716-24.
84. Zeimet AG, Reimer D, Huszar M, Winterhoff B, Puistola U, Azim SA, et al. L1CAM in early-stage type I endometrial cancer: results of a large multicenter evaluation. Journal of the National Cancer Institute. 2013;105(15):1142-50.
85. Slamon DJ, Leyland-Jones B, Shak S, Fuchs H, Paton V, Bajamonde A, et al. Use of chemotherapy plus a monoclonal antibody against HER2 for metastatic breast cancer that overexpresses HER2. N Engl J Med. 2001;344(11):783-92.
86. Hidalgo M, Amant F, Biankin AV, Budinska E, Byrne AT, Caldas C, et al. Patient-derived xenograft models: an emerging platform for translational cancer research. Cancer Discov. 2014;4(9):998-1013.
87. Husby JA, Salvesen OO, Magnussen IJ, Trovik J, Bjorge L, Salvesen HB, et al. Tumour apparent diffusion coefficient is associated with depth of myometrial invasion and is negatively correlated to tumour volume in endometrial carcinomas. Clin Radiol. 2015;70(5):487-94.
88. Cao K, Gao M, Sun YS, Li YL, Sun Y, Gao YN, et al. Apparent diffusion coefficient of diffusion weighted MRI in endometrial carcinoma-Relationship with local invasiveness. Eur J Radiol. 2012;81(8):1926-30.
89. Liu FY, Chao A, Lai CH, Chou HH, Yen TC. Metabolic tumor volume by 18F-FDG PET/CT is prognostic for stage IVB endometrial carcinoma. Gynecologic oncology. 2012;125(3):566-71.
90. Epstein E, Van Holsbeke C, Mascilini F, Masback A, Kannisto P, Ameye L, et al. Gray-scale and color Doppler ultrasound characteristics of endometrial cancer in relation to stage, grade and tumor size. Ultrasound Obstet Gynecol. 2011;38(5):586-93.
91. Thomas RM, Van Dyke T, Merlino G, Day CP. Concepts in Cancer Modeling: A Brief History. Cancer research. 2016;76(20):5921-5.
92. Kam Y, Rejniak KA, Anderson AR. Cellular modeling of cancer invasion: integration of in silico and in vitro approaches. J Cell Physiol. 2012;227(2):431-8.
93. Cekanova M, Rathore K. Animal models and therapeutic molecular targets of cancer: utility and limitations. Drug Des Dev Ther. 2014;8:1911-22.
94. Wilding JL, Bodmer WF. Cancer cell lines for drug discovery and development. Cancer research. 2014;74(9):2377-84.
95. Frese KK, Tuveson DA. Maximizing mouse cancer models. Nat Rev Cancer. 2007;7(9):645-58.
96. Begley CG, Ellis LM. Drug development: Raise standards for preclinical cancer research. Nature. 2012;483(7391):531-3.
97. Cabrera S, Llaurado M, Castellvi J, Fernandez Y, Alameda F, Colas E, et al. Generation and characterization of orthotopic murine models for endometrial cancer. Clinical & experimental metastasis. 2012;29(3):217-27.
98. Talmadge JE, Singh RK, Fidler IJ, Raz A. Murine models to evaluate novel and conventional therapeutic strategies for cancer. The American journal of pathology. 2007;170(3):793-804.
99. Cheon DJ, Orsulic S. Mouse models of cancer. Annu Rev Pathol. 2011;6:95-119.
100. Galuschka C, Proynova R, Roth B, Augustin HG, Muller-Decker K. Models in Translational Oncology: A Public Resource Database for Preclinical Cancer Research. Cancer research. 2017;77(10):2557-63.
101. Hansen K, Khanna C. Spontaneous and genetically engineered animal models; use in preclinical cancer drug development. Eur J Cancer. 2004;40(6):858-80.

102. Vandamme TF. Use of rodents as models of human diseases. Journal of pharmacy & bioallied sciences. 2014;6(1):2-9.
103. Siolas D, Hannon GJ. Patient-derived tumor xenografts: transforming clinical samples into mouse models. Cancer research. 2013;73(17):5315-9.
104. Dobbin ZK, AA. Steg, AD. Erickson, BK. Shah, MM. Alvarez, LD. et al. Using heterogeneity of the patient-derived xenograft model to identify the chemoresistant population in ovarian cancer. Oncotarget. 2014;5:8750 - 64.
105. Doll A, Gonzalez M, Abal M, Llaurado M, Rigau M, Colas E, et al. An orthotopic endometrial cancer mouse model demonstrates a role for RUNX1 in distant metastasis. International journal of cancer Journal international du cancer. 2009;125(2):257-63.
106. Che Q, Liu BY, Liao Y, Zhang HJ, Yang TT, He YY, et al. Activation of a positive feedback loop involving IL-6 and aromatase promotes intratumoral 17beta-estradiol biosynthesis in endometrial carcinoma microenvironment. International journal of cancer Journal international du cancer. 2014;135(2):282-94.
107. Kamat AA, Merritt WM, Coffey D, Lin YG, Patel PR, Broaddus R, et al. Clinical and biological significance of vascular endothelial growth factor in endometrial cancer. Clinical cancer research : an official journal of the American Association for Cancer Research. 2007;13(24):7487-95.
108. Merritt WM, Kamat AA, Hwang JY, Bottsford-Miller J, Lu C, Lin YG, et al. Clinical and biological impact of EphA2 overexpression and angiogenesis in endometrial cancer. Cancer Biol Ther. 2010;10(12):1306-14.
109. Pillozzi S, Fortunato A, De Lorenzo E, Borrani E, Giachi M, Scarselli G, et al. Over-Expression of the LH Receptor Increases Distant Metastases in an Endometrial Cancer Mouse Model. Front Oncol. 2013;3:285.
110. Theisen ER, Gajiwala S, Bearss J, Sorna V, Sharma S, Janat-Amsbury M. Reversible inhibition of lysine specific demethylase 1 is a novel anti-tumor strategy for poorly differentiated endometrial carcinoma. BMC cancer. 2014;14:752.
111. Depreeuw J, Hermans E, Schrauwen S, Annibali D, Coenegrachts L, Thomas D, et al. Characterization of patient-derived tumor xenograft models of endometrial cancer for preclinical evaluation of targeted therapies. Gynecologic oncology. 2015;139(1):118-26.
112. Winder A, Unno K, Yu Y, Lurain J, Kim JJ. The allosteric AKT inhibitor, MK2206, decreases tumor growth and invasion in patient derived xenografts of endometrial cancer. Cancer Biol Ther. 2017;18(12):958-64.
113. Schrauwen S, Coenegrachts L, Depreeuw J, Luyten C, Verbist G, Debruyne D, et al. Microsatellite instable and microsatellite stable primary endometrial carcinoma cells and their subcutaneous and orthotopic xenografts recapitulate the characteristics of the corresponding primary tumor. International journal of gynecological cancer : official journal of the International Gynecological Cancer Society. 2015;25(3):363-71.
114. De Souza R, Spence T, Huang H, Allen C. Preclinical imaging and translational animal models of cancer for accelerated clinical implementation of nanotechnologies and macromolecular agents. J Control Release. 2015;219:313-30.
115. Van Nyen T, Moiola CP, Colas E, Annibali D, Amant F. Modeling Endometrial Cancer: Past, Present, and Future. Int J Mol Sci. 2018;19(8).
116. O'Farrell AC, Shnyder SD, Marston G, Coletta PL, Gill JH. Non-invasive molecular imaging for preclinical cancer therapeutic development. Br J Pharmacol. 2013;169(4):719-35.

117. Wolf G, Abolmaali N. Preclinical molecular imaging using PET and MRI. Recent Results Cancer Res. 2013;187:257-310.
118. Nogami Y, Iida M, Banno K, Kisu I, Adachi M, Nakamura K, et al. Application of FDG-PET in cervical cancer and endometrial cancer: utility and future prospects. Anticancer research. 2014;34(2):585-92.
119. Weissleder R. Scaling down imaging: molecular mapping of cancer in mice. Nat Rev Cancer. 2002;2(1):11-8.
120. Kocher B, Piwnica-Worms D. Illuminating cancer systems with genetically engineered mouse models and coupled luciferase reporters in vivo. Cancer Discov. 2013;3(6):616-29.
121. Wang Y, Tseng JC, Sun Y, Beck AH, Kung AL. Noninvasive imaging of tumor burden and molecular pathways in mouse models of cancer. Cold Spring Harb Protoc. 2015;2015(2):135-44.
122. Currie S, Hoggard N, Craven IJ, Hadjivassiliou M, Wilkinson ID. Understanding MRI: basic MR physics for physicians. Postgraduate medical journal. 2013;89(1050):209-23.
123. Haldorsen IS, Salvesen HB. Staging of endometrial carcinomas with MRI using traditional and novel MRI techniques. Clin Radiol. 2012;67(1):2-12.
124. Vandecaveye V, Dresen R, De Keyzer F. Novel imaging techniques in gynaecological cancer. Current opinion in oncology. 2017;29(5):335-42.
125. Fasmer KE, Bjornerud A, Ytre-Hauge S, Gruner R, Tangen IL, Werner HM, et al. Preoperative quantitative dynamic contrast-enhanced MRI and diffusion-weighted imaging predict aggressive disease in endometrial cancer. Acta Radiol. 2017:284185117740932.
126. Bianchi A, Dufort S, Fortin PY, Lux F, Raffard G, Tassali N, et al. In vivo MRI for effective non-invasive detection and follow-up of an orthotopic mouse model of lung cancer. NMR Biomed. 2014;27(8):971-9.
127. Goldman LW. Principles of CT and CT technology. Journal of nuclear medicine technology. 2007;35(3):115-28; quiz 29-30.
128. Paans AM, van Waarde A, Elsinga PH, Willemsen AT, Vaalburg W. Positron emission tomography: the conceptual idea using a multidisciplinary approach. Methods. 2002;27(3):195-207.
129. Jager PL, de Korte MA, Lub-de Hooge MN, van Waarde A, Koopmans KP, Perik PJ, et al. Molecular imaging: what can be used today. Cancer imaging : the official publication of the International Cancer Imaging Society. 2005;5 Spec No A:S27-32.
130. Weber WA, Schwaiger M, Avril N. Quantitative assessment of tumor metabolism using FDG-PET imaging. Nuclear medicine and biology. 2000;27(7):683-7.
131. Soret M, Bacharach SL, Buvat I. Partial-volume effect in PET tumor imaging. Journal of nuclear medicine : official publication, Society of Nuclear Medicine. 2007;48(6):932-45.
132. Nikaki A, Angelidis G, Efthimiadou R, Tsougos I, Valotassiou V, Fountas K, et al. (18)F-fluorothymidine PET imaging in gliomas: an update. Ann Nucl Med. 2017;31(7):495-505.
133. Bai B, Bading J, Conti PS. Tumor quantification in clinical positron emission tomography. Theranostics. 2013;3(10):787-801.
134. Bollineni VR, Ytre-Hauge S, Bollineni-Balabay O, Salvesen HB, Haldorsen IS. High Diagnostic Value of 18F-FDG PET/CT in Endometrial Cancer: Systematic Review and Meta-Analysis of the Literature. Journal of nuclear medicine : official publication, Society of Nuclear Medicine. 2016;57(6):879-85.

135. Mokhtar M, Kondo K, Takizawa H, Ohtani T, Otsuka H, Kubo H, et al. Non-invasive monitoring of anticancer effects of cisplatin on lung cancer in an orthotopic SCID mouse model using [(1)(8)F] FDG PET-CT. Oncol Rep. 2014;31(5):2007-14.
136. Eschbach RS, Kazmierczak PM, Heimer MM, Todica A, Hirner-Eppeneder H, Schneider MJ, et al. (18)F-FDG-PET/CT and diffusion-weighted MRI for monitoring a BRAF and CDK 4/6 inhibitor combination therapy in a murine model of human melanoma. Cancer imaging : the official publication of the International Cancer Imaging Society. 2018;18(1):2.
137. Chen ZY, Wang YX, Yang F, Lin Y, Zhou QL, Liao YY. New Researches and Application Progress of Commonly Used Optical Molecular Imaging Technology. BioMed research international. 2014;2014:429198.
138. Ignowski JM, Schaffer DV. Kinetic analysis and modeling of firefly luciferase as a quantitative reporter gene in live mammalian cells. Biotechnology and bioengineering. 2004;86(7):827-34.
139. Kang JH, Chung JK. Molecular-genetic imaging based on reporter gene expression. Journal of nuclear medicine : official publication, Society of Nuclear Medicine. 2008;49 Suppl 2:164S-79S.
140. Keereweer S, Van Driel PB, Snoeks TJ, Kerrebijn JD, Baatenburg de Jong RJ, Vahrmeijer AL, et al. Optical image-guided cancer surgery: challenges and limitations. Clinical cancer research : an official journal of the American Association for Cancer Research. 2013;19(14):3745-54.
141. Allison RR. Fluorescence guided resection (FGR): A primer for oncology. Photodiagnosis Photodyn Ther. 2015.
142. Rocha A, Dominguez AM, Lecuru F, Bourdel N. Indocyanine green and infrared fluorescence in detection of sentinel lymph nodes in endometrial and cervical cancer staging - a systematic review. European journal of obstetrics, gynecology, and reproductive biology. 2016;206:213-9.
143. McCormack E, Mujic M, Osdal T, Bruserud O, Gjertsen BT. Multiplexed mAbs: a new strategy in preclinical time-domain imaging of acute myeloid leukemia. Blood. 2013;121(7):e34-42.
144. Wang KH, Wang YM, Chiu LH, Chen TC, Tsai YH, Zuo CS, et al. Optical imaging of ovarian cancer using a matrix metalloproteinase-3-sensitive near-infrared fluorescent probe. PloS one. 2018;13(2):e0192047.
145. Tangen IL, Krakstad C, Halle MK, Werner HM, Oyan AM, Kusonmano K, et al. Switch in FOXA1 status associates with endometrial cancer progression. PloS one. 2014;9(5):e98069.
146. Edqvist PH, Huvila J, Forsstrom B, Talve L, Carpen O, Salvesen HB, et al. Loss of ASRGL1 expression is an independent biomarker for disease-specific survival in endometrioid endometrial carcinoma. Gynecologic oncology. 2015;137(3):529-37.
147. Huvila J, Laajala TD, Edqvist PH, Mardinoglu A, Talve L, Ponten F, et al. Combined ASRGL1 and p53 immunohistochemistry as an independent predictor of survival in endometrioid endometrial carcinoma. Gynecologic oncology. 2018.
148. Engelsen IB, Stefansson IM, Akslen LA, Salvesen HB. GATA3 expression in estrogen receptor alpha-negative endometrial carcinomas identifies aggressive tumors with high proliferation and poor patient survival. Am J Obstet Gynecol. 2008;199(5):543 e1-7.
149. Berg A, Fasmer KE, Mauland KK, Ytre-Hauge S, Hoivik EA, Husby JA, et al. Tissue and imaging biomarkers for hypoxia predict poor outcome in endometrial cancer. Oncotarget. 2016;7(43):69844-56.

150. Haldorsen IS, Gruner R, Husby JA, Magnussen IJ, Werner HM, Salvesen OO, et al. Dynamic contrast-enhanced MRI in endometrial carcinoma identifies patients at increased risk of recurrence. Eur Radiol. 2013;23(10):2916-25.
151. Ytre-Hauge S, Husby JA, Magnussen IJ, Werner HM, Salvesen OO, Bjorge L, et al. Preoperative tumor size at MRI predicts deep myometrial invasion, lymph node metastases, and patient outcome in endometrial carcinomas. International journal of gynecological cancer : official journal of the International Gynecological Cancer Society. 2015;25(3):459-66.
152. Husby JA, Reitan BC, Biermann M, Trovik J, Bjorge L, Magnussen IJ, et al. Metabolic Tumor Volume on 18F-FDG PET/CT Improves Preoperative Identification of High-Risk Endometrial Carcinoma Patients. Journal of nuclear medicine : official publication, Society of Nuclear Medicine. 2015;56(8):1191-8.
153. Lorens JB, Jang Y, Rossi AB, Payan DG, Bogenberger JM. Optimization of regulated LTR-mediated expression. Virology. 2000;272(1):7-15.
154. Helland O, Popa M, Vintermyr OK, Molven A, Gjertsen BT, Bjorge L, et al. First in-mouse development and application of a surgically relevant xenograft model of ovarian carcinoma. PloS one. 2014;9(3):e89527.
155. El-Sahwi K, Bellone S, Cocco E, Casagrande F, Bellone M, Abu-Khalaf M, et al. Overexpression of EpCAM in uterine serous papillary carcinoma: implications for EpCAM-specific immunotherapy with human monoclonal antibody adecatumumab (MT201). Mol Cancer Ther. 2010;9(1):57-66.
156. Pavelic J, Radakovic B, Pavelic K. Insulin-like growth factor 2 and its receptors (IGF 1R and IGF 2R/mannose 6-phosphate) in endometrial adenocarcinoma. Gynecologic oncology. 2007;105(3):727-35.
157. McCampbell A, Broaddus R, Loose D, Davies P. Overexpression of the insulin-like growth factor I receptor and activation of the AKT pathway in hyperplastic endometrium Clinical cancer research : an official journal of the American Association for Cancer Research. 2006;21(1;12):6373-8.
158. Liang S, Huang C, Jia S, Wang B. Activated leukocyte cell adhesion molecule expression is up-regulated in the development of endometrioid carcinoma. International journal of gynecological cancer : official journal of the International Gynecological Cancer Society. 2011;21(3):523-8.
159. Fogel M, Huszar M, Altevogt P, Ben-Arie A. L1 (CD171) as a novel biomarker for ovarian and endometrial carcinomas. Expert review of molecular diagnostics. 2004;4(4):455-62.
160. Devis L, Moiola CP, Masia N, Martinez-Garcia E, Santacana M, Stirbat TV, et al. Activated leukocyte cell adhesion molecule (ALCAM) is a marker of recurrence and promotes cell migration, invasion, and metastasis in early-stage endometrioid endometrial cancer. J Pathol. 2017;241(4):475-87.
161. Haldorsen IS, Popa M, Fonnes T, Brekke N, Kopperud R, Visser NC, et al. Multimodal Imaging of Orthotopic Mouse Model of Endometrial Carcinoma. PloS one. 2015;10(8):e0135220.
162. Sharma SV, Haber DA, Settleman J. Cell line-based platforms to evaluate the therapeutic efficacy of candidate anticancer agents. Nat Rev Cancer. 2010;10(4):241-53.
163. Goodspeed A, Heiser LM, Gray JW, Costello JC. Tumor-Derived Cell Lines as Molecular Models of Cancer Pharmacogenomics. Mol Cancer Res. 2016;14(1):3-13.
164. Boretto M, Cox B, Noben M, Hendriks N, Fassbender A, Roose H, et al. Development of organoids from mouse and human endometrium showing

endometrial epithelium physiology and long-term expandability. Development. 2017;144(10):1775-86.
165. Turco MY, Gardner L, Hughes J, Cindrova-Davies T, Gomez MJ, Farrell L, et al. Long-term, hormone-responsive organoid cultures of human endometrium in a chemically defined medium. Nat Cell Biol. 2017;19(5):568-77.
166. Pauli C, Hopkins BD, Prandi D, Shaw R, Fedrizzi T, Sboner A, et al. Personalized In Vitro and In Vivo Cancer Models to Guide Precision Medicine. Cancer Discov. 2017;7(5):462-77.
167. van de Wetering M, Francies HE, Francis JM, Bounova G, Iorio F, Pronk A, et al. Prospective derivation of a living organoid biobank of colorectal cancer patients. Cell. 2015;161(4):933-45.
168. Mak IWY, Evaniew N, Ghert M. Lost in translation: animal models and clinical trials in cancer treatment. Am J Transl Res. 2014;6(2):114-8.
169. Tentler JJ, Tan AC, Weekes CD, Jimeno A, Leong S, Pitts TM, et al. Patient-derived tumour xenografts as models for oncology drug development. Nat Rev Clin Oncol. 2012;9(6):338-50.
170. Cassidy JW, Caldas C, Bruna A. Maintaining Tumor Heterogeneity in Patient-Derived Tumor Xenografts. Cancer research. 2015;75(15):2963-8.
171. Moiola CP, Lopez-Gil C, Cabrera S, Garcia A, Van Nyen T, Annibali D, et al. Patient-Derived Xenograft Models for Endometrial Cancer Research. Int J Mol Sci. 2018;19(8).
172. Unno K, Ono M, Winder AD, Maniar KP, Paintal AS, Yu Y, et al. Establishment of human patient-derived endometrial cancer xenografts in NOD scid gamma mice for the study of invasion and metastasis. PloS one. 2014;9(12):e116064.
173. Altwerger G, Bonazzoli E, Bellone S, Egawa-Takata T, Menderes G, Pettinella F, et al. In Vitro and In Vivo Activity of IMGN853, an Antibody-Drug Conjugate Targeting Folate Receptor Alpha Linked to DM4, in Biologically Aggressive Endometrial Cancers. Mol Cancer Ther. 2018;17(5):1003-11.
174. Werner HM, Trovik J, Marcickiewicz J, Tingulstad S, Staff AC, Amant F, et al. Revision of FIGO surgical staging in 2009 for endometrial cancer validates to improve risk stratification. Gynecologic oncology. 2012;125(1):103-8.
175. Jordan MA, Wilson L. Microtubules as a target for anticancer drugs. Nat Rev Cancer. 2004;4(4):253-65.
176. Fader AN, Roque DM, Siegel E, Buza N, Hui P, Abdelghany O, et al. Randomized Phase II Trial of Carboplatin-Paclitaxel Versus Carboplatin-Paclitaxel-Trastuzumab in Uterine Serous Carcinomas That Overexpress Human Epidermal Growth Factor Receptor 2/neu. Journal of clinical oncology : official journal of the American Society of Clinical Oncology. 2018;36(20):2044-51.
177. Trzpis M, McLaughlin PM, de Leij LM, Harmsen MC. Epithelial cell adhesion molecule: more than a carcinoma marker and adhesion molecule. The American journal of pathology. 2007;171(2):386-95.
178. Moestue SA, Huuse EM, Lindholm EM, Bofin A, Engebraaten O, Maelandsmo GM, et al. Low-molecular contrast agent dynamic contrast-enhanced (DCE)-MRI and diffusion-weighted (DW)-MRI in early assessment of bevacizumab treatment in breast cancer xenografts. J Magn Reson Imaging. 2013;38(5):1043-53.
179. McKinley ET, Smith RA, Zhao P, Fu A, Saleh SA, Uddin MI, et al. 3'-Deoxy-3'-18F-fluorothymidine PET predicts response to (V600E)BRAF-targeted therapy in preclinical models of colorectal cancer. Journal of nuclear medicine : official publication, Society of Nuclear Medicine. 2013;54(3):424-30.

180. Liebsch L, Kailayangiri S, Beck L, Altvater B, Koch R, Dierkes C, et al. Ewing sarcoma dissemination and response to T-cell therapy in mice assessed by whole-body magnetic resonance imaging. British journal of cancer. 2013;109(3):658-66.
181. O'Hurley G, Sjostedt E, Rahman A, Li B, Kampf C, Ponten F, et al. Garbage in, garbage out: a critical evaluation of strategies used for validation of immunohistochemical biomarkers. Molecular oncology. 2014;8(4):783-98.
182. Fons G, Hasibuan SM, van der Velden J, ten Kate FJ. Validation of tissue microarray technology in endometrioid cancer of the endometrium. J Clin Pathol. 2007;60(5):500-3.
183. Kononen J, Bubendorf L, Kallioniemi A, Barlund M, Schraml P, Leighton S, et al. Tissue microarrays for high-throughput molecular profiling of tumor specimens. Nat Med. 1998;4(7):844-7.
184. Zhang D, Salto-Tellez M, Putti TC, Do E, Koay ES. Reliability of tissue microarrays in detecting protein expression and gene amplification in breast cancer. Modern pathology : an official journal of the United States and Canadian Academy of Pathology, Inc. 2003;16(1):79-84.
185. Aas T, Borresen AL, Geisler S, Smith-Sorensen B, Johnsen H, Varhaug JE, et al. Specific P53 mutations are associated with de novo resistance to doxorubicin in breast cancer patients. Nat Med. 1996;2(7):811-4.
186. Lin B, Utleg AG, Gravdal K, White JT, Halvorsen OJ, Lu W, et al. WDR19 expression is increased in prostate cancer compared with normal cells, but low-intensity expression in cancers is associated with shorter time to biochemical failures and local recurrence. Clinical cancer research : an official journal of the American Association for Cancer Research. 2008;14(5):1397-406.
187. Bachmann IM, Halvorsen OJ, Collett K, Stefansson IM, Straume O, Haukaas SA, et al. EZH2 expression is associated with high proliferation rate and aggressive tumor subgroups in cutaneous melanoma and cancers of the endometrium, prostate, and breast. Journal of clinical oncology : official journal of the American Society of Clinical Oncology. 2006;24(2):268-73.
188. Koo TK, Li MY. A Guideline of Selecting and Reporting Intraclass Correlation Coefficients for Reliability Research. J Chiropr Med. 2016;15(2):155-63.
189. Stelloo E, Nout RA, Naves LC, Ter Haar NT, Creutzberg CL, Smit VT, et al. High concordance of molecular tumor alterations between pre-operative curettage and hysterectomy specimens in patients with endometrial carcinoma. Gynecologic oncology. 2014;133(2):197-204.
190. Oreskovic S, Babic D, Kalafatic D, Barisic D, Beketic-Oreskovic L. A significance of immunohistochemical determination of steroid receptors, cell proliferation factor Ki-67 and protein p53 in endometrial carcinoma. Gynecologic oncology. 2004;93(1):34-40.
191. Obeidat BR, Matalka, II, Mohtaseb AA, Al-Kaisi NS. Selected immuno-histochemical markers in curettage specimens and their correlation with final pathologic findings in endometrial cancer patients. Pathol Oncol Res. 2013;19(2):229-35.
192. Colombo N, Preti E, Landoni F, Carinelli S, Colombo A, Marini C, et al. Endometrial cancer: ESMO Clinical Practice Guidelines for diagnosis, treatment and follow-up. Annals of oncology : official journal of the European Society for Medical Oncology / ESMO. 2013;24 Suppl 6:vi33-8.
193. Colombo N, Creutzberg C, Amant F, Bosse T, Gonzalez-Martin A, Ledermann J, et al. ESMO-ESGO-ESTRO Consensus Conference on Endometrial Cancer: diagnosis,

treatment and follow-up. Annals of oncology : official journal of the European Society for Medical Oncology / ESMO. 2016;27(1):16-41.
194. Koh WJ, Greer BE, Abu-Rustum NR, Apte SM, Campos SM, Chan J, et al. Uterine neoplasms, version 1.2014. J Natl Compr Canc Netw. 2014;12(2):248-80.
195. Salvesen HB, Carter SL, Mannelqvist M, Dutt A, Getz G, Stefansson IM, et al. Integrated genomic profiling of endometrial carcinoma associates aggressive tumors with indicators of PI3 kinase activation. Proceedings of the National Academy of Sciences of the United States of America. 2009;106(12):4834-9.
196. Wik E, Trovik J, Kusonmano K, Birkeland E, Raeder MB, Pashtan I, et al. Endometrial Carcinoma Recurrence Score (ECARS) validates to identify aggressive disease and associates with markers of epithelial-mesenchymal transition and PI3K alterations. Gynecologic oncology. 2014;134(3):599-606.
197. O'Mara TA, Zhao M, Spurdle AB. Meta-analysis of gene expression studies in endometrial cancer identifies gene expression profiles associated with aggressive disease and patient outcome. Sci Rep. 2016;6:36677.
198. Huvila J, Laajala TD, Edqvist PH, Mardinoglu A, Talve L, Ponten F, et al. Combined ASRGL1 and p53 immunohistochemistry as an independent predictor of survival in endometrioid endometrial carcinoma. Gynecologic oncology. 2018;149(1):173-80.
199. Mehlen P, Puisieux A. Metastasis: a question of life or death. Nat Rev Cancer. 2006;6(6):449-58.
200. Tangen IL, Onyango TB, Kopperud R, Berg A, Halle MK, Oyan AM, et al. Androgen receptor as potential therapeutic target in metastatic endometrial cancer. Oncotarget. 2016;7(31):49289-98.
201. Bush LA, Herr JC, Wolkowicz M, Sherman NE, Shore A, Flickinger CJ. A novel asparaginase-like protein is a sperm autoantigen in rats. Mol Reprod Dev. 2002;62(2):233-47.
202. Cantor JR, Stone EM, Chantranupong L, Georgiou G. The human asparaginase-like protein 1 hASRGL1 is an Ntn hydrolase with beta-aspartyl peptidase activity. Biochemistry. 2009;48(46):11026-31.
203. Zhang J, Fan J, Venneti S, Cross JR, Takagi T, Bhinder B, et al. Asparagine plays a critical role in regulating cellular adaptation to glutamine depletion. Mol Cell. 2014;56(2):205-18.
204. Michalska K, Jaskolski M. Structural aspects of L-asparaginases, their friends and relations. Acta Biochim Pol. 2006;53(4):627-40.
205. Evtimova V, Zeillinger R, Kaul S, Weidle UH. Identification of CRASH, a gene deregulated in gynecological tumors. International journal of oncology. 2004;24(1):33-41.
206. Weidle UH, Evtimova V, Alberti S, Guerra E, Fersis N, Kaul S. Cell growth stimulation by CRASH, an asparaginase-like protein overexpressed in human tumors and metastatic breast cancers. Anticancer research. 2009;29(4):951-63.
207. Xiao-Feng L, Han-Qing H, Ling L, Shi-Hong C, Chen-Chen R. RNAimediated downregulation of asparaginaselike protein 1 inhibits growth and promotes apoptosis of human cervical cancer line SiHa. Molecular Medicine Reports. 2018;18:931-7.
208. Lanvers-Kaminsky C. Asparaginase pharmacology: challenges still to be faced. Cancer Chemother Pharmacol. 2017;79(3):439-50.
209. Yu M, Henning R, Walker A, Kim G, Perroy A, Alessandro R, et al. L-asparaginase inhibits invasive and angiogenic activity and induces autophagy in ovarian cancer. J Cell Mol Med. 2012;16(10):2369-78.
210. Bachet JB, Gay F, Marechal R, Galais MP, Adenis A, Ms CD, et al. Asparagine Synthetase Expression and Phase I Study With L-Asparaginase Encapsulated in Red

Blood Cells in Patients With Pancreatic Adenocarcinoma. Pancreas. 2015;44(7):1141-7.
211. Lorenzi PL, Reinhold WC, Rudelius M, Gunsior M, Shankavaram U, Bussey KJ, et al. Asparagine synthetase as a causal, predictive biomarker for L-asparaginase activity in ovarian cancer cells. Mol Cancer Ther. 2006;5(11):2613-23.
212. Yunis AA, Arimura GK, Russin DJ. Human pancreatic carcinoma (MIA PaCa-2) in continuous culture: sensitivity to asparaginase. International journal of cancer Journal international du cancer. 1977;19(1):128-35.
213. Shroyer NF. Tumor Organoids Fill the Niche. Cell Stem Cell. 2016;18(6):686-7.
214. Vahrmeijer AL, Hutteman M, van der Vorst JR, van de Velde CJ, Frangioni JV. Image-guided cancer surgery using near-infrared fluorescence. Nat Rev Clin Oncol. 2013;10(9):507-18.
215. van Driel PB, Boonstra MC, Prevoo HA, van de Giessen M, Snoeks TJ, Tummers QR, et al. EpCAM as multi-tumour target for near-infrared fluorescence guided surgery. BMC cancer. 2016;16(1):884.

I

PLOS ONE

RESEARCH ARTICLE

Multimodal Imaging of Orthotopic Mouse Model of Endometrial Carcinoma

Ingfrid S. Haldorsen[1,2], Mihaela Popa[3☯], Tina Fonnes[4☯], Njål Brekke[5], Reidun Kopperud[4], Nicole C. Visser[6], Cecilie B. Rygh[7], Tina Pavlin[7], Helga B. Salvesen[4,8], Emmet McCormack[3], Camilla Krakstad[4,8]*

1 Department of Radiology, Haukeland University Hospital, Bergen, Norway, **2** Section for Radiology, Department of Clinical Medicine, University of Bergen, Bergen, Norway, **3** Department of Clinical Science, University of Bergen, Bergen, Norway, **4** Centre for Cancer Biomarkers, Department of Clinical Science, University of Bergen, Bergen, Norway, **5** PET-centre, Department of Radiology, Haukeland University Hospital, Bergen, Norway, **6** Department of Pathology, Radboud University Medical Center, Nijmegen, The Netherlands, **7** Molecular Imaging Center, Department of Biomedicine, University of Bergen, Bergen, Norway, **8** Department of Obstetrics and Gynaecology, Haukeland University Hospital, Bergen, Norway

☯ These authors contributed equally to this work.
* camilla.krakstad@med.uib.no

Citation: Haldorsen IS, Popa M, Fonnes T, Brekke N, Kopperud R, Visser NC, et al. (2015) Multimodal Imaging of Orthotopic Mouse Model of Endometrial Carcinoma. PLoS ONE 10(8): e0135220. doi:10.1371/journal.pone.0135220

Editor: Gayle E. Woloschak, Northwestern University Feinberg School of Medicine, UNITED STATES

Received: June 8, 2015

Accepted: July 20, 2015

Published: August 7, 2015

Data Availability Statement: All relevant data are within the paper and its Supporting Information files.

Funding: Supported by Bergen Research Foundation, The Western Norway Regional Health Authority, Norwegian Research Council, The University of Bergen, The Meltzer Foundation, The Norwegian Cancer Society (The Harald Andersen's legacy), and MedViz (www.medviz.uib.no). The funders had no role in study design, data collection and analysis, decision to publish, or preparation of the manuscript.

Abstract

Background

Orthotopic endometrial cancer models provide a unique tool for studies of tumour growth and metastatic spread. Novel preclinical imaging methods also have the potential to quantify functional tumour characteristics *in vivo*, with potential relevance for monitoring response to therapy.

Methods

After orthotopic injection with luc-expressing endometrial cancer cells, eleven mice developed disease detected by weekly bioluminescence imaging (BLI). In parallel the same mice underwent positron emission tomography–computed tomography (PET-CT) and magnetic resonance imaging (MRI) employing ^{18}F-fluorodeoxyglocose (^{18}F-FDG) or ^{18}F- fluorothymidine (^{18}F-FLT) and contrast reagent, respectively. The mice were sacrificed when moribund, and post-mortem examination included macroscopic and microscopic examination for validation of growth of primary uterine tumours and metastases. PET-CT was also performed on a patient derived model (PDX) generated from a patient with grade 3 endometrioid endometrial cancer.

Results

Increased BLI signal during tumour growth was accompanied by increasing metabolic tumour volume (MTV) and increasing MTV x mean standard uptake value of the tumour (SUV_{mean}) in ^{18}F-FDG and ^{18}F-FLT PET-CT, and MRI conspicuously depicted the uterine tumour. At necropsy 82% (9/11) of the mice developed metastases detected by the applied

Competing Interests: The authors have declared that no competing interests exist.

imaging methods. ^{18}F-FDG PET proved to be a good imaging method for detection of patient derived tumour tissue.

Conclusions

We demonstrate that all imaging modalities enable monitoring of tumour growth and metastatic spread in an orthotopic mouse model of endometrial carcinoma. Both PET tracers, ^{18}F-FDG and ^{18}F-FLT, appear to be equally feasible for detecting tumour development and represent, together with MRI, promising imaging tools for monitoring of patient-derived xenograft (PDX) cancer models.

Introduction

Endometrial cancer is the most common pelvic gynaecologic malignancy in industrialized countries, and the incidence is increasing [1]. Although about 75% of the patients are treated with tumour confined to the uterine corpus, 15–20% recur [2]. In patients with distant metastases or locally recurrent disease, the effect of the conventional systemic therapy is poor with reported median survival ranging from 7–12 months [3]. Thus, there is an urgent need to develop more efficient therapies for metastatic endometrial cancer.

Preclinical testing of drug efficacy has been reliant upon subcutaneously implanted tumours originating from human cancer cell lines or tumour biopsies into immunodeficient rodents [4]. Also for endometrial cancer, subcutaneous xenograft models have long been employed to explore effect of new treatments [5]. This model enables monitoring of tumour growth by visual inspection and palpation to monitor tumour growth. However, the subcutaneous model has important limitations including non-metastatic behaviour, thus lacking immediate relevance for humans [6]. Orthotopic xenograft models, whereby molecularly defined cancer cell lines or primary patient cells are surgically implanted into the organ of origin, induce disease that more accurately reflect human metastatic patterns and response to therapeutics. Orthotopic endometrial cancer models have been successfully developed [6–8]. This has provided a valuable research platform for studies of molecular and cellular mechanisms underlying tumour growth and metastatic spread in endometrial cancer [8–13].

A challenge in such models is still to accurately determine tumour growth and drug efficacy longitudinally. Bioluminescence imaging (BLI) represents one such useful preclinical imaging method for *in vivo* monitoring of tumour growth and metastases in endometrial cancer xenograft models from human cell lines, but requires that these are transfected with luciferase gene [8, 9, 13]. Patient derived tumour xenograft (PDX) models, which better mimic the corresponding human lesion and tumour growth (i.e. molecular type, stromal tissue interaction and three dimensional growth in relevant organ) represent a more reliable tool to predict response to chemotherapy [4]. Although methods are available to genetically manipulate PDX models *ex vivo*, such manipulation cause irreversible genetic changes distancing the models from the parental tumours [14]. BLI is therefore not an optimal method for PDX models [15]. Thus, additional *in vivo* preclinical imaging methods to identify and quantify orthotopic endometrial cancer xenograft progression and response to therapy, needs to be better explored to fully exploit orthotopic PDX endometrial cancer models.

Preclinical positron emission tomography-computed tomography (PET-CT) and magnetic resonance imaging (MRI) provide both anatomical and functional information from tumour tissue [15, 16]. These novel imaging methods have been shown to predict response to therapy

in various xenografts models [16] such as in colorectal cancer [17] (based on ^{18}F-FLT and ^{18}F-FDG PET), breast cancer [18] (dynamic contrast-enhanced (DCE)-MRI and diffusion weighted imaging (DWI)) and in Ewing sarcoma [19] (whole body MRI and DWI). Characteristics for PET-CT or MRI findings in endometrial cancer orthotopic mouse models have not yet been reported, hence the feasibility of these novel imaging methods in monitoring tumour progression and metastatic spread in this setting is largely unknown.

This study presents characteristic preclinical imaging findings for *in vivo* BLI, PET-CT (with ^{18}F-FDG and ^{18}F-FLT) and MRI during tumour progression and metastatic spread in an orthotopic endometrial cancer model. These observed *in vivo* imaging findings are also related to the *ex vivo* BLI findings of single organs at necropsy and to histological characteristics for the corresponding tumour tissue.

Material and Methods

Ethics statement

For patient samples and information, all parts of the study have been approved according to Norwegian legislation, including the Norwegian Data Inspectorate, Norwegian Social Sciences Data Services, and the Western Regional Committee for Medical and Health Research Ethics, (NSD15501; REK 052.01). Participants gave written informed consent. All animal studies were approved by the Norwegian State Commission for Laboratory Animals (ID 4036) and performed according to the European Convention for the Protection of Vertebrates Used for Scientific Purposes.

Cell lines and Retroviral transfection

The human endometrial cancer cell line Ishikawa was obtained from Sigma-Aldrich (St. Louise, MO, USA) and the cell authenticity was confirmed by Short Tandem Repeat (STR) profiling (IdentiCell, Denmark). Cells were kept in Minimal Essential Medium (MEM; Lonza, Basel, Switzerland) supplemented with 5% heat-inactivated Fetal Calf Serum (FCS; Sigma-Aldrich, St. Louis, MO, USA), 2 mM L-glutamine (Lonza, Basel, Switzerland), 1% non-essential amino acids (Lonza, Basel, Switzerland), penicillin 100 IU/ml and 100 μg/ml streptomycin (Lonza, Basel, Switzerland) at 37°C in a humidified atmosphere with 5% CO_2. Ishikawa cells were stably transfected using retroviral infection as described previously [20, 21] using the luciferase expressing construct L192, combined with the tetracycline-regulated transactivator (tTA). Stably transfected Ishikawa^{Luc} cells were selected with 1 μg/ml puromycine (Sigma-Aldrich, St. Louis, MO, USA) and luciferase expression was confirmed by adding 2.5 mg/ml D-luciferin (Promega, Madison, WI, USA) before *ex vivo* optical imaging.

Orthotopic endometrial cancer model

NOD-*scid* IL2Rgamma^{null} (NSG) mice were originally a gift from Prof. Leonard D Schultz at The Jackson Laboratory (Maine, USA) and bred at the Vivarium, University of Bergen, Norway. Female 6–8 weeks old were maintained under pathogen-free conditions with food and water provided *ad libidum*. Animals were kept on a 12 hours dark/night schedule at a constant temperature of 21°C and at 50% relative humidity. Prior to surgery animals received 0.1 mg/kg Buprenorphine hydrochloride (Temgesic, Reckitt Benckiser, Berkshire, UK) intramuscular, for analgesia. Mice were anaesthetised with 250 mg/kg tribromoethanol (Sigma-Aldrich, St. Louis, MO, USA) diluted in 2 methyl-2 butanol (Sigma-Aldrich, St. Louis, MO, USA) and placed on a heating pad in dorsal decubitus. Fur on the abdomen was clipped and skin disinfected with surgical iodine and 70% ethanol. A 1cm middle line incision was made in the lower abdomen

(skin and muscles). The left uterine horn was exteriorized and $1x10^6$ of Ishikawa^{Luc} cells resuspended in 50 μl of Matrigel (BD Matrigel Basement Membrane Matrix, BD Biosciences, San Jose, CA) were injected directly into the endometrial cavity through the myometrium. A 0.3mm insulin syringe (Omnican 50, B-Braun, Melsungen, Germany) was used for the injection. The uterine horn was put back in the original position before muscles and skin was closed with 5–0 absorbable sutures. After the surgery the animals were placed in a warm environment and supervised until full recovery.

Generation and maintenance of patient derived xenograft (PDX) model

A biopsy from the primary tumour of a 69 year old woman diagnosed with grade 3 endometrioid endometrial cancer was placed on ice until processing. Tissue was mechanically dissociated using sterile scalpels and sequentially filtered through a 40 μm pore filter (Fisher) and centrifuged at 900rpm for 4 min. The cell pellet was resuspended in Matrigel and orthotopic implantation in four mice was performed as described above. The mice (F1 generation) were monitored closely for visible signs of disease development and examined using PET CT when clinical signs of disease were presented. Mice were thereafter sacrificed, and a cell suspension from the primary tumour was prepared and implanted in the next generation of mice (F2). Samples for histological examination of tumour grade and type were taken in parallel. The new generation was monitored in a similar manner until presenting clinical signs of disease, when PET CT was performed. The mouse model is continuously rederived following the same protocol.

Experimental set-up for multimodal imaging

Optical imaging. In total 15 mice were orthotopically injected with Ishikawa^{Luc} cells. All mice were subjected to weekly examination by bioluminescence to follow tumour growth and metastatic dissemination. Mice were injected intraperitoneally (i.p.) with D-luciferin (150 mg/kg) and anaesthetised with 3% isoflurane (Isoba Vet, Schering-Plough, Brussel, Belgium) 10 minutes before optical imaging using an In-Vivo FX PRO molecular imaging system (Carestream Health, Inc., Rochester, NY, USA). Total bioluminescence values were measured using manual Region of interest (ROI) of the whole abdomen using the Carestream MI software (Standard Edition, v.5.0.6.20, Carestream Health, Inc.). Three mice showed no BLI signal after four weeks, suggesting no tumour development in the uterus, possibly due to vaginal leakage of cells after surgery. One mouse died during anaesthesia for PET scan. These four mice were excluded from the experiment. The 11 remaining mice were monitored weekly and euthanized when moribund as defined by weight loss 10–15%, lethargy or ruffled fur. Ten minutes before necropsy, all mice were injected i.p. with D-Luciferin and organs were imaged *ex vivo* for evaluation of disease dissemination using Optix MX3 Small Animal Molecular Imager (ART Inc., Saint-Laurent, QC, Canada) supplied with Optix Optiview software. After BLI imaging, the tissue biopsies were fixed in 4% buffered formalin and embedded in paraffin before they were processed for histological analysis.

PET-CT. PET-CT was performed in all mice weekly from week 5/6–week 7/8 after injection of Ishikawa^{Luc} cells. In one of the mice PET-CT was also performed 12 and 13 weeks after Ishikawa^{Luc} cells injection. The PET-CT scans consisted of ^{18}F-FLT PET only (n = 2), ^{18}F-FDG-PET only (n = 3) or both ^{18}F-FLT PET and ^{18}F-FDG PET (n = 6). The last PET-CT examinations were performed 7 days (n = 1), 11 days (n = 3), 18 days (n = 1), 35 days (n = 2) and 49 days (n = 4) respectively before the mice were sacrificed, respectively. This approach was chosen in order to reduce the cost of the experiments as well as to minimize stress for individual animals also undergoing weekly BLI. For mice with slow tumour progression limited capacity of the

PET-scanner precluded PET scanning immediately prior to sacrifice. For the PDX model, the PET-CT scans consisted of ^{18}F-FLT PET in the F1 generation and ^{18}F-FDG-PET in the F2 generation. PET-CT scans were performed using the integrated PET-CT scanner nanoScan PC PET/CT (Mediso Medical Imaging Systems Ltd, Budapest, Hungary) featuring spatial resolutions of 800 μm and 30 μm of the respective PET- and CT detector systems. The PET field of view (FOV) was 9.5 x 8 cm in axial and transaxial directions allowing whole-body imaging of mice. The PET detectors consist of LYSO crystals, and acquisition was performed in 1:5 coincidence and normal count mode. Mice were scanned simultaneously without prior fasting using a dual mouse bed with integrated system for anaesthesia and heating. Animals were anaesthetised using 3% sevoflurane (Sevoflo, Abbott, Illinois, USA) and ^{18}F-FDG (mean dose of 7.3 $^{+}$/_1.6 MBq) was injected via the tail vein 30 seconds after the start of the PET scanning. Total scan time was 60 minutes, and the last 30 minutes was reconstructed into a static image. For ^{18}F-FLT PET-CT mice were anesthetised and ^{18}F-FLT (mean dose of 7.4^{+}/_2.3 MBq) was injected via the tail vein 30 minutes prior to scanning. PET acquisition time was 30 minutes. For both tracers, a whole-body CT scan (helical projections with tube energy of 50 kvP, exposure time 300 ms, 720 projections, max FOV, binning 1:4) was performed for anatomical information and attenuation correction of PET images.

Reconstruction and post-processing of PET-CT data. The PET images were reconstructed using the supplier's reconstruction algorithm Tera-Tomo 3D (OSEM), with corrections for depth-of-interaction (DOI), radionuclide decay, randoms, crystal dead time, detector normalization, and attenuation correction, and with a detector coincidence mode of 1:3, 4 iterations and 6 subsets, no filtering. CT images were reconstructed using RamLak filter. The PET and CT images were co-registered automatically. Images were reconstructed with a voxel size of 0.25×0.25×0.25 mm^3 for CT, and 0.4×0.4×0.4 mm^3 for PET. Data analyses were performed using InterView Fusion version 2.02.055.2010 (Mediso Ldt., Budapest, Hungary). For each scan a spherical volume of interest (VOI) with radius 1.5 mm were drawn manually over the muscles in the back of the neck. Standard uptake value (SUV) was calculated using the equation: SUV = $C_{PET}(T)/(ID/BW)$, where $C_{PET}(T)$ is the measured activity in tissue, ID is injected dose measured in kBq, and BW is mouse body weight in kg. SUV_{mean} is the SUV mean value of all voxels included in the VOI. SUV_{mean} in this nuchal muscle was used as a reference tissue in order to enable segmentation of putative tumour tissue having SUV ratios (SUVR) of >2 and >6 for ^{18}F-FLT and ^{18}F-FDG, respectively. VOIs of primary uterine tumours and of likely metastases were drawn semi-automatically in the PET images for estimation of metabolic tumour volumes (MTV) and their corresponding SUV_{mean}. The parameter Total Lesion Glycolysis (TLG) in the tumour was calculated based on the ^{18}F-FDG PET-CT scans using the following equation: TLG = FDG-SUV_{mean} x MTV [22]. For the ^{18}F-FLT PET-CT scans a similar parameter was calculated based on the same equation and named FLT-SUV_{mean} x MTV.

MRI. MRI was performed in one mouse at week 11 after injection of Ishikawa^{Luc} cells (3 weeks before sacrifice). The MRI scan was performed on a 7T horizontal-bore preclinical scanner (Pharmascan 70/16, Bruker Corporation, Germany), using a 40 mm ID mouse body quadrature volume resonator in a single-coil (TX/RX) configuration. During scanning, the mouse was anesthetized using 3.0% sevoflurane. Respiration rate and body temperature were monitored and kept constant at 60±20 respiratory cycles/min and 37^{+}/-2°C, respectively. For identification of tumour and estimation of tumour size, a T_2-weighted rapid acquisition with relaxation enhancement (RARE) sequence (TE/TR = 36/4300 ms, 2 averages, matrix 256x256, field of view (FOV) 3.2 x 3.2 cm, slice thickness 1 mm) and pre- and a post-contrast T_1-weighted RARE sequences (TE/TR = 9/1000 ms, 4 averages, matrix 256x256, FOV 3.2 x 3.2 cm, slice thickness 1 mm) were employed. The post-contrast images were collected after intravenous tail-vein injection of Gd-based contrast agent (Dotarem, Guerbet USA, volume 30uL, dose 0.1 mmol/kg

of body weight). In addition, apparent diffusion coefficient (ADC) maps were generated from diffusion-weighted EPI images (DWI) (TE/TR = 24.6/3100 ms, 2 averages, matrix 128x128, FOV 3.2 x 3.2 cm, slice thickness 1 mm and 3 diffusion directions with b-values of 100, 200, 400, 600, 800, 1000 s/mm^2).

Histological examination and Immunohistochemical (IHC) analysis

Formalin-fixed tissue was processed for routine histological examination. 4 μm sections were stained with Hematoxylin–Eosin (HE) and examined by a pathologist (NCMV) for typing and grading of the tumours. To verify presence of human cells, IHC staining was performed on full section to detect expression of human ERα. Briefly, sections were dewaxed with xylene, rehydrated in graded ethanol before microwave antigen retrieval, and stained for 60 min in room temperature for human ERα expression using 1:400 HC-20 (Santa Cruz Biotechnology, Dallas, TX, USA) or 1:400 Clone SP1 (Thermo Scientific, Fremont, CA, USA). Anti-rabbit secondary antibody (Dako, Denmark) was applied for 30 minutes, followed by 8 minutes with Diaminobenzidine (DAB+, Dako, Denmark) before counterstaining with hematoxylin. To verify the species specific nature of the antibody, sections were compared to the non-species specific antibody from Santa Cruz (S1 Fig), validating that the human specific antibody only detected ERα in cells of human origin.

Results

Ishikawa^{Luc} cells form primary endometrial cancers in mice

We developed an orthotopic mouse model that can be monitored by bioluminescence. Mice were monitored for up to 13 weeks and sacrificed when reaching humane endpoint. Body weight was monitored weekly (Fig 1A). A clear reduction in body weight was observed as the BLI signal increased. At 13 weeks post injection, all mice had reached a moribund disease condition (Fig 1B).

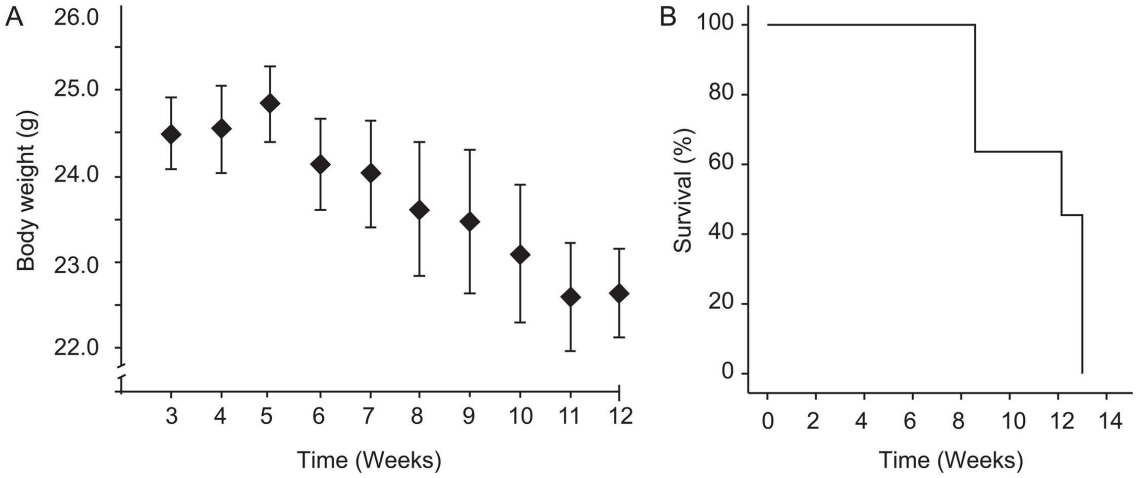

Fig 1. Orthotopic injection of Ishikawa^{Luc} cells results in weight loss and reduced survival. Mice injected with Ishikawa^{Luc} cells were monitored weekly for signs of disease development. Weight loss (A) was detected as an early sign of disease. Mice developing symptoms of severe disease were sacrificed and the overall survival is visualized in a Kaplan-Meier survival plot (B).

doi:10.1371/journal.pone.0135220.g001

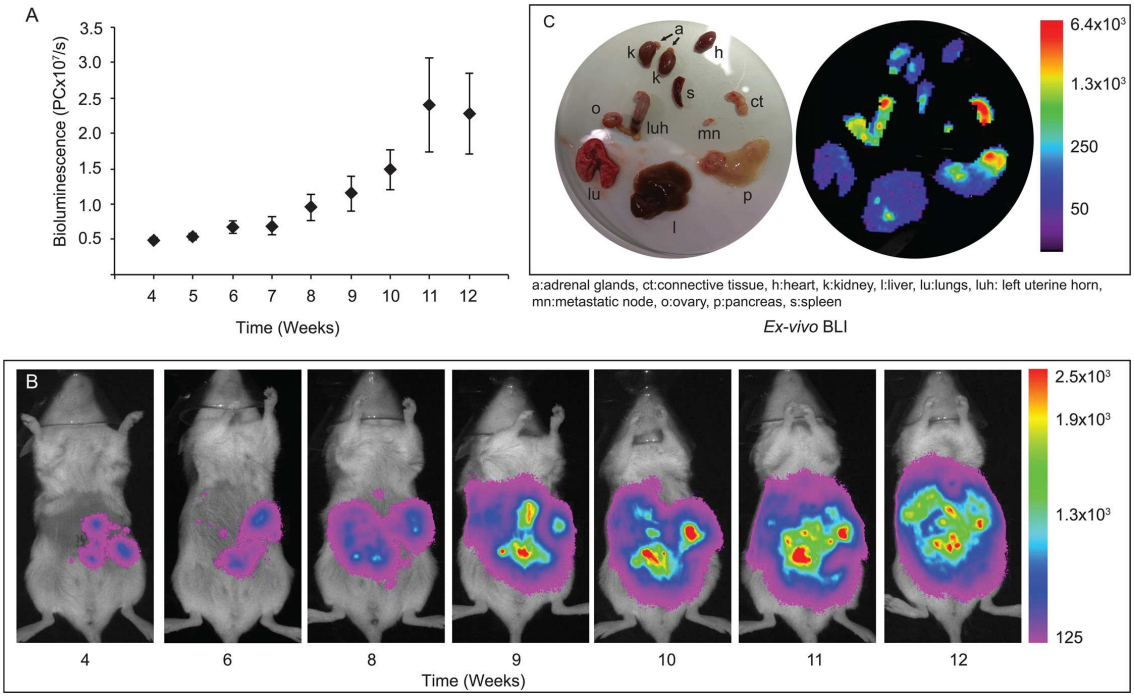

Fig 2. Tumour growth monitored by Bioluminescence Imaging (BLI). Tumour growth was monitored weekly by *in vivo* BLI and an increase in the net bioluminescence versus time was observed (A, B). Organs were also examined by BLI post-mortem to visualize metastatic spread (C). Strong BLI signals were detected at site of injection (left uterine horn; luh), right ovary (o), connective tissue surrounding the uterine horn (ct), pancreas (p) and metastatic node (mn). Spot signals were detected in the liver (l), spleen (s), kidneys (k), heart (h) and lung (lu). No signal was detected in adrenal gland (a).

doi:10.1371/journal.pone.0135220.g002

Bioluminescence monitoring of tumour growth

A bioluminescence signal restricted to the uterine area was observed the first weeks, followed by more diffuse abdominal signal as the tumour burden was increasing and the mice developed metastatic disease. The total BLI signal increased dramatically the last weeks before the animals were sacrificed (Fig 2A and 2B).

Two mice showed no signs of metastatic spread but had large tumours limited to the uterus when sacrificed. The remaining nine mice had all developed advanced disease with metastatic spread and variable amounts of ascites. After macroscopic post-mortem examination, organs were imaged *ex vivo* to detect tumour cell dissemination (Fig 2C, Table 1). A strong BLI signal was observed in the uterus of all animals. Increased BLI signal was observed in the ovaries (n = 4), pancreas (n = 7), kidney (n = 2), spleen (n = 3), liver (n = 6) and lung (n = 4) as well as in connective tissue surrounding the uterus (n = 9). Nodules suspected to be metastatic lymph nodes were also BLI positive (n = 4). No BLI signal was detected in the adrenal glands.

Histological evaluation of the model

The histology of the primary tumour and presence of metastatic spread were determined on HE stained sections (Fig 3). Histological evaluation of the organs revealed normal histology

Table 1. Tumour development and metastasis dissemination in Ishikawa^{Luc} model. *Total number of mice with organs affected by disease, defined by positive BLI signal and presence of cancer cells in histologic sections.*

Organ affected:	BLI (%)	Histology (%)
Uterus	11 (100)	11 (100)
Mice with metastases	9 (82)	9 (82)
Ascites	8 (73)	NA
Lymph nodes	4 (36)	4 (36)
Ovaries	4 (36)	4 (36)
Liver	7 (64)	4 (36)
Lungs	4 (36)	6 (55)
Connective tissue	9 (82)	9 (82)
Pancreas	7 (64)	7 (64)
Spleen	3 (27)	0
Kidneys	2 (18)	0
Adrenal glands	0 (0)	0 (0)

NA: *Not applicable*.

doi:10.1371/journal.pone.0135220.t001

with intact endometrial glands in the right uterine horn. A solid growing primary tumour was detected in the left uterine horn (at site of injection; Fig 3A) with characteristics of a grade 3 endometrioid endometrial cancer (Fig 3B), and areas of necrosis and myometrial invasion. Metastases to the ovaries (Fig 3C) were mostly solid with necrotic areas, but gland formation was also detectable in some cases. No remaining lymph node tissue was detected in metastatic nodes (Fig 3D). Larger separately growing tumour fragments were detected in the pancreas (Fig 3E). BLI positive kidneys and spleens had tumour cells in the outer surface of the organ, with no invasion of the parenchyma. This was also true for three BLI positive liver biopsies (Fig 3F). All mice with cancer cells detected in the outer lining of organs had ascites. Diffuse small tumour nodules were found in vessels in the lungs (Fig 3G), also in two lung biopsies that appeared negative in the BLI imaging (Table 1).

Cellular protein expression of human ERα was verified in human cells (S2 Fig). We found heterogeneous expression of ERα in the primary tumour, also showing myometrial infiltration (S2A Fig), consistent with reports that Ishikawa cells are ERα positive but with a tendency to lose expression of ERα with dedifferentiation. We also clearly identified presence of metastatic Ishikawa^{Luc} cells in pancreatic tissue (S2B Fig), in the capsule of the liver (S2C Fig) and in the vessels in pulmonary tissue (S2D Fig).

PET-CT monitoring of tumour progression

Evident ^{18}F-FDG/^{18}F-FLT-avid tumour tissue in the uterus (Fig 4A and 4B and Fig 5C and 5D) was observed in 6 out of 7 mice, which were scanned $\leq$ 35 days prior to sacrifice. The remaining mice (n = 4) showed no visible tumour at their last PET-CT scans, 49 days prior to sacrifice. However, these mice did develop tumour growth and metastases at a later point with increased BLI tumour signal after their last PET-CT scans.

In the mice having weekly PET-CT scans the last weeks before sacrifice, increasing MTV and SUV_{mean} x MTV was observed in both primary tumours (Fig 4A and 4C–4F) and metastases (Fig 4B and 4G–4J). The highly ^{18}F-FDG/^{18}F-FLT- avid tissue (Fig 4A and 4B), assumed to represent tumours, was histologically confirmed as primary malignant uterine tumours (Fig 4K) and metastases (Fig 4L), respectively, at necropsy. Although the absolute values for

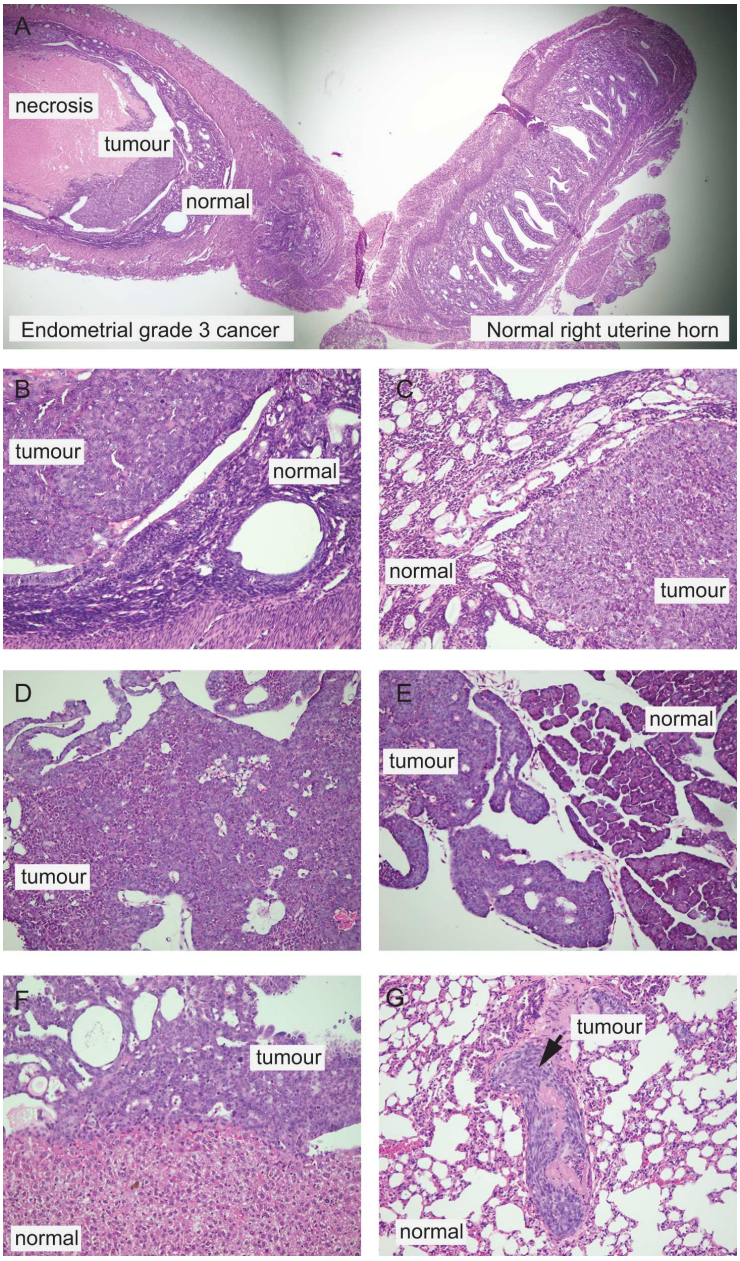

Fig 3. Histological evaluations of tumour characteristics and spread of disease. Organs were fixed in formaldehyde, sectioned and stained with HE to confirm presence of tumour tissue and for histological characterization of tumour. Sections from a representative mouse depict a large tumour mass in the left

uterine horn (A) with necrotic tissue in the centre. Normal uterine morphology is seen in the right uterine horn with endometrial glands and normal stroma and myometrium. Detail of tumour in the left uterine horn (B) reveals solid growing tumour, resembling a grade 3 endometrioid endometrial cancer. Solid tumour masses were also detected in ovaries (C). Inguinal lymph node, macroscopically suspected to be metastatic, was confirmed to represent a metastasis (D), however, without visible surrounding lymphoid tissue. Solid tumour components are depicted in the pancreas (E) with tumour tissue infiltrating surrounding fat tissue. Metastasis is observed on the outer surface of the liver (F), and tumour tissue is also detected in blood vessels of the lung (G), the latter indicating hematogenous spread.

doi:10.1371/journal.pone.0135220.g003

calculated MTV and SUV_{mean} x MTV of the tumours using different tracers on PET-CT were not directly comparable, both tracers seemed equally feasible to depict tumour tissue and monitoring tumour growth and metastatic spread at PET-CT (Fig 4A and 4B and Fig 5C and 5D).

MRI of tumour model

MRI conspicuously depicted the boundaries of the uterine tumour (Fig 5A). The tumour was hyperintense on T2-weigthed images and moderately contrast-enhancing on T1-weighted

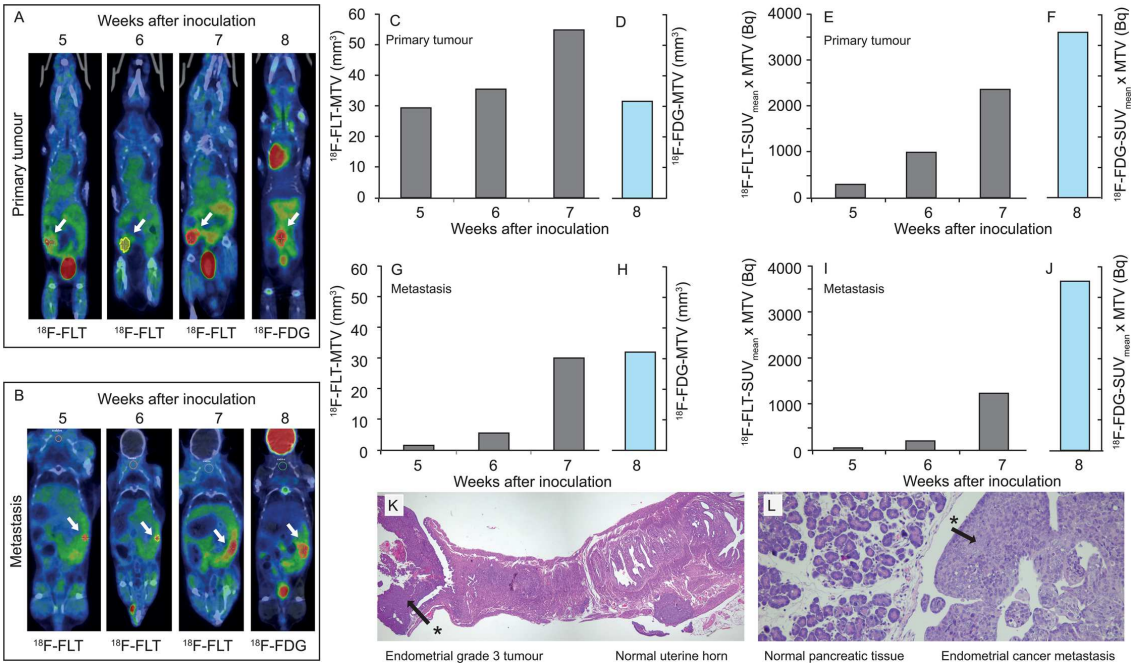

Fig 4. Tumour growth monitored by PET-CT. Tumour growth in the left uterine horn (A) and growth of abdominal metastasis (B) measured by ^{18}F-FLT PET-CT at 5, 6 and 7 weeks after inoculation of cells; and by ^{18}F-FDG PET-CT 8 weeks after inoculation (A and B) in the same mouse. Estimated metabolic tumour volume increased from 5 to 7 weeks after inoculation based on ^{18}F-FLT PET-CT but was stable or slightly decreased from 7 to 8 weeks after inoculation based on ^{18}F-FLT PET-CT (week 7) and ^{18}F-FDG PET-CT (week 8) (C/D, G/H). The estimated ^{18}F-FLT-SUV_{mean} x MTV steadily increased from 5 to 7 weeks after inoculation in both the primary tumour (E) and in the metastasis (I). Panel F and J show Total Lesion Glycolysis (^{18}F-FDG-SUV_{mean} x MTV) for primary tumor and metastasis, respectively. Histologic examination of the uterus (K) and the pancreas (L) validated presence of malignant tissue (asterisks) as detected with PET-CT.

doi:10.1371/journal.pone.0135220.g004

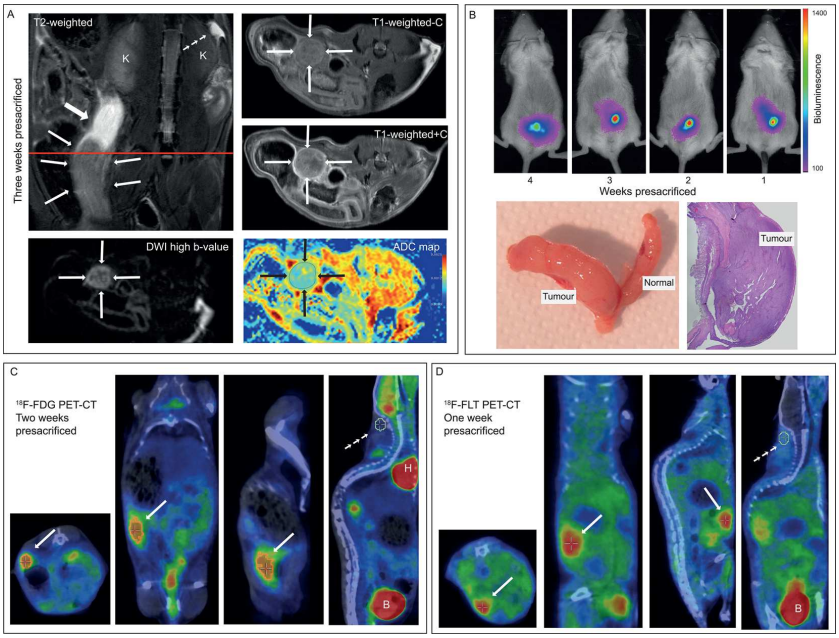

Fig 5. Multimodal imaging of the same mouse by MRI, ^{18}F-FDG PET, ^{18}F-FLT PET and BLI. MRI three weeks presacrificed (A) depicting large uterine tumour tissue in the left uterine horn (thin arrows) with intrauterine fluid cranial of the tumour (filled large arrow) and small amounts of free intraperitoneal fluid cranial to the right kidney (K) (small arrows). The tumour tissue is moderately enhancing on T1-weighted series after contrast and the tumour exhibits restricted diffusion with hyperintensity on high b-value DWI with corresponding low apparent diffusion coefficient (ADC) value (1.11 x 10^{-3} mm^2/s) on the ADC map (A). BLI 4 to 1 weeks presacrificed (B) shows increasing BLI signal corresponding to the tumour of the left uterine horn; the corresponding tumour tissue was evident macroscopically and confirmed microscopically at necropsy (B). ^{18}F-FDG PET-CT two weeks presacrificed (C) depicts a large ^{18}F-FDG-avid tumour in the left uterine horn (arrows) with estimated metabolic tumour volume of 33 ml. ^{18}F-FLT PET-CT one week presacrificed (D) depicts large ^{18}F-FLT-avid tumour in the left uterine horn (arrows) with estimated metabolic tumour volume of 44 ml. ^{18}F-FDG/^{18}F-FLT-avidity in a VOI in the nuchal muscular tissue (C and D; small arrows) was used as reference tissue to define a threshold for likely tumour tissue (activity of x2 and of x6 for ^{18}F-FLT and ^{18}F-FDG, respectively) to be included in the estimated metabolic tumour volume. B: bladder; H: heart.

doi:10.1371/journal.pone.0135220.g005

series after i.v. contrast. Restricted diffusion within the tumour tissue was striking with hyperintensity on high b-value images and corresponding low ADC value on the ADC map (Fig 5A).

The PET-CT and MRI findings of the Ishikawa^{Luc} cell model are similar to patterns detected for human endometrial cancers

The uterine tumours in the mice were highly ^{18}F-FDG-avid (Figs 4A and 4B and 5C), thus resembling the metabolic behaviour of the human endometrial cancers, which also typically exhibit marked ^{18}F-FDG-avidity (S3A, S3E Fig). Both in patients and in the preclinical model, the tumour is hyperintense on T2-weighted images (Fig 5A and S3C, S3F Fig) and moderately contrast-enhancing on T1-weighted images after intravenous contrast (Fig 5A and S3D Fig). Similarly, the restricted diffusion observed within the tumour in the mouse model (with measured tumour ADC value of 1.11 x 10^{-3} mm^2/s; Fig 5A) is quite similar to that in endometrial cancer tissue in patients (S3G and S3H Fig; tumour ADC value in this patient was 0.83 x 10^{-3} mm^2/s).

PET-CT represents a powerful tool for detection of tumour tissue in PDX model of endometrial cancer

Although orthotopic models generated from established cell lines develop tumours in the uterus, a PDX model is likely to better mimic the clinical setting relevant for disease spread and response to therapy. This PDX model was developed from a patient primary tumour (Fig 6A) with grade 3, endometrioid endometrial type. Histologic examination of the primary tumours of both the F1 (Fig 6B) and the F2 (Fig 6C) generation reveal high resemblance to the donors, and both were classified as grade 3 endometrioid, endometrial cancers by the pathologist. PET-CT was successfully used to detect tumour growth using ^{18}F-FLT in generation F1 (not shown) and ^{18}F-FDG in generation F2 (Fig 6D). Highly ^{18}F-FDG-avid tumour tissue in the uterine fundus and both the left and the right uterine horn was macroscopically verified to represent tumour tissue (Fig 6E).

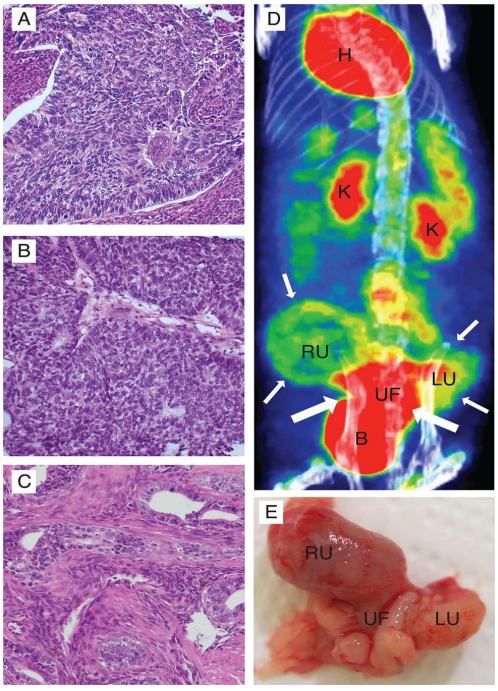

Fig 6. ^{18}F-FDG PET detects tumour in an orthotopic endometrial cancer PDX model. Mice were implanted in the uterus with cancer cells from a patient biopsy and rederived for two generations to develop a PDX model. Histological examination revealed that both the F1 (B) and the F2 (C) mice developed tumours closely resembling the parental tumour, defined as an endometrioid grade 3 endometrial cancer (A). ^{18}F-FDG PET was successfully used to detect tumour growth in both generation F1 (not shown) and generation F2 (D). Highly ^{18}F-FDG-avid tumour tissue (large arrows) in the uterine fundus (UF) and both the left and the right uterine horn (LU, RU respectively) depicted at PET-CT (D). Macroscopic examination revealed a large tumour infiltrating both the uterine horns as well as the bladder (E) and corresponded well with the tissue detected as tumour by ^{18}F-FDG PET. B, bladder; H, heart; K, kidney; LU, left uterine horn; RU, right uterine horn; UF, uterine fundus.

doi:10.1371/journal.pone.0135220.g006

Discussion

One major challenge in cancer research today is to what extent the cancer models mimic the disease in a human setting. The use of mouse models has become increasingly popular, including both sub-cutaneous and orthotopic models, in combination with cell line based and PDX models [23]. The ability to monitor disease development and response to therapy, is of great importance when choosing the model system, and several non-invasive imaging models are presently available, although not extensively explored for uterine cancer. Still, many of these are best suited for cell line based models since they ultimately rely on genetic engineering of the cells. The availability of PET tracers and small scale imaging equipment for PET-CT and MRI has improved our ability to study cancer development and metastatic spread without such use of reporter genes [24]. This study, describing the typical imaging findings based on *in vivo* BLI in parallel with PET-CT and MRI findings for the first time in an orthotopic endometrial cancer model, demonstrates an excellent feasibility of this multimodal imaging platform to monitor tumour progression and metastatic spread.

We utilized the orthotopic Ishikawa^{LUC} model of endometrial cancer to trace tumour growth using BLI and verified the methods ability to detect tumour growth and spread by macroscopic and microscopic necropsy examination of affected organs. As reported previously by others [7, 21, 25], BLI proved to be an effective imaging method for detection of tumour growth and metastases, especially when combined with *post mortem ex vivo* BLI imaging of organs. For growth of tumour cells in the peripheral margins of an organ, the *in vivo* BLI method was not able to accurately detect the exact organ specific location of the signal and *ex vivo* BLI or microscopic examination was necessary. In spite of these limitations, BLI is a powerful imaging tool to monitor cancer cell line growth, however with limited value for monitoring tumour growth in orthotopic PDX models. We therefor explored the same mice in parallel by PET-CT and MRI to explore the potential for these methods to detect tumour development.

PET-CT was performed using two different tracers enabling imaging of different metabolic properties of the tumour tissue. ^{18}F-FLT is a nucleoside analogue that is taken up in proliferating cells in the S-phase. ^{18}F-FLT enters cells via passive diffusion and active nucleoside transporters. It undergoes phosphorylation by the enzyme thymidine kinase 1 (TK1) and is trapped intracellularly [26]. The uptake of ^{18}F-FLT is thus related to the metabolism of the nucleosides and is considered a marker for cell proliferation [16]. ^{18}F-FDG is a glucose analogue that tends to accumulate in tissue with upregulated glucose transporter expression and/or increased metabolic activity [16]. Most cancers show an increased aerobic glycolysis leading to an increased uptake of ^{18}F-FDG. Whereas ^{18}F-FDG-avidity is nonspecific for tumour tissue, and a characteristic also of inflammatory or infectious disease, ^{18}F-FLT-avidity is believed to almost uniformly indicate presence of viable tumour cells [16]. Interestingly, both tracers seemed equally feasible of depicting and monitoring tumour growth and metastatic dissemination in this mouse model.

The uptake of both ^{18}F-FDG and ^{18}F-FLT in a tumour is considered to reflect tumour viable cell densities, and the product SUV_{mean} x MTV, referred to as Total Lesion Glycolysis when using ^{18}F-FDG as tracer, is thus a measure of the total number of viable tumour cells in the tumour [22]. Interestingly, we observed a gradual increase in SUV_{mean} x MTV prior to sacrifice both in the primary tumour and in the metastasis (Fig 4E/4F and 4I/4J, respectively), whereas estimated MTV in a mouse decreased in the primary tumour and was stable in the metastasis at the last study when ^{18}F-FDG replaced ^{18}F-FLT (Fig 4C/4D and 4G/4H, respectively). A plausible explanation of this finding regarding estimated MTV when using different tracers may be differences in tracer characteristics for the same tumour, as well as the applied thresholds for the two tracers to estimate MTV. Further studies are needed to establish optimal PET imaging

parameters and PET tracers for reliable estimation of tumour burden and progression as well as response to therapy in this mouse model.

The ability of PET-CT to validly detect and to monitor tumour growth quantitatively is affected by various known factors such as tumour size, surrounding background activity, spatial resolution of the PET-CT scanner and reconstruction algorithms of the scanner [27]. The recorded spatial resolution of 800 μm and 30 μm for the respective PET- and CT detector systems of the PET-CT scanner in this study, would ideally allow detection of very small lesions down to 0.8 mm. However, we found that early detection of the very small uterine tumours and metastases were difficult due to radiotracer uptake in neighbouring organs i.e. the bladder and kidneys and often also the intestines. However, when a gradual increase of radiotracer activity was depicted in the uterus and at the same extrauterine sites on consecutive images (suggesting metastases), the evidence of tumour growth seemed obvious, and the tissue of increased tracer uptake was confirmed to represent tumours at the corresponding sites at necropsy.

A limitation of this study is its ineligibility to compare the estimated MTV at PET to tumour volumes based on necropsy, which would be highly interesting. Such a comparison would allow an analysis of the optimal threshold for discriminating the tumour from the surrounding tissue and for estimating the corresponding correct tumour volumes. However, in order to perform such a comparison meaningfully, the PET-CT should be performed immediately prior to sacrifice. Since this was not done in the present study, we plan to do so in a follow-up study in order to further refine and validate the MTV measurements based on PET-CT.

The imaging findings presented in this study during tumour growth and metastatic spread apply to untreated mice. Future studies will thus be needed to explore the feasibility of the same multimodal imaging platform to evaluate treatment response during therapy. However, the ability to visualize and quantify the tumor burden before treatment is a prerequisite in order to succeed in the evaluation of treatment response. Thus, we propose that the presented findings in untreated mice make the same imaging methods very promising for evaluation of treatment response, although this remains to be demonstrated in future studies. Furthermore, including preclinical ultrasound scanning during tumor growth and therapy may represent an intriguing addition to the multimodal imaging platform already explored in this study. Ultrasound may be especially translatable to the clinic, since patients with symptoms of endometrial cancer are often subjected to vaginal ultrasound as primary imaging examination.

Interestingly, the functional tumour characteristics based on PET-CT and MRI are very similar to that observed in human endometrial cancer, supporting a promising translational relevance of this imaging integrated tumour model for assessing tumour growth. The findings in this model derived from human endometrial cancer cell lines, as well as the PDX model, open the avenue for further exploring the value of PET-CT and MRI in monitoring tumour growth and metastatic spread in PDX models of endometrial cancer. This may prove highly clinically relevant since PDX models are likely to have an increased translational relevance for drug testing with relevance for a human tumour setting.

Conclusion

We have demonstrated the feasibility of a multimodal imaging platform using BLI, ^{18}F-FDG PET, ^{18}F-FLT PET, and MRI to detect and monitor tumour progression in an orthotopic endometrial cancer model derived from human cell lines. The latter three imaging methods are well suited also in patients derived tumour models in which BLI is ineligible. PET-CT is also demonstrated to detect tumour tissue in a PDX model. PET-CT and MRI may thus represent

powerful tools for monitoring tumour progression and functional changes for preclinical testing of systemic therapy in orthotopic models more reliably mimicking human endometrial cancer.

Supporting Information

S1 Fig. Identification of human specific anti-Estrogen Recetor α antibody. Immunohistochemical staining was performed according to a standard protocol. Paraffin sections from mouse uterus implanted with Ishikawa human endometrial cancer cells were stained with 1:50 anti-ERα (A; sc-543 Santa Cruz Biotechnologies) or 1:400 anti-ERα (B; SP1, Thermo) for detection of endometrial cells expressing ERα. Both antibodies are raised in rabbit and selected to avoid crossreaction with mouse immunoglobulins. The Santa Cruz antibody (A) was found to detect both mouse and human ERα, while the Thermo antibody SP1(B) was human specific. The SP1 antibody was selected to specifically detect localization and spread of implanted cells.
(PDF)

S2 Fig. Detection of metastatic spread by IHC staining for human ERα. To verify presence of the ERα positive human Ishikawa^{Luc} cell line spread to distant organs, sections were stained for expression of human Estrogen Receptor α. Myometrial tumour infiltration was detected in the uterus (A) and metastases were detected in the pancreas (B), liver (C) and in the lungs (D); for all tumour sites positive staining for human ERα confirming spread of the human tumour cells.
(PDF)

S3 Fig. Example of human endometrial carcinoma assessed by preoperative imaging and estrogen receptor staining in histological section. ^{18}F-FDG PET-CT (A, E), CT (B), T2-weighed (C, F) and contrast enhanced T1-weighed (D) MRI, diffusion weighted imaging (b = 1000 s/mm^2) (G) with corresponding apparent diffusion coefficient (ADC) map (H) and positive immunohistochemical staining for estrogen receptor of the uterine tumour tissue (I) from an 80-year old female with FIGO stage 2, endometrioid endometrial cancer. ^{18}F-FDG PET-CT shows a highly ^{18}F-FDG-avid uterine tumour (A, E; arrows) with an estimated metabolic tumour volume of 22 ml. The tumour is also conspicuously depicted at CT (B) and MRI (C-D, F-H; arrows) exhibiting restricted diffusion on the ADC map (H) with tumour ADC value of 0.83 x 10^{-3} mm^2/s.
(PDF)

Acknowledgments

We thank Ellen Valen, Britt Edvardsen and Bendik Nordanger for excellent technical assistance.

Author Contributions

Conceived and designed the experiments: ISH EMC HBS CK. Performed the experiments: MP TF RK CK TP CBR. Analyzed the data: ISH TF NB TP NCV CBR CK. Wrote the paper: ISH CK.

References

1. Amant F, Moerman P, Neven P, Timmerman D, Van Limbergen E, Vergote I. Endometrial cancer. Lancet. 2005; 366(9484):491–505. doi: 10.1016/S0140-6736(05)67063-8 PMID: 16084259.

2. Salvesen HB, Haldorsen IS, Trovik J. Markers for individualised therapy in endometrial carcinoma. The Lancet Oncology. 2012; 13(8):e353–61. Epub 2012/08/01. doi: 10.1016/S1470-2045(12)70213-9 PMID: 22846840.
3. Oza AM, Elit L, Tsao MS, Kamel-Reid S, Biagi J, Provencher DM, et al. Phase II study of temsirolimus in women with recurrent or metastatic endometrial cancer: a trial of the NCIC Clinical Trials Group. Journal of clinical oncology: official journal of the American Society of Clinical Oncology. 2011; 29 (24):3278–85. doi: 10.1200/JCO.2010.34.1578 PMID: 21788564; PubMed Central PMCID: PMC3158598.
4. Tentler JJ, Tan AC, Weekes CD, Jimeno A, Leong S, Pitts TM, et al. Patient-derived tumour xenografts as models for oncology drug development. Nature reviews Clinical oncology. 2012; 9(6):338–50. doi: 10.1038/nrclinonc.2012.61 PMID: 22508028; PubMed Central PMCID: PMC3928688.
5. Vollmer G. Endometrial cancer: experimental models useful for studies on molecular aspects of endometrial cancer and carcinogenesis. Endocrine-related cancer. 2003; 10(1):23–42. PMID: 12653669.
6. Doll A, Gonzalez M, Abal M, Llaurado M, Rigau M, Colas E, et al. An orthotopic endometrial cancer mouse model demonstrates a role for RUNX1 in distant metastasis. International journal of cancer Journal international du cancer. 2009; 125(2):257–63. doi: 10.1002/ijc.24330 PMID: 19384951.
7. Cabrera S, Llaurado M, Castellvi J, Fernandez Y, Alameda F, Colas E, et al. Generation and characterization of orthotopic murine models for endometrial cancer. Clinical & experimental metastasis. 2012; 29(3):217–27. Epub 2011/12/27. doi: 10.1007/s10585-011-9444-2 PMID: 22198674.
8. Kamat AA, Merritt WM, Coffey D, Lin YG, Patel PR, Broaddus R, et al. Clinical and biological significance of vascular endothelial growth factor in endometrial cancer. Clinical cancer research: an official journal of the American Association for Cancer Research. 2007; 13(24):7487–95. doi: 10.1158/1078-0432.CCR-07-1017 PMID: 18094433.
9. Che Q, Liu BY, Liao Y, Zhang HJ, Yang TT, He YY, et al. Activation of a positive feedback loop involving IL-6 and aromatase promotes intratumoral 17beta-estradiol biosynthesis in endometrial carcinoma microenvironment. International journal of cancer Journal international du cancer. 2014; 135(2):282–94. doi: 10.1002/ijc.28679 PMID: 24347287.
10. Che Q, Liu BY, Wang FY, He YY, Lu W, Liao Y, et al. Interleukin 6 promotes endometrial cancer growth through an autocrine feedback loop involving ERK-NF-kappaB signaling pathway. Biochemical and biophysical research communications. 2014; 446(1):167–72. doi: 10.1016/j.bbrc.2014.02.080 PMID: 24582558.
11. Merritt WM, Kamat AA, Hwang JY, Bottsford-Miller J, Lu C, Lin YG, et al. Clinical and biological impact of EphA2 overexpression and angiogenesis in endometrial cancer. Cancer biology & therapy. 2010; 10 (12):1306–14. PMID: 20948320; PubMed Central PMCID: PMC3047089.
12. Pillozzi S, Fortunato A, De Lorenzo E, Borrani E, Giachi M, Scarselli G, et al. Over-Expression of the LH Receptor Increases Distant Metastases in an Endometrial Cancer Mouse Model. Frontiers in oncology. 2013; 3:285. doi: 10.3389/fonc.2013.00285 PMID: 24312898; PubMed Central PMCID: PMC3832806.
13. Theisen ER, Gajiwala S, Bearss J, Sorna V, Sharma S, Janat-Amsbury M. Reversible inhibition of lysine specific demethylase 1 is a novel anti-tumor strategy for poorly differentiated endometrial carcinoma. BMC cancer. 2014; 14:752. doi: 10.1186/1471-2407-14-752 PMID: 25300887; PubMed Central PMCID: PMC4197342.
14. Siolas D, Hannon GJ. Patient-derived tumor xenografts: transforming clinical samples into mouse models. Cancer Res. 2013; 73(17):5315–9. doi: 10.1158/0008-5472.CAN-13-1069 PMID: 23733750; PubMed Central PMCID: PMC3766500.
15. O'Farrell AC, Shnyder SD, Marston G, Coletta PL, Gill JH. Non-invasive molecular imaging for preclinical cancer therapeutic development. British journal of pharmacology. 2013; 169(4):719–35. doi: 10.1111/bph.12155 PMID: 23488622; PubMed Central PMCID: PMC3687654.
16. Wolf G, Abolmaali N. Preclinical molecular imaging using PET and MRI. Recent results in cancer research Fortschritte der Krebsforschung Progres dans les recherches sur le cancer. 2013; 187:257–310. doi: 10.1007/978-3-642-10853-2_9 PMID: 23179885.
17. McKinley ET, Smith RA, Zhao P, Fu A, Saleh SA, Uddin MI, et al. 3'-Deoxy-3'-18F-fluorothymidine PET predicts response to (V600E)BRAF-targeted therapy in preclinical models of colorectal cancer. Journal of nuclear medicine: official publication, Society of Nuclear Medicine. 2013; 54(3):424–30. doi: 10.2967/jnumed.112.108456 PMID: 23341544; PubMed Central PMCID: PMC3633462.
18. Moestue SA, Huuse EM, Lindholm EM, Bofin A, Engebraaten O, Maelandsmo GM, et al. Low-molecular contrast agent dynamic contrast-enhanced (DCE)-MRI and diffusion-weighted (DW)-MRI in early assessment of bevacizumab treatment in breast cancer xenografts. Journal of magnetic resonance imaging: JMRI. 2013; 38(5):1043–53. doi: 10.1002/jmri.24079 PMID: 23908122.
19. Liebsch L, Kailayangiri S, Beck L, Altvater B, Koch R, Dierkes C, et al. Ewing sarcoma dissemination and response to T-cell therapy in mice assessed by whole-body magnetic resonance imaging. Br J

Cancer. 2013; 109(3):658–66. doi: 10.1038/bjc.2013.356 PMID: 23839490; PubMed Central PMCID: PMC3738111.

20. Lorens JB, Jang Y, Rossi AB, Payan DG, Bogenberger JM. Optimization of regulated LTR-mediated expression. Virology. 2000; 272(1):7–15. Epub 2000/06/30. doi: 10.1006/viro.2000.0353 PMID: 10873744.

21. Helland O, Popa M, Vintermyr OK, Molven A, Gjertsen BT, Bjorge L, et al. First in-mouse development and application of a surgically relevant xenograft model of ovarian carcinoma. PLoS One. 2014; 9(3): e89527. Epub 2014/03/07. doi: 10.1371/journal.pone.0089527 PMID: 24594904; PubMed Central PMCID: PMC3942384.

22. Bai B, Bading J, Conti PS. Tumor quantification in clinical positron emission tomography. Theranostics. 2013; 3(10):787–801. doi: 10.7150/thno.5629 PMID: 24312151; PubMed Central PMCID: PMC3840412.

23. Frese KK, Tuveson DA. Maximizing mouse cancer models. Nature reviews Cancer. 2007; 7(9):645–58. doi: 10.1038/nrc2192 PMID: 17687385.

24. Weissleder R. Scaling down imaging: molecular mapping of cancer in mice. Nature reviews Cancer. 2002; 2(1):11–8. doi: 10.1038/nrc701 PMID: 11902581.

25. Kocher B, Piwnica-Worms D. Illuminating cancer systems with genetically engineered mouse models and coupled luciferase reporters in vivo. Cancer discovery. 2013; 3(6):616–29. doi: 10.1158/2159-8290.CD-12-0503 PMID: 23585416; PubMed Central PMCID: PMC3679270.

26. Sanghera B, Wong WL, Sonoda LI, Beynon G, Makris A, Woolf D, et al. FLT PET-CT in evaluation of treatment response. Indian journal of nuclear medicine: IJNM: the official journal of the Society of Nuclear Medicine, India. 2014; 29(2):65–73. doi: 10.4103/0972-3919.130274 PMID: 24761056; PubMed Central PMCID: PMC3996774.

27. Soret M, Bacharach SL, Buvat I. Partial-volume effect in PET tumor imaging. Journal of nuclear medicine: official publication, Society of Nuclear Medicine. 2007; 48(6):932–45. doi: 10.2967/jnumed.106.035774 PMID: 17504879.

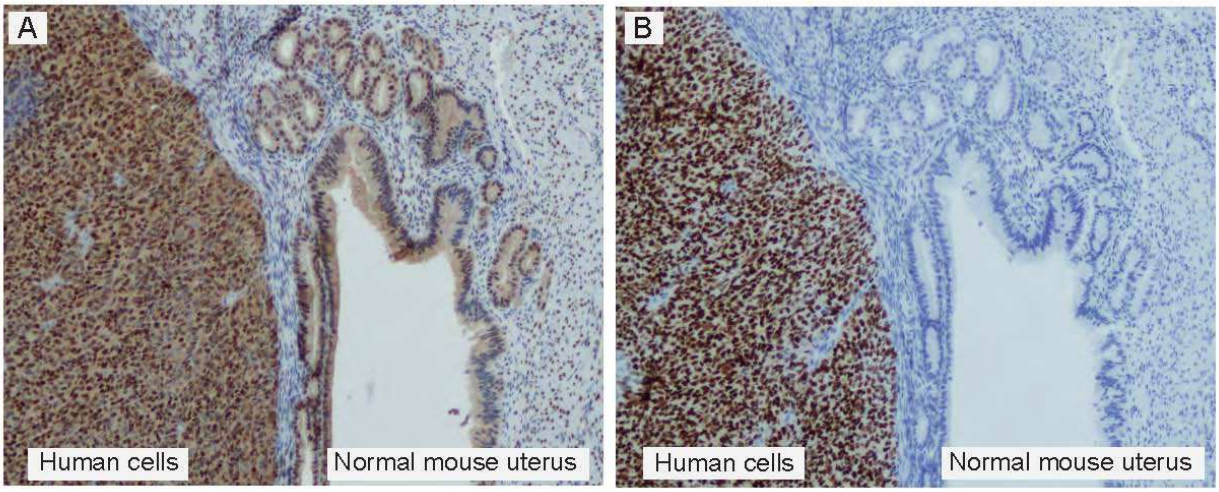
A
Human cells
Normal mouse uterus
B
Human cells
Normal mouse uterus

Figure S1.

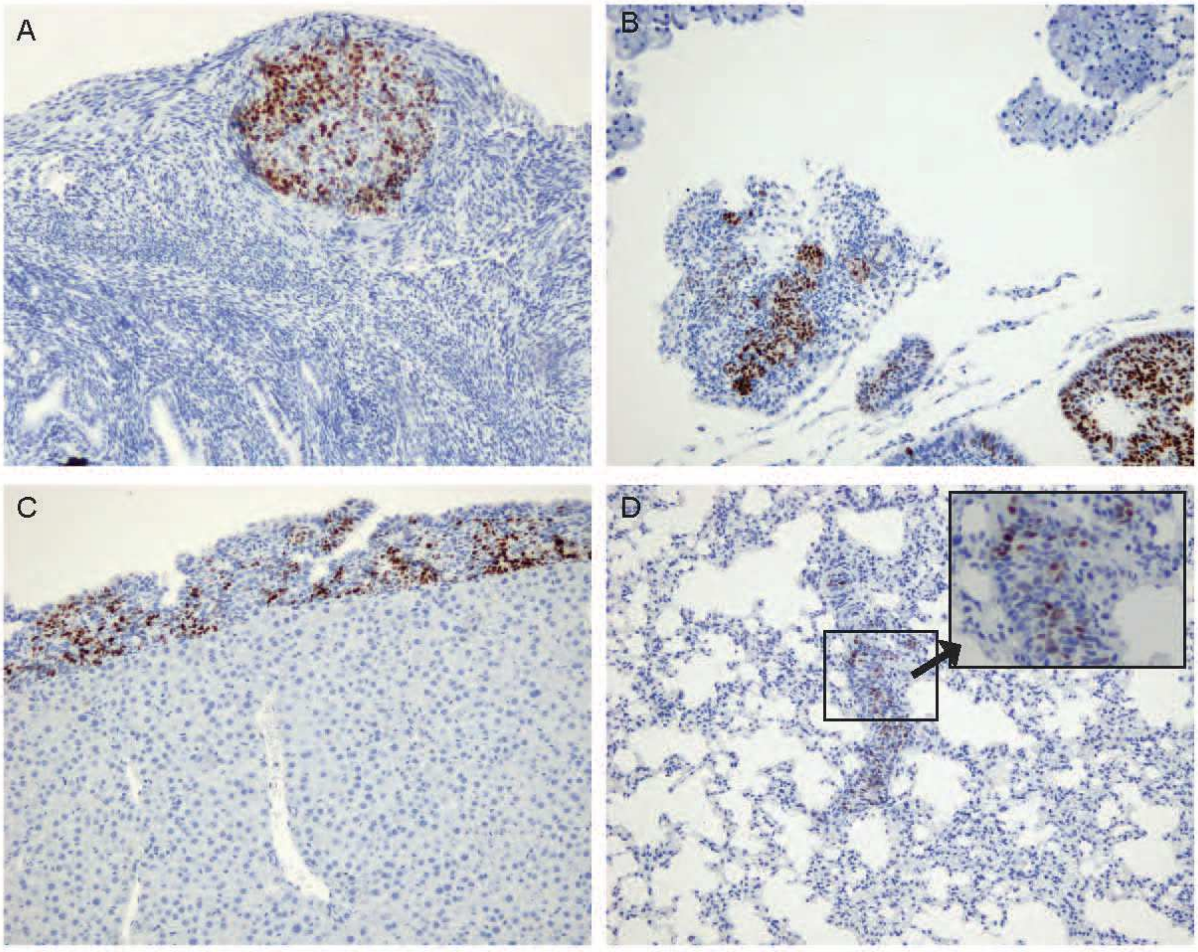

Figure S2.

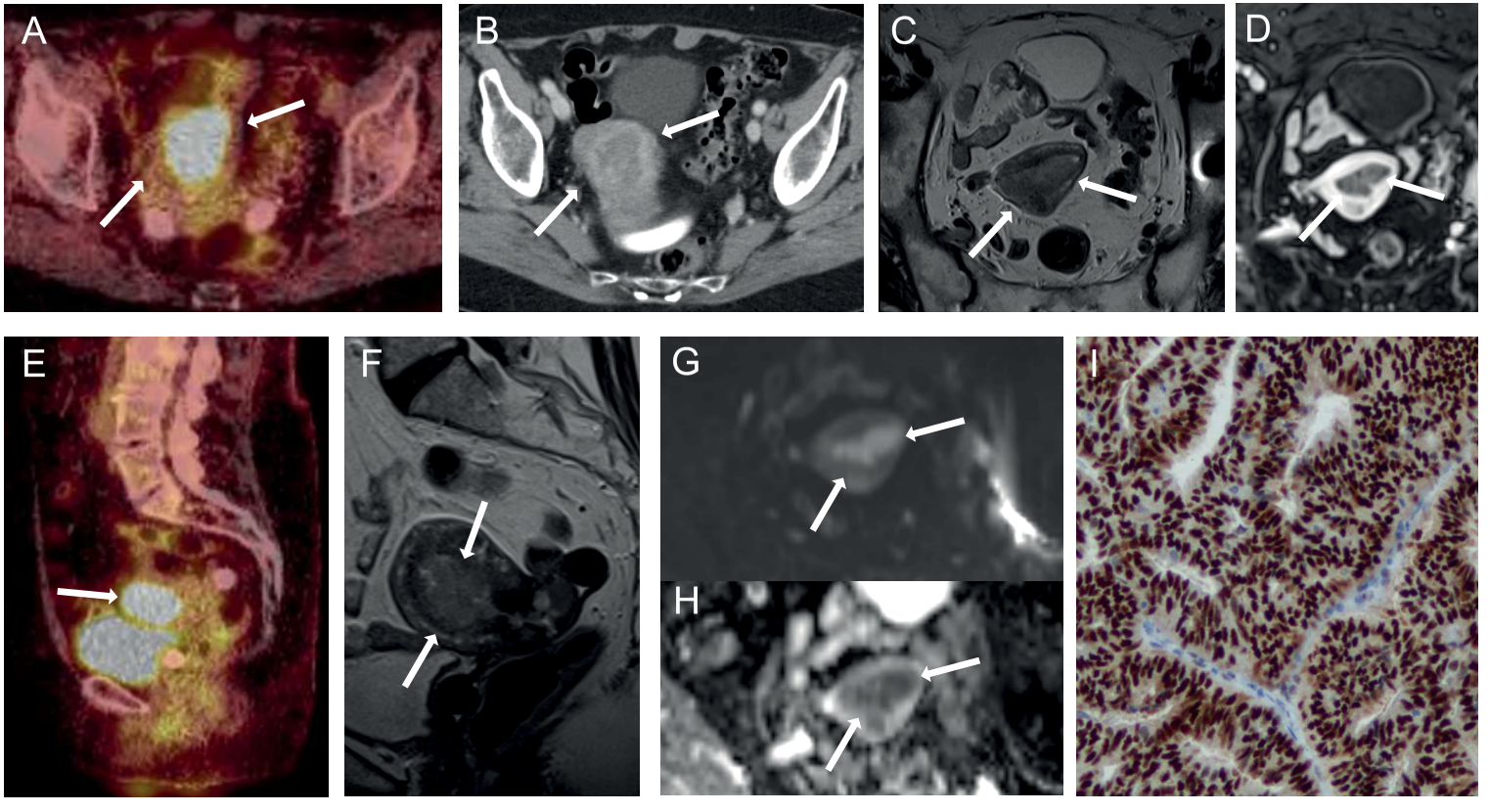

Figure S3

III

Gynecologic Oncology 148 (2018) 197–203

Contents lists available at ScienceDirect

Gynecologic Oncology

journal homepage: www.elsevier.com/locate/ygyno

Asparaginase-like protein 1 is an independent prognostic marker in primary endometrial cancer, and is frequently lost in metastatic lesions

Tina Fonnes [a,b], Hege F. Berg [a,b], Therese Bredholt [a,b], Per-Henrik D. Edqvist [c,d], Kristina Sortland [e], Anna Berg [a,b], Helga B. Salvesen [a,b], Lars A. Akslen [f,g], Henrica M.J. Werner [a,b], Jone Trovik [a,b], Ingvild L. Tangen [a,b], Camilla Krakstad [a,b,*]

[a] Centre for Cancer Biomarkers, Department of Clinical Science, University of Bergen, Bergen, Norway
[b] Department of Obstetrics and Gynecology, Haukeland University Hospital, Bergen, Norway
[c] Department of Immunology, Genetics and Pathology, Uppsala University, Uppsala, Sweden
[d] Science for Life Laboratory, Uppsala, Sweden
[e] Department of Biomedicine, University of Bergen, Bergen, Norway
[f] Department of Pathology, Haukeland University Hospital, Bergen, Norway
[g] Centre for Cancer Biomarkers, Department of Clinical Medicine, Section for Pathology, University of Bergen, Bergen, Norway

HIGHLIGHTS

- ASRGL1 validates as a prognostic marker in a prospective setting.
- Low ASRGL1 protein and *ASRGL1* mRNA expression predicts poor outcome.
- ASRGL1 expression has independent impact on survival.
- Precursor lesions express high ASRGL1 levels.
- The majority of metastases have low ASRGL1 expression.

ARTICLE INFO

Article history:
Received 29 September 2017
Received in revised form 20 October 2017
Accepted 23 October 2017
Available online 31 October 2017

Keywords:
Endometrial carcinoma
Hysterectomy
Prognostic
Biomarker
ASRGL1

ABSTRACT

Objective. Loss of Asparaginase-like protein 1 (ASRGL1) has been suggested as a prognostic biomarker in endometrial carcinoma. Our objective was to validate this in a prospectively collected, independent patient cohort, and evaluate ASRGL1 expression in endometrial carcinoma precursor lesion and metastases.

Methods. 782 primary endometrial carcinomas, 90 precursor lesions (complex atypical hyperplasia), and 179 metastases (from 87 patients) were evaluated for ASRGL1 expression by immunohistochemistry in relation to clinical and histopathological data. *ASRGL1* mRNA level was investigated in 237 primary tumors and related to survival and ASRGL1 protein expression.

Results. Low expression of ASRGL1 protein and *ASRGL1* mRNA predicted poor disease specific survival ($P < 0.001$). In multivariate survival analyses ASRGL1 had independent prognostic value both in the whole patient cohort (Hazard ratio (HR): 1.53, 95% confidence interval (CI): 1.04–2.26, $P = 0.031$) and within the endometrioid subgroup (HR: 2.64, CI: 1.47–4.74, $P = 0.001$). Low ASRGL1 expression was less frequent in patients with low grade endometrioid primary tumors compared to high grade endometrioid and non-endometrioid primary tumors, and ASRGL1 was lost in the majority of metastatic lesions.

Conclusions. In a prospective setting ASRGL1 validates as a strong prognostic biomarker in endometrial carcinoma. Loss of ASRGL1 is associated with aggressive disease and poor survival, and is demonstrated for the first time to have independent prognostic value in the entire endometrial carcinoma patient population.

1. Introduction

Endometrial carcinoma is a malignancy originating in the female reproductive tract, and is the fourth most diagnosed cancer in European women after breast, colorectal and lung cancer [1]. Primary surgical

* Corresponding author at: Department of Clinical Science, University of Bergen, Jonas Lies Vei 72, 5020 Bergen, Norway.
E-mail address: camilla.krakstad@med.uib.no (C. Krakstad).

https://doi.org/10.1016/j.ygyno.2017.10.025
0090-8258/

treatment of endometrial carcinoma is curative for most patients, but 15–20% suffers a relapse within few years [2,3]. Prognosis for recurrent endometrial carcinoma is often poor, especially in patients with systemic recurrence [3]. Little improvement in treatment and survival has been achieved over the last decades, highlighting the need of targeted therapies and more individualized cancer treatment [4]. Discovering, validating and implementing new biomarkers that can identify high-risk endometrial carcinoma patients is crucial as such markers can potentially guide physicians planning treatment for individual patients [2]. Asparaginase-like protein 1 (ASRGL1) is an enzyme classified as a N-terminal nucleophile (Ntn) hydrolase, exhibiting both L-asparaginase and β-aspartyl peptidase activity [5]. It was first described as a novel protein sharing 77% of its genetic sequence with a sperm autoantigen found in rats [6]. The role of ASRGL1 in cancer development and progression is not clear. For several malignancies including mammary, ovarian, and prostate cancer high levels of ASRGL1 in tumor have been reported [7,8]. In endometrial carcinoma loss of the gene encoding ASRGL1 has previously been reported as part of a 29-gene signature associated with features of aggressive disease and poor recurrence-free survival [9,10]. Loss of ASRGL1 in primary endometrial carcinoma has also been suggested to be an independent biomarker for disease-specific survival in a subgroup of patients with endometrioid endometrial carcinoma [11]. In the present study we aimed to validate ASRGL1 as a prognostic biomarker in endometrial carcinoma, and to evaluate the expression of ASRGL1 in clinical specimens from a large, prospectively collected patient cohort including precursor lesions (complex atypical hyperplasias – CAH), primary tumors, and metastases.

2. Material and methods

2.1. Patient series

Women diagnosed with endometrial carcinoma at Haukeland University Hospital, Norway, were prospectively included during the period 2001–2015. Haukeland University Hospital is a referral hospital for Hordaland County, and the patient series is representative of the Norwegian population due to similar incidence rates and patient characteristics for this region compared to the whole of Norway [12]. Primary tumor tissue from 782 patients was collected during hysterectomy and prepared as formalin fixed and paraffin embedded (FFPE) tissue. This corresponds to 76% of endometrial carcinoma patients included in the local biobank during this time period. Cases not represented in TMAs include inoperable patients, patients with sparse tumor material in hysterectomy specimen, and cases with poor technical quality of TMA tissue cylinders. Fresh frozen tissue was collected in parallel when possible. Clinical information was retrieved from medical records as previously described [13], including age at primary treatment, International Federation of Gynaecology and Obstetrics (FIGO) stage (according to 2009 criteria), histopathological type and grade, and follow-up data. Biopsies from precursor lesions were obtained from 90 patients diagnosed with CAH. Samples from metastatic tissue were available for 87 patients (179 lesions in total). All parts of the study have been approved according to Norwegian legislation, including the Norwegian Data Inspectorate, Norwegian Social Sciences Data Services and Western Regional Committee for Medical and Health Research Ethics (REK 2009/2315). All participants were informed and gave written consent prior to inclusion.

2.2. Immunohistochemistry (IHC)

FFPE tissue was used to generate tissue microarrays (TMA) as previously described [14]. The tumor area with highest tumor content was identified on hematoxylin and eosin stained slides. Using a custom made precision instrument (Beecher instruments, Silver Spring, MD, USA) tissue cylinders (0.6 mm) (three tissue cylinders for primary tumors and CAHs and one tissue cylinder for metastatic lesions) were punched out of the donor block and mounted in a recipient paraffin block. TMAs were stained by automated IHC using a previously published polyclonal anti-ASRGL1antibody (HPA029725, diluted 1:375) [11], or a monoclonal anti-ASRGL1 antibody (AMAb90907, diluted 1:1000) (Both; Atlas Antibodies, Stockholm, Sweden). ASRGL1 staining in tumor cells was evaluated without considering sub-cellular localization [11]. A staining index (SI) was calculated for each patient based on all three cylinders by multiplying staining intensity (range 0–3) and area of positive stained tumor cells ($1 \leq 10\%$, $2 = 10–50\%$, $3 \geq 50\%$) as previously reported [15]. For statistical analyses cases were ranked by staining index, and categorized into quartiles based on frequency distribution and size of the subgroups. The upper three quartiles were combined based on similarities in survival, and defined as "ASRGL1 high". The lower quartile was defined as "ASRGL1 low", corresponding to SI: 0–2 (HPA029725) or SI: 0–1 (AMAb90907). Random TMA slides were scored by three independent observers (TF, KS and ILT) blinded for patient characteristics and outcome, and an intraclass correlation coefficient (ICC) was calculated to assess interrater reliability for each of the two antibodies. The ICC of HPA029275 score in two groups was 0.71 (95% confidence interval (CI): 0.64–0.78, $n = 126$ patients), while AMAb90907 score in two groups had an ICC of 0.95 (CI: 0.93–0.96, $n = 105$ patients). Staining and scoring of estrogen receptor α (ERα) have previously been described, defining loss of ERα as SI: 0–3 [16].

2.3. Gene expression

RNA was extracted from fresh frozen tissue using the RNeasy Mini Kit (Qiagen, Hilden, Germany) according to the manufacturer's instructions. Samples were hybridized to Agilent Whole Human Genome Microarrays 44 k (Cat. No. G4112F) prior to scanning and normalization as previously reported [16]. In total, RNA was extracted from 237 primary tumors. For survival analyses based on mRNA levels patients were ranked by *ASRGL1* expression and divided into quartiles. The cut-off for low *ASRGL1* was defined as the lower quartile of cases.

2.4. Statistical analyses

SPSS Statistics software (version 24.0; IBM Corp., Armonk, NY, USA) was used for statistical analyses. All statistical tests were two-sided, and P-values ≤ 0.05 were considered statistically significant. ICC estimates were calculated by a single rater absolute agreement, two-way random effects model. Analyses of categorical variables were performed using the Pearson Chi-square test or Fisher's exact test, while continuous variables were evaluated using the Mann-Whitney *U* test. Disease-specific survival curves were generated using the Kaplan-Meier method, and survival between groups was compared using the log rank (Mantel-Cox) test. Time of primary surgery was used as entry date, and time to death due to endometrial carcinoma was defined as endpoint. Cox proportional hazard regression model was used to evaluate the independent prognostic impact of ASRGL1 in multivariate survival analyses.

3. Results

782 patients treated for endometrial carcinoma at Haukeland University Hospital were prospectively included in this study. Of these patients, 79% ($n = 616$) were classified as "ASRGL1 high" (Fig.1A) and 21% ($n = 166$) as "ASRGL1 low" (Fig.1B) when evaluating ASRGL1 expression in primary tumors by IHC. Validation of antibody was performed by staining 607 primary tumors with two different antibodies (AMAbb90907 and HPA029725). These antibodies had significantly correlated scoring indexes ($P < 0.001$) and similar prognostic value. The ICC estimate for AMAb90907 (ICC: 0.95, CI: 0.93–0.96) indicates excellent interrater reliability [17], and was higher than for HPA029725 (ICC: 0.71, CI: 0.64–0.68). AMAb90907 score was therefore selected for further analyses. Low ASRGL1 protein expression was significantly associated with clinicopathological characteristics of aggressive endometrial

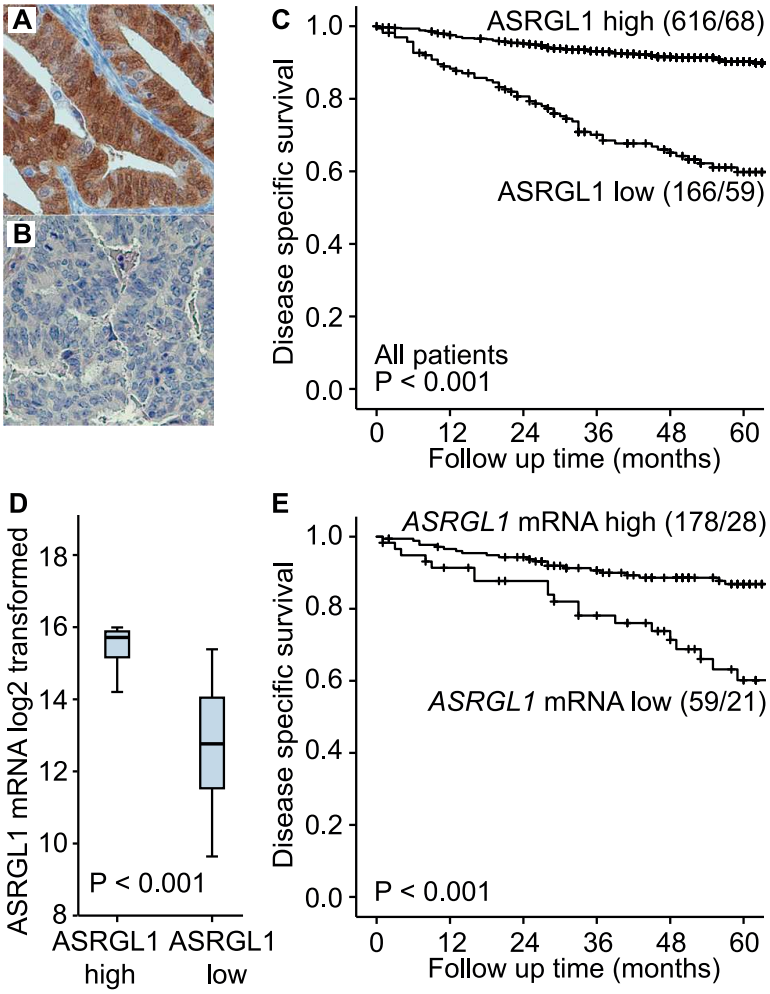

Fig. 1. Low expression of ASRGL1 predicts poor survival. Immunohistochemical staining of ASRGL1 (AMAb90907), demonstrating "high" (A) and "low" (B) staining index. Low protein expression of ASRGL1predicts poor disease specific survival in the whole patient population (C). *ASRGL1* mRNA and protein expression is found to significantly correlate, using the Mann-Whitney *U* test (D), and the quartile of patients with the lowest *ASRGL1* mRNA expression have significantly poorer disease specific survival than patients with higher *ASRGL1* mRNA expression (E).

carcinoma such as high age, high FIGO stage, ERα loss and non-endometrioid histology ($P < 0.001$ in all) (Table 1). The proportion of patients with low ASRGL1 expression was particularly high among carcinosarcomas and undifferentiated endometrial tumors (71% and 86%, respectively), but also 8% of patients with endometrioid grade 1–2 tumors expressed low ASRGL1 levels (Table 1). In a univariate survival analysis, low ASRGL1 level predicted poor disease-specific survival in the whole patient population (Fig. 1C). ASRGL1 was also found to have an independent prognostic impact on survival in a multivariate survival analysis after adjusting for age, FIGO stage, histological type and grade (Hazard ratio (HR): 1.53, CI: 1.04–2.26, $P = 0.031$) (Table 2). The *ASRGL1* gene has been reported up-regulated in several cancer forms and mRNA expression levels might be an alternative prognostic biomarker in gene-based applications. A significant overlap between *ASRGL1* mRNA and protein level was observed in 237 patients with both IHC and microarray data available ($P < 0.001$) (Fig. 1D), and patients with low *ASRGL1* mRNA expression had significantly worse 5 year disease specific survival (DSS) compared to patients with high *ASRGL1* mRNA expression (5 year DSS of 0.60 and 0.87, respectively, $P < 0.001$, Fig. 1E).

ASRGL1 was evaluated by IHC in 90 patients with complex atypical hyperplasia, a precursor lesion of endometrial carcinoma. ASRGL1 expression was mainly intact in this group, and 70% of patients had strong positive staining (SI: 6–9). Only one patient (1%) demonstrated low ASRGL1 level (Fig. 2A). The proportion of lesions with low ASRGL1 expression increased significantly with higher grade within the endometrioid endometrial carcinoma subgroup ($P < 0.001$) (Fig. 2A). Of the non-endometrioid tumors 56% had low expression of ASRGL1, which was significantly higher than for the endometrioid grade 3 tumors ($P = 0.012$). In the subgroup of endometrioid endometrial carcinoma patients where less aggressive disease is presumed [18], low expression of ASRGL1 was significantly associated with

Table 1
ASRGL1 protein expression related to clinicopathological variables in 782 patients with endometrial carcinoma.

Variable	N	ASRGL1		P-value (x^2)
		High *n* (%)	Low *n* (%)	
Age	782			<**0.001**
<66	405	341 (84)	64 (16)	
≥66	377	275 (73)	102 (28)	
FIGO stage 2009	782			<**0.001**
I–II	659	551 (84)	108 (16)	
III–IV	123	65 (53)	58 (47)	
Histologic type	782			<**0.001**
Endometrioid	635	551 (87)	84 (13)	
Clear cell	29	15 (52)	14 (48)	
Serous	70	38 (54)	32 (46)	
Carcinosarcoma	34	10 (29)	24 (71)	
Undifferentiated	14	2 (14)	12 (86)	
Histologic grade	623			<**0.001**
Grade 1–2	511	471 (92)	40 (8)	
Grade 3	112	68 (61)	44 (39)	
Metastatic lymph nodes	630			<**0.001**
Negative	559	457 (82)	102 (18)	
Positive	71	37 (52)	34 (48)	
Ploidy	**490**			<**0.001**
Diploid	381	302 (79)	79 (21)	
Aneuploid	109	57 (52)	52 (48)	
Myometrial infiltration	779			<**0.001**
<50%	483	410 (85)	73 (15)	
≥50%	296	205 (69)	91 (31)	
ERα	741			<**0.001**
Positive	555	514 (93)	41 (7)	
Negative	186	75 (40)	111 (60)	

Abbreviations: Asparaginase-like protein 1 (ASRGL1), Estrogen receptor α (ERα), International Federation of Gynaecology and Obstetrics (FIGO).
Missing information on histologic grade for 12 patients, metastatic nodes for 152 patients, ploidy for 292 patients, myometrial infiltration for 3 patients, and ERα status for 41 patients.
[a] Endometrioid cases only.

characteristics of aggressive disease (Supplementary Table S1) and poor disease-specific survival (P < 0.001, Fig. 2B). ASRGL1 was also found to have independent prognostic value within the endometrioid endometrial carcinoma patients after adjusting for age and histologic grade (HR: 2.64, CI: 1.47–4.74, P = 0.001, Table 3). In the non-endometrioid subgroup ASRGL1 did however not have an independent impact on survival when adjusted for age and FIGO stage (HR: 1.37, CI: 0.83–2.26, P = 0.226).

ASRGL1 expression was investigated by IHC in 179 metastatic lesions from 87 patients with available corresponding primary tumors. Of these 87 patients, 43% of primary tumors and 77% of metastases expressed low ASRGL1 levels (Fig. 3A and Supplementary Fig. S1). Within the endometrioid subgroup, patients with grade 1 and 2 endometrioid endometrial carcinoma had fewer metastases with low ASRGL1 level (53% and 44% of lesions, respectively) than grade 3 endometrioid endometrial carcinoma patients (80% of lesions). Overall, patients with endometrioid endometrial carcinoma had a lower proportion of metastatic lesions with low ASRGL1 expression compared to patients with non-endometrioid endometrial carcinoma (63% and 90% of metastases, respectively, Supplementary Fig. S1). Of 50 patients with "ASRGL1 high" primary tumors, only 10% had some metastases with high and some metastases with low ASRGL1 level. 46% of patients had intact ASRGL1 expression in all metastases, while 44% of patients had ASRGL1 loss in all metastatic lesions (Fig. 3B). 37 patients had low ASRGL1 expression in primary tumor, and the majority of these (89%) also had low ASRGL1 level in all metastatic lesions. 4 patients had high ASRGL1 expression in some, but not all metastases. None of the patients with ASRGL1 low primary tumors had high ASRGL1 expression in all metastatic lesions (Fig. 3C). For patients with more than one available metastatic lesion, the expression pattern of ASRGL1 was similar between the different metastases in individual patients in most cases (Supplementary Fig. S1). Information regarding ERα status in metastases was included when known, and was available for a total of 158 lesions. A similar expression of ASRGL1 and ERα in metastases was observed. 73% of metastatic lesions with high ASRGL1 levels had intact ERα, and 72% of lesions with low ASRGL1 had low levels of ERα. ASRGL1 was more frequently lost in metastatic lesions than ERα (77% and 60% of lesions respectively, P = 0.001, Supplementary Fig. S1).

4. Discussion

New, robust biomarkers are needed to tailor treatment for individual endometrial carcinoma patients. To achieve clinical implementation, novel biomarkers should be validated in independent studies with sufficient number of patients to ensure statistical power. Validation studies should also be performed in patient groups that are representative for the population where the biomarker potentially will be used [19]. In the current study we validate loss of ASRGL1 expression as a prognostic marker for poor survival in endometrial carcinoma, in a large, independent, population-based patient cohort. This is the first study investigating the prognostic potential of ASRGL1 expression in a prospective setting in endometrial carcinoma, as ASRGL1 previously only has been explored in retrospectively collected cohorts with lower number of patients [11].

In the present study ASRGL1 expression was evaluated using the staining index, where low expression is defined as 0–1 and high

Table 2
Multivariable survival analyses of endometrial carcinoma patients according to the Cox' proportional hazards regression model.

Variable	n[a]	Unadj.HR	95% CI	P-value	Adj.HR	95% CI	P-value
Age (mean = 65)				<0.001			<0.001
	770	1.05	1.04–1.07		1.03	1.02–1.05	
FIGO stage				<0.001			<0.001
I/II	648	1			1		
III/IV	122	8.77	6.17–12.45		5.08	3.49–7.39	
Histologic type				<0.001			0.001
Endometrioid	623	1			1		
Non-endometrioid	147	6.73	4.71–9.60		2.29	1.42–3.70	
Histologic grade				<0.001			0.050
1/2	511	1			1		
3	259	6.11	4.16–8.96		1.73	1.00–2.97	
ASRGL1[b]				<0.001			0.031
High	604	1			1		
Low	166	4.10	2.89–5.82		1.53	1.04–2.26	

[a] Cases with data available for all variables included in the univariate analyses (N = 770).
[b] Evaluated in hysterectomy samples by IHC (high = 2–9, low = 0–1).

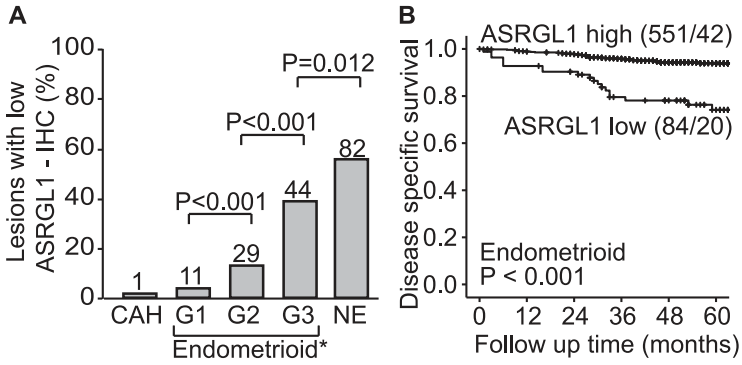

Fig. 2. ASRGL1 protein level decreases with dedifferentiation, and predicts survival in EEC. The proportion of tumors with low ASRGL1 expression is increasing with higher grade within the endometrioid endometrial carcinoma patients, and is higher in non-endometrioid patients compared to endometrioid grade 3 patients. Numbers on bars represent the number of patients with low ASRGL1. *P*-values were calculated using the Fisher's exact test (A). Low protein expression of ASRGL1 is associated with poor survival in patients with endometrioid endometrial carcinoma (B). Abbreviations: CAH: complex atypical hyperplasia, G: grade, NE = non-endometrioid. *Information on grade missing for 12 patients.

expression as 2–9. An earlier study defined positive staining in >75% of cells as cut-off for high ASRGL1 expression regardless of staining intensity [11]. The fact that different scoring methods and cut-offs for ASRGL1 demonstrate prognostic impact supports its robustness as a prognostic marker in endometrial carcinoma.

Low ASRGL1 protein expression has been linked to aggressive disease and poor survival in endometrial carcinoma, and is reported to be an independent prognostic marker in endometrioid endometrial carcinoma [11]. This is consistent with our findings, and we are the first to demonstrate that ASRGL1 has independent prognostic value also in the whole patient population.

No IHC biomarkers are currently clinically used to recommend adjuvant chemotherapy in endometrial carcinoma patients [20–22], and risk stratification is based on traditional parameters such as FIGO stage and histological grade. Low ASRGL1 expression can potentially be used as a biomarker aiding in the selection of patients that may benefit from adjuvant treatment. Patients with grade 1–2 endometrioid endometrial carcinoma are generally assumed to have low risk disease and are not recommended for adjuvant therapy [20]. Interestingly, 8% of the patients in our cohort with grade 1–2 endometrioid endometrial carcinoma have low ASRGL1 level, and it is tempting to speculate whether these patients could benefit from more extensive treatment.

Chemotherapy is often related to adverse effects and reduced quality of life, and biomarkers that can identify patients that may not benefit from additional treatment could potentially improve quality of life for those patients as well as reduce medical costs. We observed that high expression of ASRGL1 is associated with a favorable outcome, both in the endometrioid subgroup and in the whole patient cohort. It would be interesting to further explore if high ASRGL1 expression could be used to select patients that may be spared from the detrimental effects associated with adjuvant treatment.

Loss of the hormone receptor ERα is associated with aggressive disease and poor survival in endometrial carcinoma patients [23,24], and ERα is currently one of the best validated prognostic molecular biomarkers in endometrial carcinoma [25]. An estrogen response element has been identified in the promotor of the *ASRGL1* gene [8], suggesting a link between this steroid hormone and expression of ASRGL1. A potential regulatory role of estrogen on ASRGL1 expression could explain the association between hormone receptor status and ASRGL1 levels found in both primary tumor and metastatic lesions in our study.

ASRGL1 status in metastases has not previously been investigated. In the current study we describe the protein expression of ASRGL1 in 179 metastatic lesions and their corresponding primary tumors from 87 patients, also linking this to histology and ERα status. Interestingly, in most cases where primary tumor has a low ASRGL1 level, ASRGL1 expression is also low in corresponding metastases. In most patients with multiple metastases, similar expression of ASRGL1 is found in all metastatic lesions from the same individual. This is in contrast to hormone receptors, where the expression pattern of metastatic lesions in individual patients seems to be more heterogeneous [26]. 4 patients with ASRGL1 low primary tumors had high expression of ASRGL1 in some but not all metastases. Possible explanations include that these lesions originate from cells that metastasized at an earlier time point where primary tumor expressed ASRGL1, or that small ASRGL1 positive regions in primary tumor were missed when collecting biopsies or selecting areas for preparation of TMAs. It must be emphasized that our study only includes sampled metastatic lesions with corresponding primary tumors. Patients may have metastases that are surgically unavailable or that have not been sampled for other reasons. However, we find this to be interesting descriptive observations that should be explored further in future studies.

ASRGL1 is demonstrated to degrade both L-asparagine and isoaspartyl peptides *in vitro* [5], but the functional role in normal and cancerous cells is not known. Asparagine is reported to suppress apoptosis [27], and isoaspartyl peptides generated in proteins by non-enzymatic damage leads to misfolding, dysfunction and reduced degradation [5,28]. This indicates that loss of ASRGL1 function could lead to both elevated cellular asparagine levels and accumulation of dysfunctional proteins. Investigating the cellular effects of ASRGL1 activity as well as molecular mechanisms related to loss of ASRGL1 expression would be interesting, and could be performed through *in vitro* and eventually also *in vivo* studies. L-Asparaginase has been used to treat acute lymphoblastic leukemia and Non-Hodgkin lymphoma for several

Table 3
Multivariable survival analyses of endometrioid endometrial carcinoma patients according to the Cox' proportional hazards regression model.

Variable	n[a]	Unadj.HR	95% CI	P-value	Adj.HR	95% CI	P-value
Age (mean = 64)	622	1.06	1.03–1.08	<0.001	1.06	1.03–1.08	<0.001
Histologic grade				<0.001			0.008
1/2	510	1			1		
3	112	3.28	1.96–5.47		2.12	1.21–3.70	
ASRGL1[b]				<0.001			0.001
High	539	1			1		
Low	83	3.40	1.99–5.79		2.64	1.47–4.74	

[a] Cases with data available for all variables included in the univariate analyses ($N = 622$).
[b] Evaluated in hysterectomy samples by IHC (high = 2–9, low = 0–1).

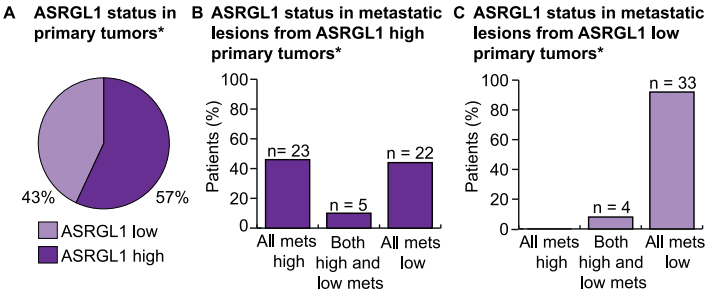

Fig. 3. ASRGL1 protein expression in metastatic lesions. 87 primary tumors with corresponding metastatic lesions were stained for ASRGL1 expression. Of these, 57% were defined as "ASRGL1 high", while 43% were defined as "ASRGL1 low" (A). Graphs showing the ASRGL1 status of metastatic lesions in patients with primary tumors defined as "ASRGL1 high" (B) or "ASRGL1 low" (C). *Only patients with primary tumors and corresponding metastatic lesions were included.

decades, and the therapeutic potential of L-asparaginase is now being explored in several solid tumors [29–32]. As ASRGL1 is proposed to display proteolytic activity against L-asparagine and loss of this enzyme is associated with aggressive disease and poor prognosis, L-asparaginase could potentially be a candidate drug for treatment of endometrial carcinoma.

We have validated ASRGL1 as a strong prognostic marker in endometrial carcinoma in a prospective setting, and find that loss of both mRNA and protein expression predicts poor outcome. Low ASRGL1 expression had independent prognostic value both in the endometrioid subgroup and in the endometrial carcinoma population in general, and its clinical utility as a prognostic marker should be further evaluated through clinical trials.

Supplementary data to this article can be found online at https://doi.org/10.1016/j.ygyno.2017.10.025.

Acknowledgements

The authors would like to thank Britt Edvardsen, Ellen Valen and Bendik Nordanger for excellent technical assistance.

Financial support

This study was supported by the University of Bergen, Helse Vest, the Norwegian Cancer Society (628837), the Research Council of Norway (239840), and Bergen Research Foundation.

Conflict of interest

Per-Henrik Edqvist has a pending patent on ASRGL1 in endometrial cancer. The remaining authors have nothing to disclose.

References

[1] J. Ferlay, I. Soerjomataram, R. Dikshit, S. Eser, C. Mathers, M. Rebelo, et al., Cancer incidence and mortality worldwide: sources, methods and major patterns in GLOBOCAN 2012, Int. J. Cancer 136 (2015) E359–86.
[2] H.B. Salvesen, I.S. Haldorsen, J. Trovik, Markers for individualised therapy in endometrial carcinoma, Lancet Oncol. 13 (2012) e353–61.
[3] L.S. Bradford, J.A. Rauh-Hain, J. Schorge, M.J. Birrer, D.S. Dizon, Advances in the management of recurrent endometrial cancer, Am. J. Clin. Oncol. 38 (2015) 206–212.
[4] S. Lheureux, M. Wilson, H.J. Mackay, Recent and current phase II clinical trials in endometrial cancer: review of the state of art, Expert Opin. Investig. Drugs 23 (2014) 773–792.
[5] J.R. Cantor, E.M. Stone, L. Chantranupong, G. Georgiou, The human asparaginase-like protein 1 hASRGL1 is an Ntn hydrolase with beta-aspartyl peptidase activity, Biochemistry 48 (2009) 11026–11031.
[6] L.A. Bush, J.C. Herr, M. Wolkowicz, N.E. Sherman, A. Shore, C.J. Flickinger, A novel asparaginase-like protein is a sperm autoantigen in rats, Mol. Reprod. Dev. 62 (2002) 233–247.
[7] V. Evtimova, R. Zeillinger, S. Kaul, U.H. Weidle, Identification of CRASH, a gene deregulated in gynecological tumors, Int. J. Oncol. 24 (2004) 33–41.
[8] U.H. Weidle, V. Evtimova, S. Alberti, E. Guerra, N. Fersis, S. Kaul, Cell growth stimulation by CRASH, an asparaginase-like protein overexpressed in human tumors and metastatic breast cancers, Anticancer Res. 29 (2009) 951–963.
[9] H.B. Salvesen, S.L. Carter, M. Mannelqvist, A. Dutt, G. Getz, I.M. Stefansson, et al., Integrated genomic profiling of endometrial carcinoma associates aggressive tumors with indicators of PI3 kinase activation, Proc. Natl. Acad. Sci. U. S. A. 106 (2009) 4834–4839.
[10] E. Wik, J. Trovik, K. Kusonmano, E. Birkeland, M.B. Raeder, I. Pashtan, et al., Endometrial carcinoma recurrence score (ECARS) validates to identify aggressive disease and associates with markers of epithelial-mesenchymal transition and PI3K alterations, Gynecol. Oncol. 134 (2014) 599–606.
[11] P.H. Edqvist, J. Huvila, B. Forsstrom, L. Talve, O. Carpen, H.B. Salvesen, et al., Loss of ASRGL1 expression is an independent biomarker for disease-specific survival in endometrioid endometrial carcinoma, Gynecol. Oncol. 137 (2015) 529–537.
[12] Cancer Registry of Norway. Cancer in Norway, Cancer Incidence, Mortality, Survival and Prevalence in Norway, Cancer Registry of Norway, Oslo, 2015 2016.
[13] C. Krakstad, I.L. Tangen, E.A. Hoivik, M.K. Halle, A. Berg, H.M. Werner, et al., ATAD2 overexpression links to enrichment of B-MYB-translational signatures and development of aggressive endometrial carcinoma, Oncotarget 6 (2015) 28440–28452.
[14] I.L. Tangen, C. Krakstad, M.K. Halle, H.M. Werner, A.M. Oyan, K. Kusonmano, et al., Switch in FOXA1 status associates with endometrial cancer progression, PLoS One 9 (2014), e98069. .
[15] I.M. Stefansson, H.B. Salvesen, L.A. Akslen, Prognostic impact of alterations in P-cadherin expression and related cell adhesion markers in endometrial cancer, J. Clin. Oncol. Off. J. Am. Soc. Clin. Oncol. 22 (2004) 1242–1252.
[16] C. Krakstad, J. Trovik, E. Wik, I.B. Engelsen, H.M. Werner, E. Birkeland, et al., Loss of GPER identifies new targets for therapy among a subgroup of ERalpha-positive endometrial cancer patients with poor outcome, Br. J. Cancer 106 (2012) 1682–1688.
[17] T.K. Koo, M.Y.A. Li, Guideline of selecting and reporting Intraclass correlation coefficients for reliability research, Am. J. Chin. Med. 15 (2016) 155–163.
[18] X. Matias-Guiu, B. Davidson, Prognostic biomarkers in endometrial and ovarian carcinoma, Virchows Archiv: Int. J. Pathol. 464 (2014) 315–331.
[19] M.J. Duffy, C.M. Sturgeon, G. Soletormos, V. Barak, R. Molina, D.F. Hayes, et al., Validation of new cancer biomarkers: a position statement from the European group on tumor markers, Clin. Chem. 61 (2015) 809–820.
[20] N. Colombo, E. Preti, F. Landoni, S. Carinelli, A. Colombo, C. Marini, et al., Endometrial cancer: ESMO Clinical Practice Guidelines for diagnosis, treatment and follow-up, Ann. Oncol. Off. J. Eur. Soc. Med. Oncol. ESMO. 24 (Suppl. 6) (2013) vi33–8.
[21] N. Colombo, C. Creutzberg, F. Amant, T. Bosse, A. Gonzalez-Martin, J. Ledermann, et al., ESMO-ESGO-ESTRO consensus conference on endometrial cancer: diagnosis, treatment and follow-up, Ann. Oncol. Off. J. Eur. Soc. Med. Oncol. ESMO. 27 (2016) 16–41.
[22] W.J. Koh, B.E. Greer, N.R. Abu-Rustum, S.M. Apte, S.M. Campos, J. Chan, et al., Uterine neoplasms, version 1.2014, J. Natl. Compr. Cancer Netw. 12 (2014) 248–280.
[23] E. Wik, M.B. Raeder, C. Krakstad, J. Trovik, E. Birkeland, E.A. Hoivik, et al., Lack of estrogen receptor-alpha is associated with epithelial-mesenchymal transition and PI3K alterations in endometrial carcinoma, Clin. Cancer Res. 19 (2013) 1094–1105.
[24] V. Jongen, J. Briet, R. de Jong, K. ten Hoor, M. Boezen, A. van der Zee, et al., Expression of estrogen receptor-alpha and -beta and progesterone receptor-A and -B in a large cohort of patients with endometrioid endometrial cancer, Gynecol. Oncol. 112 (2009) 537–542.
[25] H.M. Werner, H.B. Salvesen, Current status of molecular biomarkers in endometrial cancer, Curr. Oncol. Rep. 16 (2014) 403.
[26] I.L. Tangen, T.B. Onyango, R. Kopperud, A. Berg, M.K. Halle, A.M. Oyan, et al., Androgen receptor as potential therapeutic target in metastatic endometrial cancer, Oncotarget 7 (2016) 49289–49298.
[27] J. Zhang, J. Fan, S. Venneti, J.R. Cross, T. Takagi, B. Bhinder, et al., Asparagine plays a critical role in regulating cellular adaptation to glutamine depletion, Mol. Cell 56 (2014) 205–218.
[28] K. Michalska, M. Jaskolski, Structural aspects of L-asparaginases, their friends and relations, Acta Biochim. Pol. 53 (2006) 627–640.
[29] A.A. Yunis, G.K. Arimura, D.J. Russin, Human pancreatic carcinoma (MIA PaCa-2) in continuous culture: sensitivity to asparaginase, Int. J. Cancer 19 (1977) 128–135.

[30] P.L. Lorenzi, W.C. Reinhold, M. Rudelius, M. Gunsior, U. Shankavaram, K.J. Bussey, et al., Asparagine synthetase as a causal, predictive biomarker for L-asparaginase activity in ovarian cancer cells, Mol. Cancer Ther. 5 (2006) 2613–2623.
[31] M. Yu, R. Henning, A. Walker, G. Kim, A. Perroy, R. Alessandro, et al., L-asparaginase inhibits invasive and angiogenic activity and induces autophagy in ovarian cancer, J. Cell. Mol. Med. 16 (2012) 2369–2378.
[32] J.B. Bachet, F. Gay, R. Marechal, M.P. Galais, A. Adenis, Ms CD, et al., Asparagine synthetase expression and phase I study with L-asparaginase encapsulated in red blood cells in patients with pancreatic adenocarcinoma, Pancreas 44 (2015) 1141–1147.

Supplementary Table S1. ASRGL1 protein expression related to clinicopathological variables in 635 patients with endometrioid endometrial carcinoma.

		ASRGL1		
Variable	**N**	**High *n* (%)**	**Low *n* (%)**	**P-value (x^2)**
Age	**635**			0.475
< 66	363	318 (88)	45 (12)	
≥ 66	272	233 (86)	39 (14)	
FIGO stage 2009	**635**			**<0.001**
I-II	561	505 (90)	56 (10)	
III-IV	74	46 (62)	28 (38)	
Histologic grade	**623**			**<0.001**
Grade 1-2	511	471 (92)	40 (8)	
Grade 3	112	68 (61)	44 (40)	
Metastatic nodes	**506**			**<0.001**
Negative	466	414 (89)	52 (11)	
Positive	40	25 (63)	15 (37)	
Ploidy	**381**			**0.007**
Diploid	322	275 (85)	47 (15)	
Aneuploid	59	42 (71)	17 (29)	
Myometrial infiltration	**634**			**<0.001**
<50%	406	371 (91)	35 (9)	
≥50%	228	180 (79)	48 (21)	
ERα	**602**			**<0.001**
Positive	503	476 (95)	27 (5)	
Negative	99	50 (51)	49 (49)	

Abbreviations: Asparaginase-like protein 1 (ASRGL1), Estrogen receptor α (ERα), International Federation of Gynaecology and Obstetrics (FIGO).

Missing information on histological grade for 12 patients, metastatic nodes for 129 patients, ploidy for 254 patients, myometrial infiltration for 1 patient, and ERα status for 33 patients.

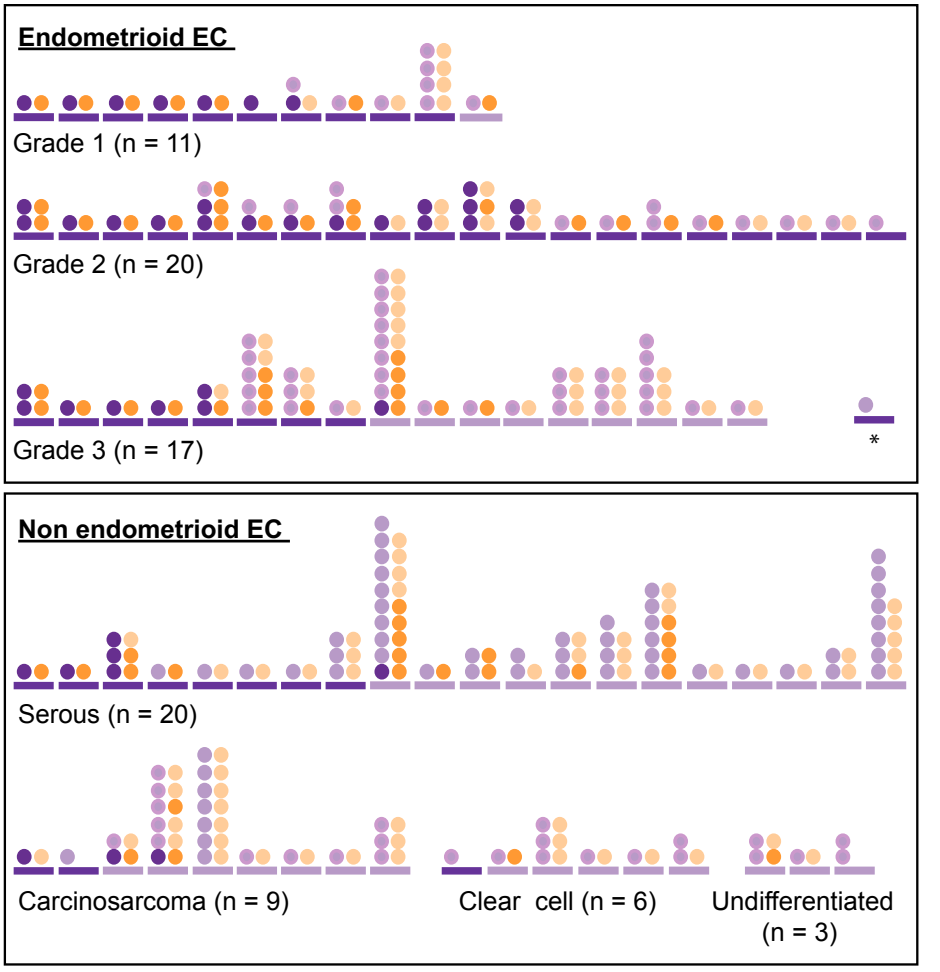

Supplementary figure S1. ASRGL1 status in individual metastatic lesions. Expression pattern of ASRGL1 in sampled metastatic lesions with corresponding primary tumors from patients diagnosed with endometrial carcinoma. Rectangles represent primary tumorsof individual patients and each line of circles one metastasis, illustrationg the status of ASRGL1 (purple) and ERα (yellow) for that lesion. *Information on grade missing for one patient. Abbreviations: EC = endometrial carcinoma, ERα = estrogen receptor α

Graphic design: Communication Division, UiB / Print: Skipnes Kommunikasjon AS

uib.no

ISBN: 978-82-308-3619-4